1968

Finite Element Analysis of Salt Pillar Models.

William Joseph Bergeron
Louisiana State University and Agricultural & Mechanical College

FINITE ELEMENT ANALYSIS OF SALT PILLAR MODELS

A Dissertation

Submitted to the Graduate Faculty of the
Louisiana State University and
Agricultural and Mechanical College
in partial fulfillment of the
requirements for the degree of
Doctor of Philosophy

in

The Department of Engineering Mechanics

by
William Joseph Bergeron
B.S., University of Southwestern Louisiana, 1959
M.S., Louisiana State University, 1961
August, 1968

ACKNOWLEDGEMENT

The author wishes to express his gratitude to Dr. Robert L. Thoms for having suggested the problem presented herein and for his quidance, assistance, and encouragement throughout its solution. He also wishes to express his thanks to the rest of his committee and to the staff of the Engineering Mechanics Department for making his stay at L.S.U. not only a beneficial one, but also a pleasant one.

Special acknowledgement is also due his wife Rena and children Stephanie, Renée, Angelle, and Bryan for their understanding and patience while he completed his education.

TABLE OF CONTENTS

LIST OF FIGURES

NOMENCLATURE

A	= area; constant
a	= inner diameter of steel rings; constant
B	= constant
b	= outer diameter of steel ring; constant
$[B]$	= matrix function used to obtain strains
C	= constant
c	= constant
D	= constant; diameter of circular pillar model
$[D]$	= elasticity matrix
$[D_o]$	= that part of [D] which depends only on ν
$[D_{ec}]$	= 'elasto-creep' matrix
E	= elastic modulus
E_m	= Maxwell elastic modulus (instantaneous elastic modulus)
E_k	= Kelvin elastic modulus (delayed or retarded elastic modulus)
e	= 2.7183; general element
$\{F\}^e$	= nodal forces on e
$[f]$	= displacement field
f_1, f_2	= functions
G_1	= elastic shear modulus
G_2	= retarded shear modulus

$\{g\}$ = distributed external load per unit area

H = height of pillar model

I = identity matrix

I_1, I_2, I_3 = integrals

i, j, m = nodal points of element e

K_o = octahedral shearing strength

$[K]$ = stiffness matrix of entire structure

$[k]^e$ = stiffness matrix of element e

m = constant; slope of $\dot{\epsilon}$ vs t on log-log plot (negative)

$[N]$ = matrix function used in obtaining displacement field

n = constant; slope of $\dot{\epsilon}$ vs σ on log-log plot (positive); number of nodes

$\{P\}^e$ = distributed body force per unit volume of material

p_i = internal pressure applied to steel rings

R = radial component of body force

$\bar{R}$ = radial force per unit length of the circumference of a node

$\{R\}$ = external forces applied at the nodes

$\bar{r}$ = r-coordinate of centroid of element e

$[S]$ = stress matrix

T = absolute temperature ($^\circ$K)

t = time

U = component of nodal force in r-direction

u = component of displacement in r-direction

V = component of nodal force in z-direction

v = component of displacement in z-direction

W = width of square pillar model

Z = axial component of body force

$\bar{Z}$ = axial force per unit length of the circumference of a node

$\bar{z}$ = z-coordinate of centroid of element e

α = coefficient of thermal expansion; constant

β = constant

γ = shear strain

γ_o = octahedral shear strain

Δ = area of triangle e

$\{\delta\}$ = displacement vector

ϵ = strain

ϵ_{z_o} = pillar cumulative deformation ($in.in.^{-1}$)

$\dot{\epsilon}_{z_o}$ = pillar strain rate

ζ_1 = viscoelastic constant

ζ_2 = viscoplastic constant

η_k, η_1, η_2 = Kelvin viscosity

η_m = Maxwell viscosity

θ^e = temperature rise in element e

ν = Poisson's ratio

π = 3.1416

σ = stress

$\bar{\sigma}$ = effective stress

σ_{z_o} = average applied axial pillar stress

τ = shear stress

τ_o = octahedral shear stress

τ_i = τ_o at t = 0

Supercripts

e = element e

T = transposed

$\bar{}$ = evaluated at $\bar{r}$, $\bar{z}$

$'$ = corrective term

Subscripts

b = boundary force

c = creep

e = elastic

i, j, k = 1st, 2nd, 3rd nodes respectively of element e

LA	= laterally applied
o	= initial
p	= body force
pl	= plastic
r	= radial
t	= thermal
z	= axial
I,II,...,V	= partition numbers
ϵ_o	= initial strain
θ	= tangential

ABSTRACT

The creep characteristics of rock salt were studied in an application of the finite element method. A creep law was proposed for rock salt and creep and large displacement modifications proposed for the finite element method. The scope of this study was limited to the use of physical constants of rock salt available from other investigators.

An analysis was made of the proposed creep law and the proposed creep modifications and these were shown to complement each other. A computer program was written to solve the problem and was shown to produce small errors.

The actual problem solved was the determination of stresses and displacements in an axi-symmetric salt pillar model when it was subjected to a pillar load of 6,000 psi at 300°K for total times of two, five, and ten days. Included with the results were computer obtained plots of the original finite element salt pillar model and the deformed finite element salt pillar model.

Deformations obtained for the finite element salt pillar model correlated very well with deformations observed in recent publications showing actual deformed salt pillar models.

CHAPTER I

INTRODUCTION

THE WASTE DISPOSAL PROBLEM

Concern for the hazards created by radioactive fallout from weapon testing programs prompted an investigation by Parker et al. (1)* into the source, magnitude, and disposition of the other radioactive debris generated in our nuclear age. It was noted that the major source of radioactive wastes from peacetime uses of nuclear energy will be that produced by the irradiation of fissionable fuel in stationary power reactors. According to predictions by Lane (2), this radioactive waste per year produced will be over five hundred times as much as that produced in bomb tests, and by the year 2000, over a thousand times as much. Therefore, it is imperative that a safe means be found to handle the radioactive waste products from nuclear reactors.

This high-level radioactive waste which is separated from the reuseable unconsumed uranium in the reprocessing of spent reactor fuel has far too much radioactivity to

---

*Numbers in parentheses pertain to references appended to this paper.

allow disposal to the living environment. With the growth of the nuclear power industry, this disposal problem is becoming increasingly serious and thus necessitates the development of a total and safe containment procedure. At the present time, the majority of the wastes produced in all countries are stored either as acid liquors in stainless steel tanks or as alkaline liquors in mild steel tanks in underground locations at the processing plants (3). However, as the nuclear power industry expands throughout the world, storage of hundred of millions of gallons of liquid wastes with obvious hazards and with the cost of monitoring and tank replacement over the centuries becomes less attractive. Therefore, considerable research has been in progress for the past ten years to devise methods for the conversion of these high-level liquid wastes into solids. These processes are only treatment steps, however, and they must be followed by a disposal operation. Thus, an ultimate disposal operation is required that will insure that the fission products are safely contained for centuries without further attention or need for monitoring.

DISPOSAL IN SALT MINES

The Earth Science Division of the National Research Council organized in 1955 at Princeton University a

meeting (4) of sixty-five geologist, engineers, and personnel from other related disciplines to propose and discuss the disposal of radioactive wastes in geologic formations.

The storage of radioactive wastes in salt formations aroused considerable interest at this conference and in 1957, the report of the committee on Waste Disposal (5) suggested disposal of solid form wastes in cavities mined in salt beds and salt domes as the possibility promising the most practical immediate solution of the problem.

Some of the advantages cited for salt were:

(1) Rock salt is widely distributed and abundant: United States reserves are estimated at greater than 6×10^{13} tons (1,6).

(2) The thermal conductivity of rock salt (2.5 Btu/hr-ft-F^{o} at 200^{o} F) is higher than most rocks and will enable larger quantities of heat to be dissipated (7).

(3) Rock salt has a compressive strength similar to that of concrete, but unlike concrete and most other rocks, salt will flow plastically and relieve stress concentration produced by mining and heating. Under normal mining conditions, the stress concentrations and temperatures are sufficiently low that supports are not needed.

(4) Salt formations in the United States are located in areas of low seismicity.

(5) Salt is essentially impermeable due to its plastic nature when under pressure. Any cracks which might develop in the salt formation would be expected to be self-healing, as indicated by the lack of solution caverns similar to those found in limestone formations.

(6) The cost of mining salt is less than most other rocks. In reference to the first advantage; if the estimated waste solution through the year 2000 A.D. is converted to solids and ultimately stored in salt mines, an area of about 1200 acres will be required (3). This is not considered unreasonable for the size of the nuclear economy involved and for the quantity of rock salt available.

As a result of the above reports, the ORNL initiated studies on the disposal of high-level radioactive wastes in salt cavities. The economics of an actual disposal facility in a salt mine, the heat transfer from the waste to the salt, and the effects of heat and radiation on the properties of salt were considered. The following major conclusions drawn from these studies were (8,9,10):

(1) The "in situ" heat-transfer properties of rock salt are sufficiently close to the values determined in the laboratory on single crystals so that confidence can

be placed on theoretical heat-transfer calculations.

(2) Elevated temperatures will cause accelerated creep, but the exact effect on structural stability of the mine cannot be predicted from the present studies with sufficient accuracy to allow the design of a disposal facility making the optimum use of mine space.

(3) Most bedded-salt deposits contain trapped moisture which is released by shattering of the salt at temperatures above 250°C. By limiting the maximum salt temperature in a disposal operation to 200°C, this problem can be avoided.

(4) Rock salt is comparable to concrete for gamma radiation shielding.

(5) A radiation dose of 5×10^8 R produces some changes in the structural properties of rock salt (i.e., about a 10% reduction in compressive strength); however, because of the shielding characteristics of salt, the effect produced will be limited to the salt near the radiation source.

(6) Gamma radiation may produce some free chlorine within the salt structure; however, the amount released is expected to be negligible.

(7) The relative stability at ambient temperature of a salt mine used for waste disposal can be predicted from observed conditions in existing mines.

(8) The economics of a salt mine facility for disposal of future high-level power reactor wastes indicate that costs will be of the order of 0.01-0.02 mils/kwh of electricity generated.

"PROJECT SALT VAULT"

These studies were only in preparation for the actual final goal of the ORNL program on radioactive waste disposal in underground salt formations. This goal was to demonstrate the equipment and operations necessary to carry out safe and economical disposal of high-level solidified wastes in a typical disposal operation in the Carey Salt Mine at Lyons, Kansas. Considerable emphasis in the United States has been placed on this demonstration project which is called "Project Salt Vault" (11,12,13,14,15,16). The objectives of this salt mine study were:

(1) to confirm the feasibility of disposal in salt mines;

(2) to demonstrate the required waste-handling equipment and techniques;

(3) to determine the possible gross effects of radiation on hole closure, floor uplift, salt-shattering temperatures, etc., in an area where the salt temperature is in a range of 100-200°C;

(4) to determine the possible release of radiolytically produced chlorine; and

(5) to collect information on creep and plastic flow of salt at elevated temperatures which can be used later in the design of an actual disposal facility.

The last objective of the study is the one with which this report is concerned.

A newly mined experimental area was created at the periphery of the mine at a higher level than the existing abandoned mine and of the most desirable geometry, so as to have the purest salt strata in the floor where the radioactive source was to be located. Four experimental rooms (Figure 1.1) were mined and in November, 1965, fourteen irradiated fuel assemblies (10^6 curi) from the Engineering Test Reactor, contained in seven cans, were placed in the floor in the first room. A series of electrical heaters in the same geometric array as the main radioactive array was placed in the fourth room as a control to determine the effect of heat only. The final portion of the demonstration was a pillar heating experiment where a large mass of salt underlying a mine pillar was heated by electrical heaters to about 100°C beneath the pillar. This portion of the project was set up to obtain information on mine stability as a result of

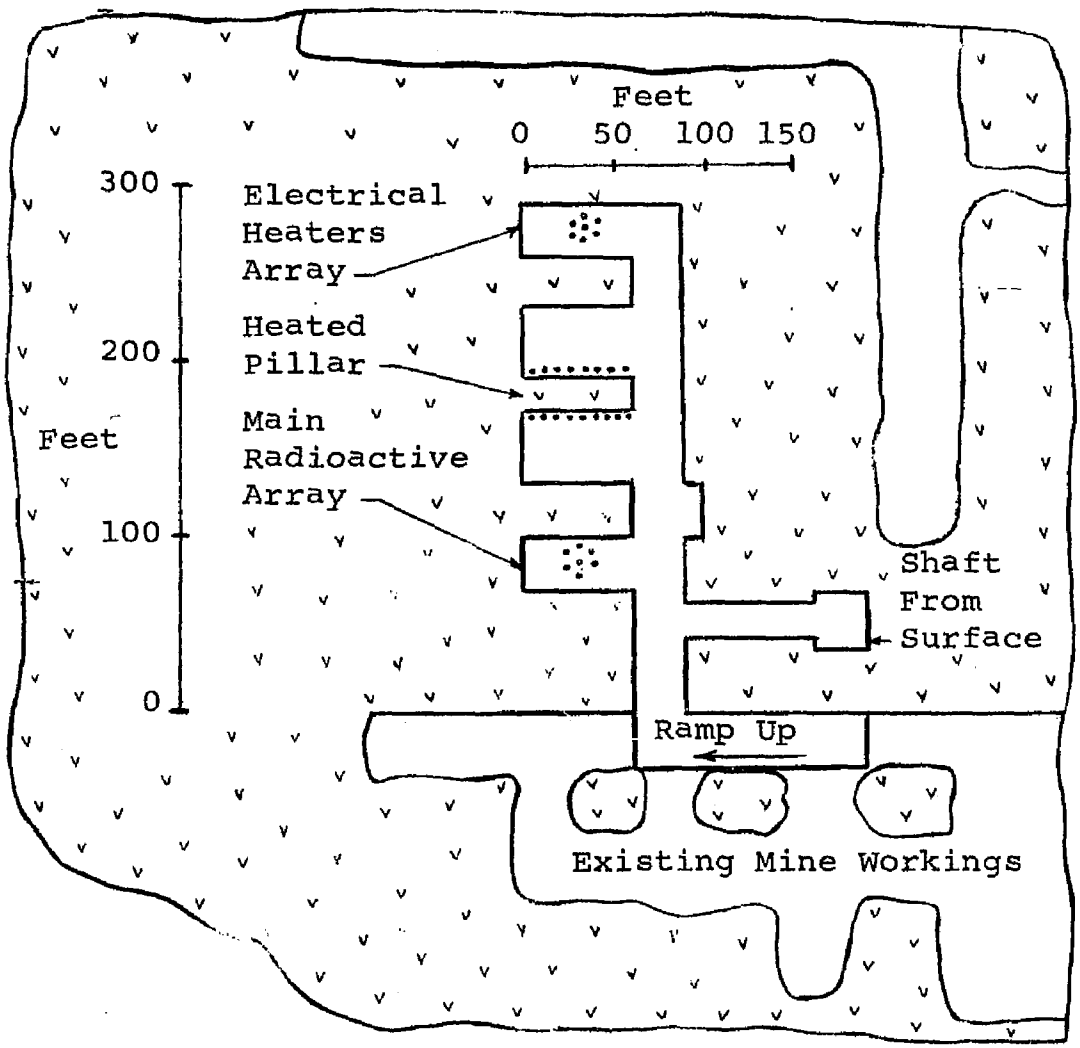

Figure 1.1. Layout of Experimental Area

increased salt temperatures. However, it was delayed until the end of 1966 since it was assumed that extreme salt movement would take place. The temperature, flow rate, and overburden load transfer in the center pillar were monitored by means of thermocouples, strain gages, and strain change meters located in and around the experimental area and throughout the mine. Experiments were also performed in the laboratory on models of the salt pillars to complement the data obtained from the mine.

The following conclusions were presented by Bradshaw and associates to the First Congress of the International Society of Rock Mechanics, Lisbon, Portugal in September and October of 1966 (15).

(1) The pillar-model tests have proven themselves to be useful for understanding the way in which salt movement takes place, and it is reasonable to expect that predictions based on the elevated temperature models will also be valid.

(2) No measurable effects of radiation on the flow of salt were expected or observed.

(3) Thermal expansion of the floor and increased transverse expansion rates in the pillars adjacent to the array rooms have been about as expected with acceleration of movement in the ceiling exceeding expectation. However,

these movements should not cause trouble during the time when a room is still being filled with radioactive wastes.

Considerable laboratory tests (8,9,10,15,17,18,19,20, 21,22,23,24) were carried out to measure the effects of temperature and radiation on plastic flow and on the stability of salt, and the test area in the mine was well instrumented to compare the actual conditions with theoretical predictions. Thus, the salt-flow data obtained in this experiment should, when combined with the results of laboratory and theoretical studies on the structural stability of rock salt at elevated temperatures and pressures, allow the establishment of a basis for the design of an actual disposal facility for optimum use of salt mine space.

THE SALT PILLAR MODEL

The study of this report is a theoretical one in which the salt pillar model is analyzed by numerical procedures. This model is the one proposed by Obert (19) and is the one which has evolved as the standard test model in all the many recent laboratory tests. However, as of this date, there is no evidence of any theoretical creep studies performed on the salt pillars or on this salt pillar model. This model, its development, its description, and its value are discussed in detail in Chapter II.

THE MECHANICAL BEHAVIOR OF ROCK SALT

In order to study the creep behavior of the salt pillar model, information on rock salt's mechanical behavior is necessary. A review of the laboratory experiments conducted in this area is presented in Chapter III and the relative merits of the various experiments are discussed. The mechanical models of salt presented by investigators who worked with the salt pillar models are discussed in Chapter V and a new mechanical model is proposed and fitted to the data obtained by Bradshaw and his associates (21).

THE FINITE ELEMENT METHOD

The numerical procedure used in studying the creep of the salt pillar model is the 'Finite Element Method'. A general discussion of the method and the actual mathematical analysis of an axi-symmetric elastic problem is presented in Chapter IV. In order to account for creep behavior, the analysis is then extended into the nonlinear range by the introduction of a 'variable elasticity' procedure. The application of this procedure to the creep law adopted for this analysis is discussed in Chapter V.

CHAPTER II

THE SALT PILLAR MODEL

INTRODUCTION

Salt pillars are the unexcavated areas of salt left within the limits of a salt mine and, as such, they are the most important element in stabilizing the underground structure. In the salt mines, these pillars undergo continuous deformation (creep). The creep rate of the pillar depends on the average pillar stress (which in turn depends on the extraction ratio and the depth of the mine), the shape and height of the pillars, the temperature of the salt and the time since creation of the pillars.

Sufficient data on existing salt mines were available to enable predictions to be made on the stability of mines at ambient temperatures, but no data or experience were available which were directly applicable at elevated temperatures. Studies performed by Serata (18) and Obert (14) [1964] at ambient temperatures have shown that creep in rock salt mines may be approximated by testing scale-model specimens uniaxially by providing proper horizontal restraints over the floor and roof portions of the model. These horizontal restraints produced triaxial stress

conditions similar to those found in the pillars in the salt mines. Lomenick and Bradshaw [1965] (20) studied the behavior of these scale model pillars (D/H = 4) at temperatures up to 200°C and stresses up to 10,000 psi for time periods of several thousand hours.

DEVELOPMENT OF THE PILLAR MODEL

Serata and Obert in their developments of a model pillar each investigated the effects of specimen shape and end constraints on the strength and deformational behavior of salt. Following is a general discussion of these investigations.

The most important difference of a mine pillar from a laboratory specimen is the continuous medium of the upper and lower formations over and under the exposed pillar portion. Thus, they each insisted that a pillar model should reflect the proper relation of the pillar to the surrounding medium of an infinite extent since the pillar in the mine is actually a part of a continuous medium. Furthermore, the medium is subjected to both the lateral earth pressure and strain confinement in addition to the overburden load. The influence of the continuous medium on the behavior of the pillar portion is manifold. It adds to the axially

loaded pillars the following effects which virtually change its behavior:

1. Friction and cohesive forces acting on both ends of the pillar.
2. Room for elastic and time dependent deformations to reduce localized stress developed in the pillar.
3. Transfer of the formation's lateral pressure onto the pillar.
4. Confinement against lateral expansion of the pillar at both ends.

Serata demonstrated in the laboratory these effects of the continuous medium by testing specimens with various degrees of confinement. His experimental results are summarized in Figure 2.1 in which the stress-strain curves of four types of specimens are compared. All the specimens have similar square pillars, but different friction and confinement conditions on the ends. The Type A specimen is a 3-inch cube uniaxially loaded with a friction reducer attached to each end of the specimen. The Type B specimen is an identical 3-inch cube uniaxially loaded with the loading ends directly exposed to the steel surface of the loading plungers. Thus, the only difference between the two is the degree of friction created on the specimens in the process of loading. However, the failure strength of

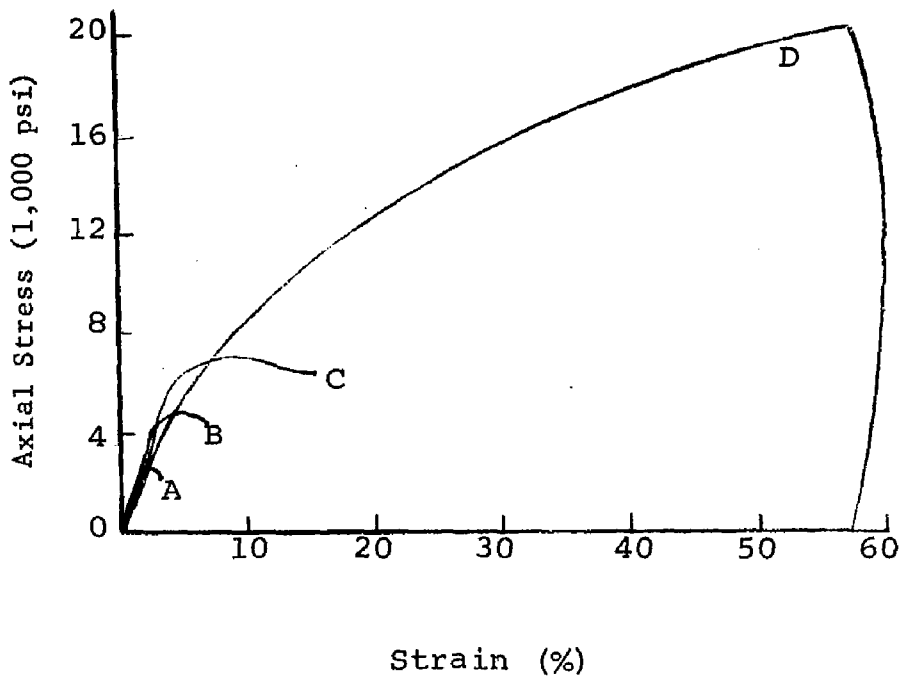

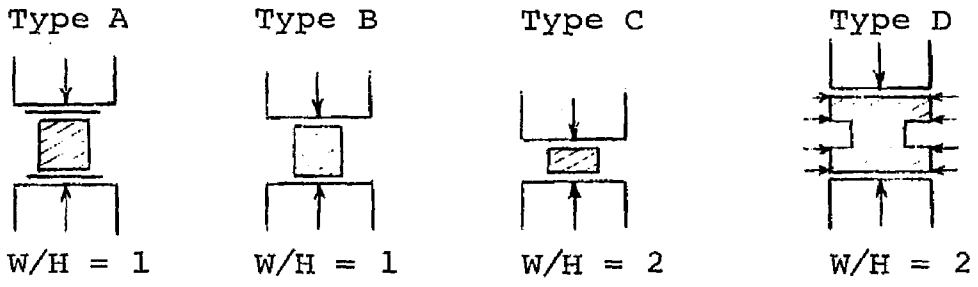

Figure 2.1. Behavior of Pillar Models Under Various Loading Conditions

the Type B specimen was twice as large as the other. This strength increase was credited to the larger lateral friction developed over the steel contact surfaces of the Type B specimen. The Type C specimen is identical to the Type B specimen except for its height which is only half as great. This reduction in the height increased the failure strength of the same material to approximately three times the true uniaxial strength. The Type D specimen has a pillar located in the center of the specimen exactly the same as Type C but has in addition a confined continuous medium at each end of the pillar. This medium at the top and at the bottom of the specimen represents, respectively, the roof and floor of the mine. This simulates closely the natural conditions of a mine pillar.

Experiments performed by Obert produced the same results, i.e., (1) the end constraints strongly affect the specimen strength with confined conditions at the ends of the pillar increasing the strength, and (2) as the ratio W/H was increased, the specimens lost their brittle characteristics and tended to flow rather than fracture.

The stress-strain curves for the different specimens illustrated in Figure 2.1 show the effects of the medium confinement. Due to the difference in degree of end-confinement conditions and to the addition of media at

each end to simulate the continuous medium, a significant increase of the failure strength and in the time dependent creep was observed for the Type D specimen. This is graphically illustrated in Figure 2.2. In this figure, the distribution of axial stress and lateral stress in the pillar section is considered in the three different pillar models. These pillar models have the same width but different heights. Serata indicates that very little or no lateral stress appears in the middle portion of the tall pillar, in which $H_3 = 2W$, since he assumed that the end effects would not reach this far. This condition is similar to the Type A specimen of Figure 2.1.

Serata, assuming the octahedral shearing stress criterion, proposed the following general equation for the maximum pillar stress.

$$\sigma_{z_{o_{max}}} = \frac{1}{A}\int_A \sigma_z \, dA$$

$$= \frac{1}{A}\int_A \left[(\sigma_z - \sigma_L) + \sigma_L\right] dA$$

$$= \frac{3}{\sqrt{2}} K_o + \sigma_{L_{av}} \, . \qquad (2.1)$$

He applied Equation 2.1 to the tall pillar of Figure 2.2, in which the average lateral stress is nearly zero, and

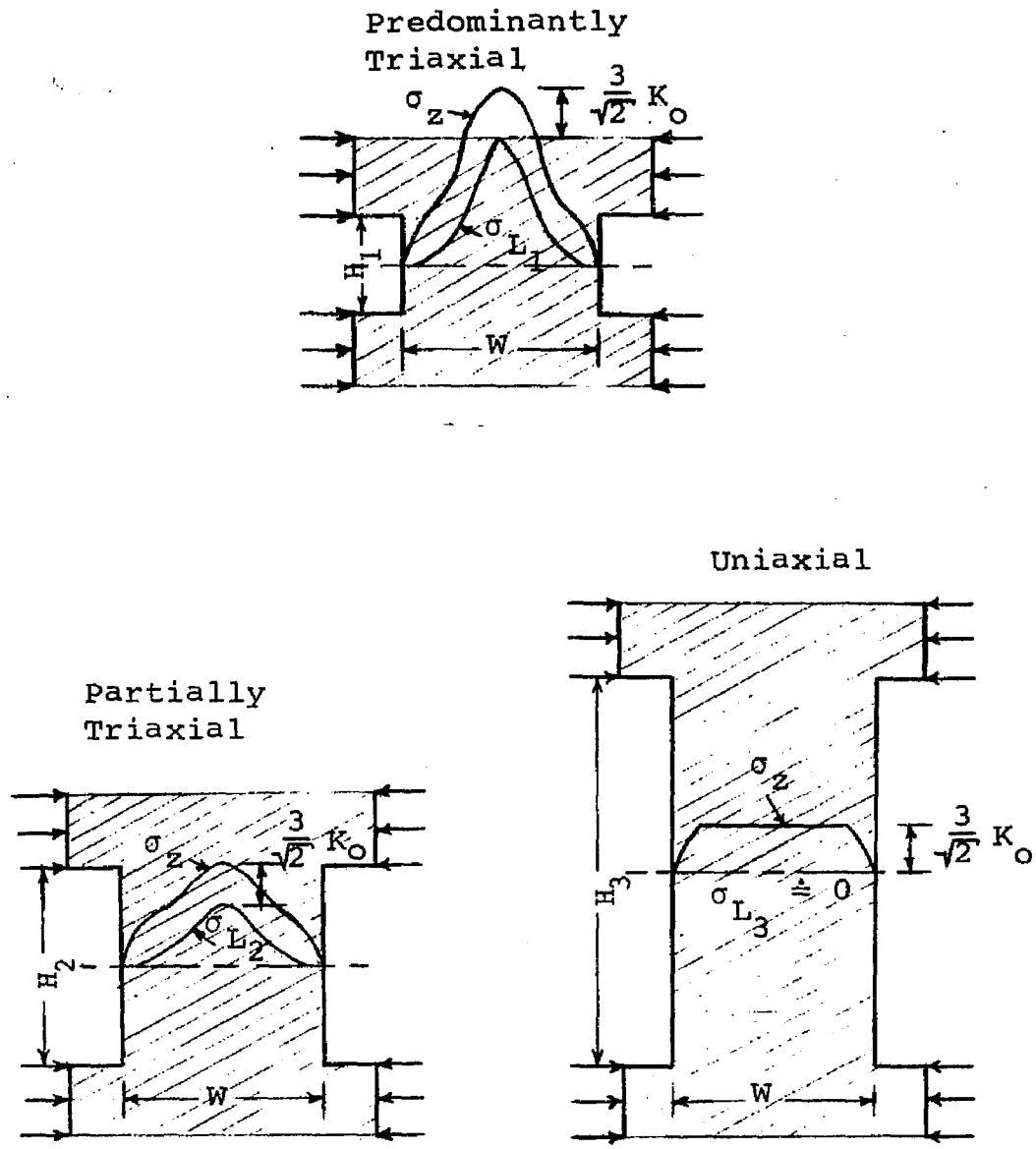

Figure 2.2. Development of Lateral Stress for Various W/H Ratios of the Pillar Model

obtained the value of σ_{max_T} = 3,200 psi. This was fairly close to the laboratory strength which he obtained for the Type A pillar of Figure 2.1.

The medium pillar resembles Types B and C specimens of Figure 2.1, since a considerable amount of the lateral stress reaches the middle part of this pillar. The maximum strength of the medium pillar is calculated by Equation A in which $\sigma_L > 0$ as:

$$\sigma_{max_M} = \frac{3}{\sqrt{2}} K_o + \sigma_{L_{av}} \qquad (2.2)$$

Thus, the medium pillar should be stronger than the tall pillar by the amount of the average lateral stress $\sigma_{L_{av}}$ existing at the middle of the pillar.

The short pillar of Figure 2.2 with its secure confinement and reduced height gives a greatly increased lateral stress magnitude. This is the condition for the Type D specimen of Figure 2.1.

Obert arrived at similar results in his laboratory, i.e., as the W/H ratio of the pillar model was increased, the compressive strength also increased and there was an increase also in the tendency for the models to flow rather than fracture.

DESCRIPTION OF THE PILLAR MODEL

Since the deformational behavior of salt was so strongly dependent on the end constraints, model pillars made from salt had to provide some means of controlling and determining the magnitude of this factor. Obert found the model shown in Figure 2.3 to satisfy these requirements. The model is cylindrical* in shape with a portion of the center ground out to form the pillar and surrounding rooms. To supply the confining pressures to the roof and floor portions, steel rings (3/4 inch thick by 1 inch height) were cemented to the ends of the model with an epoxy cement that completely filled the gap between the salt and the rings. The ends of the model were allowed to extend past the steel rings 1/8 inch so that when it was loaded no axial force was applied to the steel rings. Two dial gages were mounted 180° apart on the steel rings to provide means of measuring the cavity closure of the pillar model. Three resistance strain gages, oriented to respond to tangential strain, were cemented to the periphery of each ring at 120° intervals. The internal pressure applied to the ring was

*Cross section of mine pillars are not circular, but model studies by Obert show that the relation between compressive strength and diameter/height or width/height ratio are virtually identical if the width of a pillar is taken as its smaller lateral dimension.

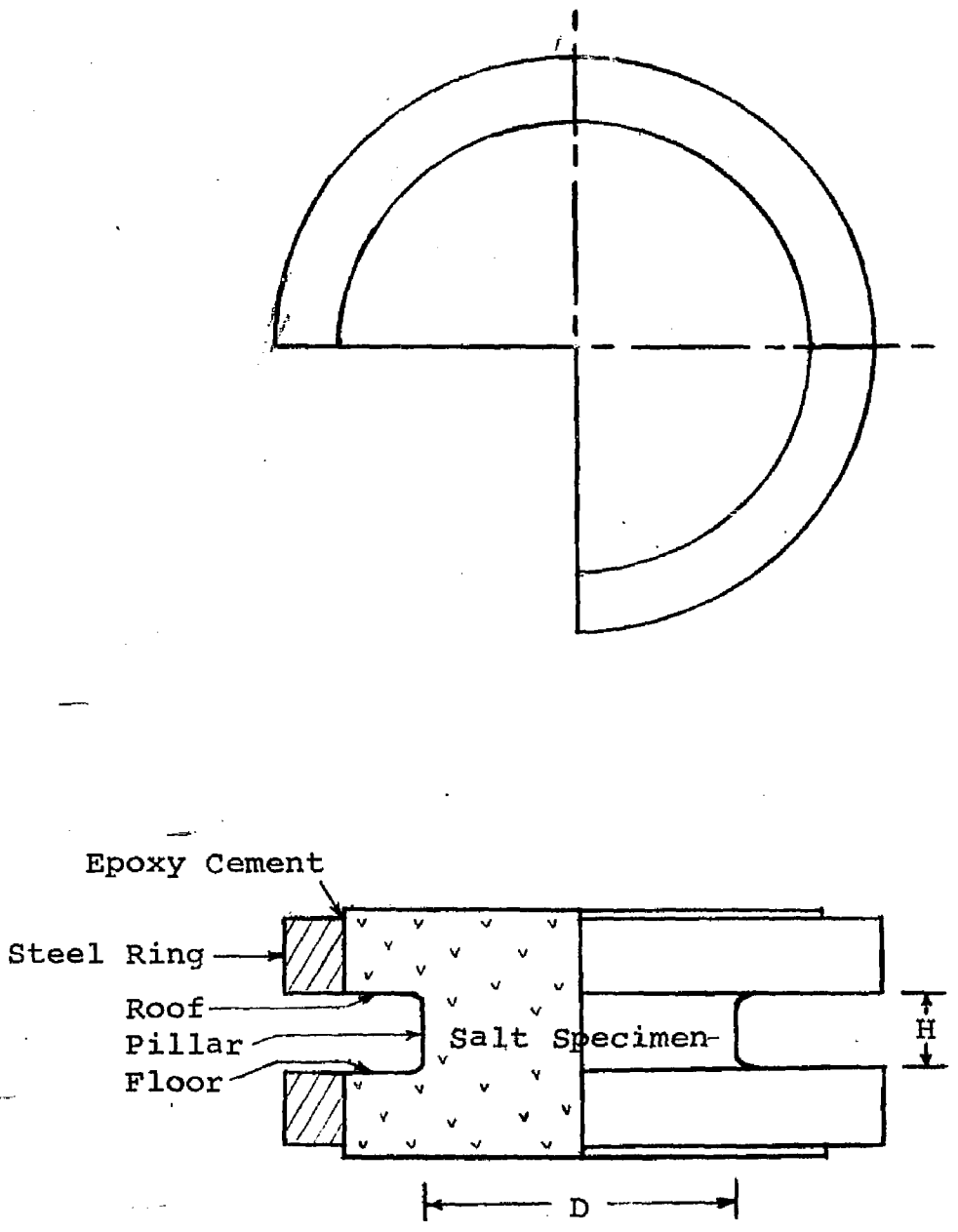

Figure 2.3. Salt Pillar Model (3/4 Section)

determined by the equation for thick wall rings,

$$p_i = \frac{E\,\epsilon_\theta (b^2 - a^2)}{2a^2} \qquad (2.3)$$

Under the assumption that the lubricant on the bearing plates reduced the end constraints to a negligible value, the radial stress σ_r in the pillar model was obtained from

$$\sigma_r = - p_i . \qquad (2.4)$$

Bradshaw (15) and associates found from pillar model tests that the radial stress was equal to about 50% of the average vertical pillar stress. It should be observed, however, that this stress is actually not in the pillar portion itself as was assumed, but, in the floor and roof sections at the interface between the salt and the steel rings.

VALUE OF THE PILLAR MODEL

Obert found through laboratory experimentation with rock salt that the mode of failure and the strength of the above model pillars were virtually the same as that for the conventional compression specimen having the same pillar D/H ratio tested without end lubricants. However, the above pillar model was considered a much better model since there was no discontinuity in the model material at the roof and

floor and since the steel rings permitted a means of determining and controlling the magnitude of the end constraints. Bradshaw (21) and associates performed a correlation of convergence measurement in salt mines with laboratory creep-test data and found a reasonable agreement with the rates measured in the Kansas mines. They also observed that the horizontal expansions of the pillars did not seem to be great enough to account for the apparent shortening of the pillars. A plausible explanation accepted by them at that time was that part of the pillar volume expanded into the room via the floor and roof. Again the pillar model proved valuable, for in a later paper (15), this was shown to actually take place in the testing of pillar models.

Bradshaw and associates (15) performed research in the laboratory with model pillars (at temperatures up to 200° C and stresses up to 14,000 psi) and in a 1,000 feet deep salt mine ("Project Salt Vault") using reactor fuel and electrical heaters. Measurements of convergence, strain, strain rates and stress changes were obtained. Again, the model tests were found to correlate well with underground measurements and observations. Also, these pillar model tests, since they indicate the radial stress developed,

have shown in a qualitative way why roof-sags and floor-heaves take place in the salt mines.

Thus, the pillar model test performed have shown that these salt pillar models can give useful information about salt movement in the mines both at ambient and at elevated temperatures.

CHAPTER III

THE MECHANICAL BEHAVIOR OF ROCK SALT

INTRODUCTION

The problem of accurately determining the stress, strain, and creep in a rock structure in the earth's crust is a rather complex one. Theoretical studies differ widely in many of the basic assumptions about the physical properties of the rock itself. Some solutions of problems in underground stress analysis assume that rock is elastic, homogeneous and isotropic in character, and that its physical properties are neither time nor temperature dependent; others assume that rocks are nonhomogeneous, anisotropic, plastic, viscoplastic, viscoelastic, time and temperature dependent, or a combination thereof.

The study of the physical properties of rock salt, the member of the rock family considered here, is especially complicated by its viscoplastic, viscoelastic, time, temperature, and pressure dependent characteristics. In the underground structure, the pressure involved is a function of the depth, stratigraphy, the percentage of salt excavated, and the configuration of the excavation. The temperature is a function of the depth, the size and shape

of the structure, the rate of heat production of the stored material and the thermal conduction in the surrounding salt. Although rock salt is somewhat nonhomogeneous and anisotropic (because of impurities in the salt such as anhydrites and shale, and more so in the bedded salt than in the dome salt, and because of flow bands in dome salt which formed as the salt crept from a deeper source to its present position), the rock salt of the salt pillar model considered in this study will be assumed to be homogeneous and isotropic. The time, temperature, and pressure dependent characteristics will, however, be considered in this analysis.

Another complication is that the physical properties of rock salt depend upon the testing method. The major factors which affect the testing results are the size of the test specimen, cross-sectional form of the specimen, ratio of specimen width (or diameter) to height, degree of friction on the loading surface of the specimen, confining pressure, geometry of loading, rate of loading and size of crystalline grains. In this analysis, the results of the testing procedure which are consistent with the salt pillar model's material, size, shape, and loading conditions will be used.

Experiments to describe the creep phenomena and to determine the physical properties of rock salt were rather

limited before 1959. Since that time, investigators such as Bradshaw, Serata, Obert, LeCompte, Boresi, Deere, and others have performed a number of varied experiments under different test conditions.

PREVIOUS WORK: GENERAL

Stocke and Borchert [1936] (25) performed a few two-hour test on natural polycrystalline rock salt. These test were conducted at room temperature and atmospheric pressure with axial stresses ranging from 372 psi to 3,900 psi.

Griggs [1939] (26) conducted a creep test of 42 days on a prism of a single crystal of halite loaded in uniaxial compression to 900 psi at room temperature and atmospheric pressure.

Kendall [1958] (27) carried out creep experiments on cylinders of a single crystal of halite at room temperature under confining pressures of 0 psi and 2,000 psi and with stress differences ranging from 500 psi to 4,000 psi.

Gunter and Parker [1959] (28) made some uniaxial creep tests at room temperature and with an axial stress of 2,500 psi on natural dome salt and bedded salt to determine the effects of radiation on the creep behavior of rock salt. Some structural properties at room temperature and at 200°C

for irradiated and unirradiated natural dome salt and bedded salt were also determined.

Brown and Jessen [1959] (29) studied the effects of pressure and temperature on a 2 inch, cylindrical cavity contained in a 6 inch long by 6 inch diameter salt core under triaxial pressure conditions. They determined rates of closure of these cavities under axial stresses of 1,000 psi to 8,000 psi and temperatures of 32°C to 204°C.

Serata and Gloyna's work [1959] (30) on the mechanical properties of rock salt was the most extensive up to that time. Except for a few runs with synthetic single crystals, most of their work was carried out on fine-grained natural polycrystalline rock salt. They presented a theoretical analysis of stress distribution around various forms of cavities. Experiments were conducted in the laboratory and in a salt mine to investigate the strength of these cavities. Using uniaxial compression, they investigated the following properties of rock salt: strength, Young's Modulus, Poisson's ratio, and strain-hardening. They also studied the effects of triaxial compression on the strength of rock salt from various test data and the effects of temperature and pressure on the creep rates.

Serata and Gloyna [1960] (31) followed their earlier work with a discussion of the theoretical principles of

structural stability of underground salt cavities and of the significance of the principles as they relate to other cavities. They applied the theory of plasticity to the evaluation of stress and strain conditions of salt cavities. The concept of a yielded zone which develops around the cavities was introduced, and a theoretical development of the extent and stress distribution of the zone was illustrated through the use of ideal spherical and cylindrical cavities under uniform triaxial compression. Application of the concept to actual conditions such as cavity irregularities, brittleness of formation, and nonhydrostatic loading was also discussed.

LeCompte [1964] (24) investigated the effects of temperature to 300°C, confining pressures to 14,500 psi, stress difference to 2,000 psi, and different grain sizes on the creep behavior of rock salt. These creep test were carried out on artificial polycrystalline rock salt specimens and on one single crystal. In this study and in an earlier one [1960] (34), he fitted the equation $\epsilon = A + Bt^n$ to his creep data and experimentally evaluated the constants A, B, and n for different temperatures and confining pressures.

PREVIOUS WORK: "PROJECT DRIBBLE"

With Deere as consultant to Holmes and Narver, Inc., who represented the AEC, a comprehensive test program, "Project Dribble," was outlined for determining the significant physical properties of rock salt. The Engineering Laboratories, Bureau of Reclamation, United States Department of the Interior, Denver, Colorado, performed some of the triaxial test [1962] (22) at 73°F with lateral pressures ranging from zero to 5,000 psi on a series of 4 15/16 inch diameter rock salt cores from Tatum Dome near Jackson, Mississippi. The purpose of these tests was to determine shear strength characteristics in terms of the equation of Mohr's envelope. The majority of the tests [1963] (32) were performed at the United States Army Engineer Waterways Experimental Station, Corps of Engineers, Vicksburg, Mississippi. These test, on the same type core as above, included petrographic examination of cores, uniaxial compressive cyclic loading test, specific gravity, porosity, permeability and interstitial fluid determinations, nondestructive dynamic tests, and creep test of uniaxial compressive and triaxial extensive types.

Boresi and Deere [1963] (23) presented a report in which the triaxial compression tests (Bureau of Reclamation) and the creep tests (Corps of Engineers) were used in

assessing the probable behavior of the cavity to be excavated at Tatum Dome, Mississippi. By a curve fitting process, they obtained and presented the following equation relating strain, stress and time:

$$\epsilon = K \sigma^{n} t^{m} . \qquad (3.1)$$

RECENT WORK: SALT PILLAR MODELS AND "PROJECT SALT VAULT"

Serata [1964] (18) studied the triaxial properties of rocks and the underground stress field in order to establish a theoretical basis for mathematical analysis of underground openings and support systems. Rock salt of uniform quality was used as the model material in the various models of the structures to test his theoretical conclusions on the behavior of these systems. A new testing method designated the "transition test" was developed in the Michigan State University Laboratory in order to supplement the shortcomings of the conventional triaxial testing method and to provide a condition similar to an infinite continuous medium. It was used to determine the triaxial properties of the rock salt. Using a single specimen, all the following material property coefficients of a continuous rock salt medium were determined:

Young's modulus, $E = 0.86 \times 10^{6}$ psi

Poisson's ratio, $\nu = 0.16$

Octahedral shearing strength, $K_o = 1{,}500$ psi

Elastic shear modulus, $G_1 = 0.39 \times 10^6$ psi

Retarded elastic shear modulus, $G_2 = 0.0042 \times 10^6$ psi

Viscoelastic constant, $\zeta_2 = 150 \times 10^6$ psi-minutes

Viscoplastic constant, $\zeta_1 = 2{,}000 \times 10^6$ psi-minutes

Assuming five fundamental property coefficients for rocks, G_1, G_2, ζ_1, ζ_2, and K_o, a five-element time-dependent mechanical model of the triaxial behavior of the material was presented.

The effects of the individual factors which influence the physical properties of rock salt in testing procedures were investigated in order to design laboratory models of underground structures which were free from these influences. A model of an underground cylindrical opening was developed, and its behavior was in good agreement with the proposed theory and with field observations conducted in various salt mines. This led to the development of models for underground supporting systems. A square pillar model with confined continuous medium on both ends of the pillar (Type D specimen of Chapter II) was thus developed to simulate the natural conditions of a mine pillar. Its behavior was also in good agreement with the proposed theory and with field observations.

Serata concluded that the deformation of the pillar consisted of three independent components of elastic, viscoelastic, and viscoplastic deformations, and that the individual deformations associated with each component could be analyzed by the theory developed with the property coefficients obtained and with the initial underground stress field. The model pillar was also used for studying the long-term behavior of a mine pillar in which the time-dependent deformation was expressed by

$$\frac{d\varepsilon_{z_o}}{dt} = \frac{\left(\sigma_{z_o} - \sigma_{LA}\right)}{3\,\tau_o}\left[\frac{\tau_i - K_o}{\zeta_1}\cdot e^{-\left(G_1/\zeta_1\right)^t} + \frac{\tau_o}{\zeta_2}\cdot e^{-\left(G_2/\zeta_2\right)^t}\right]. \tag{3.2}$$

Equation (3.2) is thus a separation into two exponential components of the effects of viscoplasticity and viscoelasticity.

Serata also proposed a mechanical model for rock salt and is shown in Figure 3.1.

Obert [1964] (19) investigated the effects of specimen shape and end constraints on the strength and deformational behavior of salt and trona specimens. From these preliminary tests, he developed a pillar model that has proven

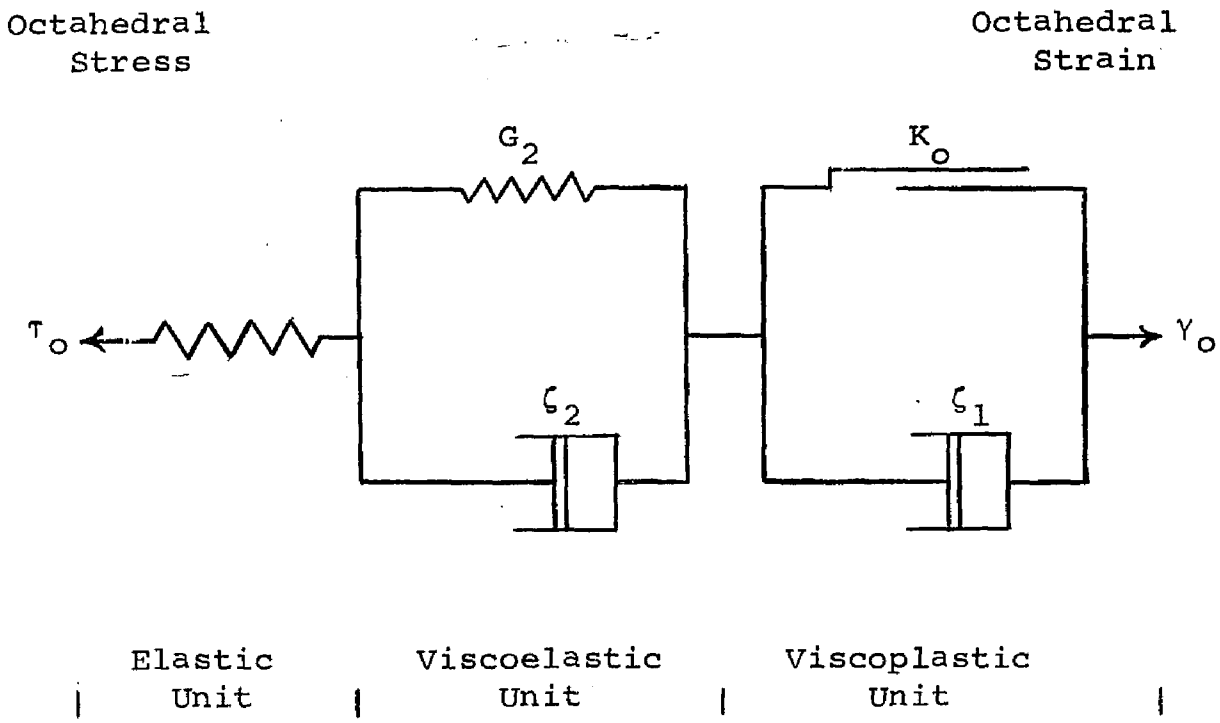

Figure 3.1. Mechanical Model of Rock Salt
(by Serata)

to be realistically related to its prototype in the mine and which has been adopted as the standard test pillar model (15,16,20,21). He then studied the strength and deformational behavior of pillar models made from salt, potash, and trona tested under constant applied loads at ambient temperature. This pillar model was the one used by Bradshaw and associates in their model studies connected with "Project Salt Vault" and is the one considered in this study (Figure 2.3).

Obert also performed creep tests with this pillar model in which he used a D/H ratio of 4 and a constraining ring thickness of 3/4 inch. He fitted to the data from the creep tests a general expression of the form

$$\varepsilon_{z_o} = A + Bt + Cf(t), \qquad (3.3)$$

where: $A = \frac{\sigma_{z_o}}{E_m}$, elastic strain

$B = \frac{\sigma_{z_o}}{3\eta_m}$, steady-state creep

$C = \frac{\sigma_{z_o}}{E_k}$

$f(t) = (1 - e^{-E_k t/3\eta_k})$, initial or transient-creep/C.

The mechanical model corresponding to this expression is presented in Figure 3.2. He found that although Equation 3.3 could be fitted to any given creep data by proper selection of the constants, no set of constants would provide a fit for the family of curves for any rock type, primarily because $3\eta_m$ was not constant for different values of σ_{z_o}. For a family of curves, he found that the steady-state strain rate $\dot{\epsilon}_{z_{o_m}}$ could be expressed by

$$\dot{\epsilon}_{z_{o_m}} = D\,\sigma_{z_o}^{n} \tag{3.4}$$

where for Kansas salt, n = 3.0 for σ_{z_o} = 4,000 psi to 10,000 psi and where the "in situ" pillar stress can be reasonably approximated from the depth and extraction ratio.

Bradshaw and associates [1964] (21) at the request of the Oak Ridge National Laboratory were furnished data by L. Obert of the Applied Physics Laboratory of the United States Bureau of Mines on a series of creep test on Obert's salt pillar model. The results of these tests were compared with actual measurements in salt mines in order to gain more information on the design parameters involved in "Project Salt Vault". Obert performed 1,000 hour creep tests at ambient temperature on the salt pillar models of

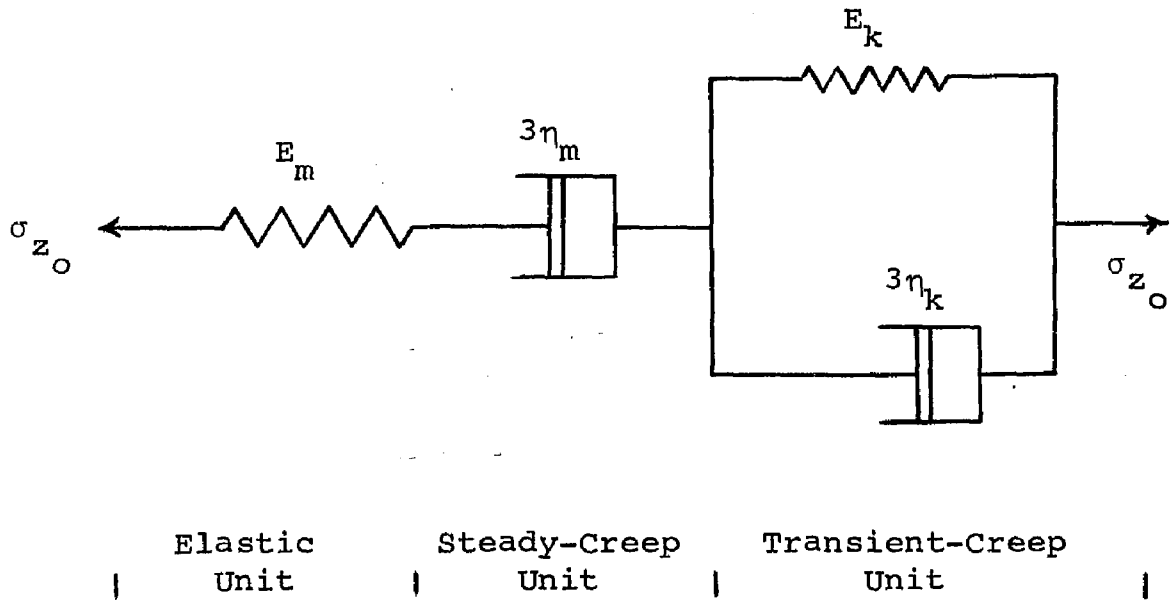

Figure 3.2. Mechanical Model of Rock Salt (by Obert)

D/H ratio of 4 and with average pillar stresses of 4,5,6, 7,8,10, and 12,000 psi. Vertical shortening of the pillars, as a function of time and stress, was measured by means of the two dial gauges attached to the steel restraining rings of the pillar model. Bradshaw and associates plotted creep rate vs. time from Obert's cumulative deformation curves by taking their tangents. They then fitted to these curves an equation of the form

$$\dot{\epsilon}_{z_o} = B\, \sigma_{z_o}^{m}\, t^{n} . \qquad (3.5)$$

It was found that a reasonable fit was obtained with

$$\dot{\epsilon}_{z_o} = 9 \times 10^{-8}\, \sigma_{z_o}^{3.1}\, t^{-0.6}\ \mu \text{ in.in.}^{-1} \text{ day}^{-1} \qquad (3.6)$$

They observed that the value of m was in reasonable agreement with those obtained by the USBM using salt samples from other mines, but that the value of n differed significantly. However, the use of the above equation to extrapolate the creep rate out to 70 years produced predicted creep rates which were in good agreement with those actually measured in the mine from which the samples came. Therefore, they concluded that salt from one mine may have different mechanical properties from salt in other mines.

Bradshaw and associates [1965-1967] (15,16,20) after having obtained predicted creep rates, which were in good

agreement with the creep-closure rates measured in the Kansas mines since 1959, extended the model test to elevated temperatures. They studied the behavior of the salt pillar models at temperatures ranging up to 200°C and stresses up to 10,000 psi. A sizeable increase in the deformation of the pillars was observed with increasing load, but, even more significant was the greatly accelerated creep rates of the salt at the elevated temperatures. Cavity closure vs. time curves at 22.5°C, 60°C, and 100°C for loads of 4,000 psi and 6,000 psi were plotted. All curves were in general similar in shape, exhibiting an initial high creep rate that decreased with time and continued to do so in tests of duration in excess of 5,000 hours. These curves gave support to a previously developed hypothesis (33) that the effect of elevating the temperature is effectively the same as that of increasing the average pillar stress and that the relationship between creep rate and axial stress follows the same power law regardless of temperature. However, it was observed that at temperatures of 100°C and above, the deformational behavior of the models departs somewhat from that produced by increased stress.

To the data obtained by Bradshaw and associates at the Oak Ridge National Laboratory, the following approximate

empirical equations were fitted for times from 10 hours on

$$\dot{\epsilon}_{z_o} = 9.2 \times 10^{-36} T^{10.9} \sigma_{z_o}^{3.2} t^{0.35} + A \qquad (3.7)$$

$$\dot{\epsilon}_{z_o} = 3.2 \times 10^{-36} T^{10.9} \sigma_{z_o}^{3.2} t^{-0.65} \qquad (3.8)$$

CHAPTER IV

THE FINITE ELEMENT METHOD

INTRODUCTION

The stress analysis of some of the present day complex structures of arbitrary shape, subject to thermal and mechanical loads, is not only of considerable academic interest, but in some cases, practical and necessary. In some of these problems, the governing differential equations have been known for many years, but closed form solutions have been obtained for only a limited number of severely idealized situations. Thus, the stress analyst must rely on experimental and/or numerical techniques. With the rapid development of digital computers and with the associated advance in numerical procedures, such as the one considered here, the expensive experimental models now often used in design of structures are rapidly becoming replaced by more economic computation.

Before numerical, computer-based solutions of real problems dealing with complex continua can be solved, it is necessary to limit their infinite degrees of freedom to a finite, although sometimes large, number of unknowns. The most popular of the numerical techniques using this

process of discretization has been the finite difference method. However, for some problems such as structures of composite materials or of arbitrary geometry, this procedure is difficult to apply. An alternative approach, that of finite elements, appears to offer considerable advantages and its relatively simple logic makes it ideally suited for the computer. Thus, this will be the numerical solution used in the analysis of the salt core and restraining steel ring of the axi-symmetric salt pillar model considered in this study.

Review of Literature

The finite-element method was originally developed in the aircraft industry and was introduced as a method of direct structural analysis (35). Since that time, it has been the subject of investigation by many workers interested in approximate solutions of elasto-static boundary value problems. The method has proven to be extremely effective for the treatment of problems in plane stress and plane strain (36-41), and several computer programs for solutions of plane elasticity problems are now in existence (38-40).

On a smaller scale, the applicability of the method to plate and shell bending problems has been demonstrated (42-45) and impressive results were obtained in the analysis

of axi-symmetric shells approximated by a series of truncated cone elements (45,46). Recently, this procedure was recognized to be equivalent to the well known Rayleigh-Ritz procedure which when applied to the same problem resulted in exactly the same formulation as that achieved previously by the structural approach (41,47,48). Thus, this procedure was extended to a variety of physical problems in which an 'extremum' principle exists (48-52). Although the general concept is clearly applicable to the analysis of three-dimensional solids, only preliminary investigations of this type have been reported (37,53-55).

Recently, the finite element method was applied to the structural analysis of axi-symmetric solids with considerable success (56-58). Another recent extension of the method has been in the area of non-linear problems, where plasticity, creep, and large deformations are considered (37,48,59,60).

Advantages of the Finite Element Method

The advantages of the finite element method in comparison to other numerical approaches are numerous. Unlike the finite difference method which is difficult to apply for structures of arbitrary geometry or of composite materials, the finite element method is completely general

with respect to geometry and material properties. Complex bodies composed of many different materials are easily represented. Since anisotropic materials are automatically included in the formulation, filament structures are readily handled. The shape of the element can be chosen to best fit the particular problem considered and the size of these elements can be varied in accordance with the anticipated stress gradients. Displacement or stress boundary conditions may be specified at any node (or nodal circle) within the finite element system. Arbitrary thermal, mechanical, and acceleration loads are possible. Mathematically, it can be shown that the method converges to the exact solution as the number of elements is increased (44,61); therefore, any desired degree of accuracy may be theoretically obtained. In addition, the finite element approach generates equilibrium equations which produce a symmetric, positive-definite matrix which may be placed in band form and solved with a minimum of computer storage and time. With the recent recognition of this procedure as an equivalent Rayleigh-Ritz procedure, the method now has a much broader basis which permits applications to be extended to almost all problems where a variational formulation is possible. In addition, procedures have been suggested for this method which allows extension into the area of non-linear problems, thereby including plasticity, creep, and large deformations.

Concept of Analysis

The numerical analysis is based upon finding an alternative form of the governing equations which is easier to solve than the governing differential equations of the continuous solid. The discretization process reduces the problem from solving a system of differential equations to solving an equivalent set of algebraic equations. Therefore, the ultimate goal is to derive the governing equations of the idealized solid.

The concept of finite elements, as originally introduced by Turner et al. (35), handles the problem of discretization by assuming that the real continuum is divided into a finite number of discrete structural elements interconnected only at a finite number of joints or nodal points at which some fictious forces, representative of the distributed stresses acting on the element boundaries, are introduced. The finite elements are formed by figuratively cutting the original continuum into a number of appropriately shaped pieces, retaining in the elements the properties of the original material. In the analysis, these assumed structural elements are entirely equivalent to the components of an ordinary framed structure. Thus, the analysis process consists merely in the normal operations of satisfying compatibility and equilibrium conditions

at the nodal points, using any standard structural analysis procedure.

In practice, the displacement formulation (36,41) of structural analysis generally has been found most convenient for treating finite element idealizations of elastic continua, and this will be the method used in this analysis. Thus, in summary, the finite element analysis may be viewed as a generalization of structural analysis theory that makes possible the analysis of two- and three-dimensional elastic continua by the same procedure used in the analysis of ordinary framed structures.

The Finite Element

Several types of elements may be used in the representation of a structure. In the plane stress analysis of a thin slice, the most frequently used element is the triangular shape element, e, as defined by the nodes i, j, and m numbered in counter-clockwise order and by the straight line boundaries as indicated by Figure 4.1. In the finite element approximation of axi-symmetric solids, the continuous structure is replaced by a system of axi-symmetric elements which are interconnected at circumferential joints or nodal circles. In the axi-symmetric stress analysis, which is mathematically two-dimensional in nature, the

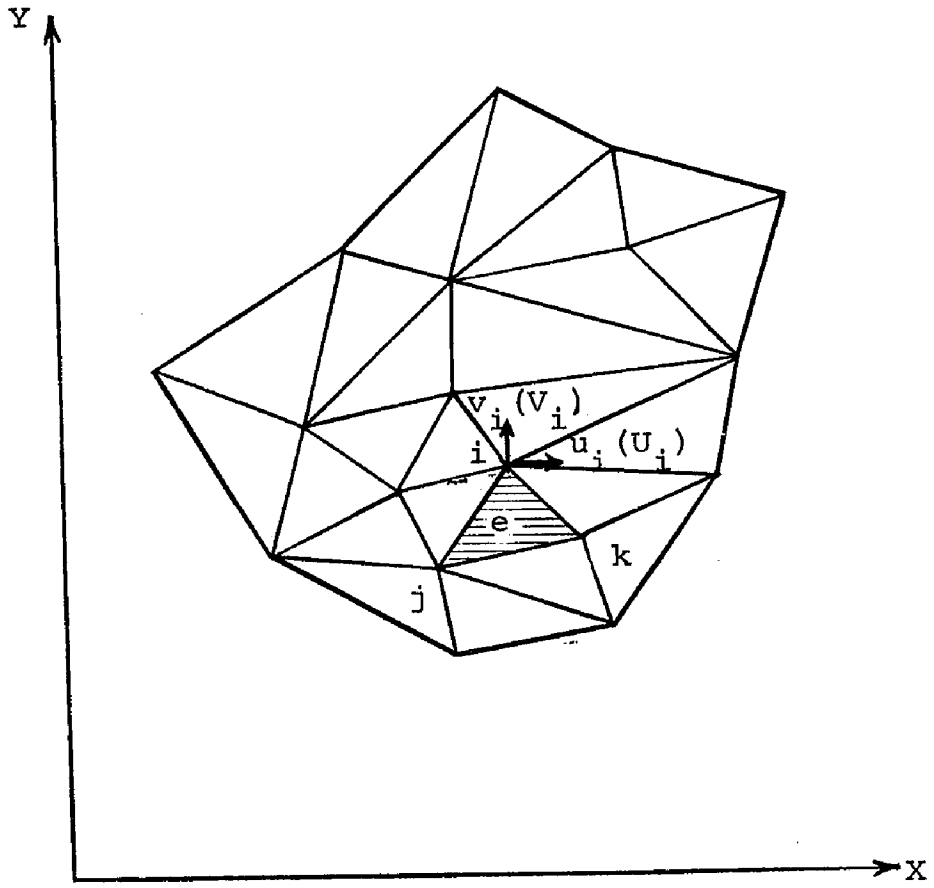

Figure 4.1. A Plane Stress Region Divided Into Triangular Shaped Elements

triangular shaped element of the plane stress analysis becomes the cross section of the ring elements. (See Figure 4.2 and Figure 4.3.) It should be recognized that the finite elements that are shown here are actually complete rings in the third dimension (extending through the angle $\theta = 2\pi$), and that the nodal 'points' at which they are connected are in reality circular lines in plan view. Otherwise, the system shown is entirely equivalent to a finite element plane stress or plane strain problem.

The Axi-Symmetric 'Two-Dimensional' Problem

The axi-symmetric structure to be considered in this analysis is shown in Figure 4.2-A. Because of the symmetry of the structure and its loading about the vertical Z axis, the two components of displacement in any plane sectioning the body along its axis of symmetry define completely the state of strain and therefore, the state of stress. Thus, displacements of the system will be developed only in the radial and vertical directions; tangential displacements do not exist. Furthermore, stresses and strains do not vary in the tangential direction.

From a mathematical point of view, this class of system is two-dimensional in nature and may be represented as shown in Figure 4.2-B. An appropriate idealization of

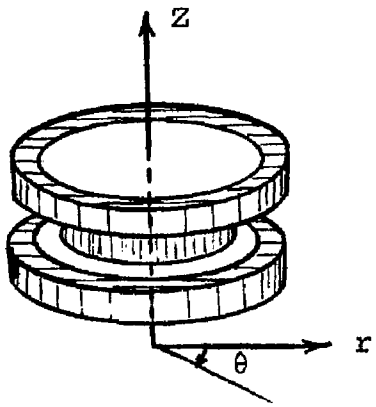

A. Axi-Symmetric Solid

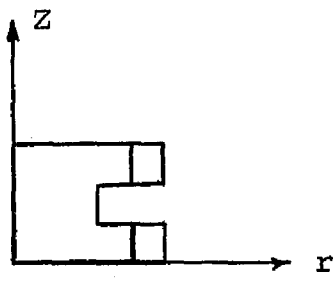

B. Two-Dimensional View of Axi-Symmetric Continuum

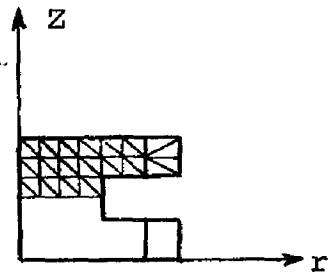

C. Two-Dimensional View of Finite Element Idealization of Axi-Symmetric Continuum

Figure 4.2. Axi-Symmetric Idealization

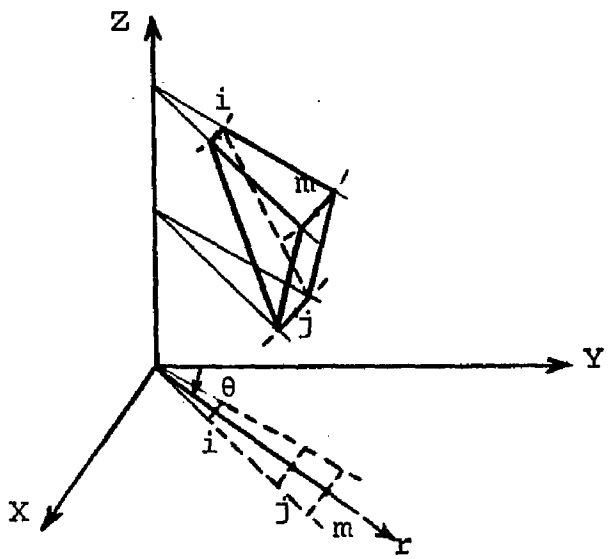

A. Typical Triangular Axi-Symmetric Element

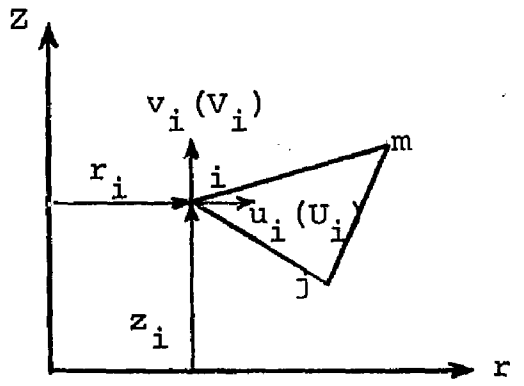

B. Two-Dimension View of Axi-Symmetric Element

Figure 4.3. Axi-Symmetric Elements

this 'two-dimensional' system, using triangular finite elements, is shown in Figure 4.2-C. Thus, the system shown is entirely equivalent in degree of mathematical complexity to a finite element plane stress or plane strain problem, and standard plane stress computer programs may be adapted to the solution of this class of system. It is necessary merely to develop stiffness and load matrices appropriate to the 'ring type' finite elements, taking proper account of the fact that tangential stresses and strains result from radial displacements in the axi-symmetric system.

The Computer Program

Finite element plane stress computer programs provide a significant contribution to the analysis of axi-symmetric solids by finite elements since these programs can be modified to solve the latter problems. Thus, some of the programming efforts represented by existing plane stress programs can be incorporated into an axi-symmetric analysis program.

The general finite element analysis program can be divided into three phases:

1. The element stiffnesses and the element loads are computed.
2. The stiffness matrix and the load matrix for the

complete structure are formed (by superposing individual element effects) and the resulting nodal displacements are computed.

3. The element stresses are evaluated.

In the axi-symmetric analysis, the plane stress program must be modified by substituting into phase one the appropriate axi-symmetric element stiffness and load subroutines in place of the corresponding plane stress routines. The assembly and solution of the 'two-dimensional' equilibrium equations of phase two are left unchanged. Phase three is unchanged in principle; the stresses in each element, e, are still calculated as in the plane stress program. However, the displacement matrix now represents the nodal displacements associated with the axi-symmetric element. Thus, it is necessary to refer to the appropriate axi-symmetric expressions for each of these matrices, but no modification of the program is required.

The input data required for the axi-symmetric analysis and for the plane stress analysis is identical. The physical property data concerning each finite element, the geometric co-ordinates of each nodal point, the loading associated with each element, and certain miscellaneous items concerning boundary conditions, etc., must be supplied in both computer programs.

The output data is equivalent to that obtained from the plane stress program except that one additional item is obtained; the stress in the θ-direction.

Convergence Criteria

The dependability of the finite element method is strongly controlled by the assumed shape functions since they limit the infinite degrees of freedom of the system. Thus, the exact solution may never be reached, irrespective of the fineness of the mesh. To insure convergence to the correct result, certain simple requirements have to be satisfied (44,48,56,57).

1. The assumed displacements must be continuous over the elements and must be continuously differentiable up to and including the highest derivative required in the formulation of the element strains.

2. The deformation between adjacent elements must be compatible since no gaps or overlaps are permitted in the deformed finite element system. With nodal displacements selected as generalized displacements, this requirement is easily satisfied. The displacements along any side of the element are selected so that they depend only on the displacements at the nodes bounding the side. For triangular two-dimensional elements, this boundary compatibility

condition is satisfied by assuming displacements that vary linearly in each direction. The edges of each element will then displace as straight lines, and no gaps can develop between them as long as nodal continuity is maintained. If complete compatibility can be maintained (internally and on the boundary), then the finite element method can be demonstrated to converge to these exact results as the mesh size is reduced (44,61).

3. The displacement function must be a linear function of the generalized displacements. This is necessary so that the load-displacement equation will be linear. In the displacement expression, as a consequence, the coefficient of the nodal displacement must be non-dimensional so as to satisfy dimensional requirements.

4. The displacement function must be of such a form that if nodal displacements are compatible with a constant strain condition, such constant strain will, in fact, be obtained. This incorporates the requirement that it does not permit straining of an element to occur when the nodal displacements are caused by a rigid body displacement, since rigid body displacements are a particular case of constant strain - with a value of zero.

It should be noted that all of the above stipulations are independent of element shape, material characteristics, and the smallness of strains and displacements.

Alternate Energy Approach

Although the 'structural analysis' approach is direct and physically interpretable, the concept of replacing the distributed stresses on the element boundaries by 'equivalent' static loads raised some questions of the exact physical conditions that were being imposed and what approximations were, in fact, made by the process. Recently, this problem was approached via an alternate route which led to the recognition of the equivalence of the finite element-structural analysis approach with a minimization process (41,47,48). Thus was shown the similarity of the formulation with the well-known Rayleigh-Ritz methods.

The finite element method based on energy principles differs from the usual Rayleigh-Ritz procedure in the choice of displacement functions. Instead of the smooth displacement function of the Rayleigh-Ritz method, extending over the entire solid, the finite element method uses many displacement functions, each restricted to a small part of the solid. Also, contrary to the Rayleigh-Ritz procedure, quantities with obvious physical meaning are chosen as the variable parameters. This allows the analyst to maintain at all times a direct physical 'contact' with the real problem being examined.

In the minimization process, it was shown that if the system of displacements was defined throughout the structure by the element displacement functions, with the nodal displacements acting as undetermined parameters, then the procedure of minimization of the total potential energy of the system results in precisely the same formulation as that achieved by the 'structural analysis' approach. Therefore, there now exist two equivalent, alternate formulations. In the first, an equation is written and its direct solution attempted. In the second, the problem is to find a function minimizing a certain specified functional over the field involved.

A list of but a few of the many problems encountered in engineering practice which can be solved by finite element-energy method is:

heat conduction,

bending of prismatic beams,

seepage through porous media,

irrotational flow of ideal fluids,

distribution of electric (or magnetic) potential,

torsion of prismatic shafts, etc.

Thus was opened the door of application of finite elements beyond that of structural analysis to the much wider range of almost all problems where a variational formulation is possible.

METHOD OF ANALYSIS

General Steps

Using the displacement method of the 'structural analysis' procedure, the finite element analysis procedure can be summarized as follows:

1. Idealization. The axi-symmetric elastic continuum is separated by imaginary surfaces into a system of triangular shape ring elements which are then reduced to equivalent triangular plane elements for the mathematical analysis.

2. Element Analysis. Assuming that the triangular elements are interconnected at their three vertex nodal points, a displacement function is used to define uniquely the state of displacement within each finite element in terms of its three nodal displacements. Thus, the state of strain within each element is defined in terms of its nodal displacements by the displacement functions, and together with any initial strain and the elastic properties of the material, so is the state of stress throughout the element and, hence, also on its boundaries. A system of forces concentrated at the nodes and equilibrating the boundary stresses and any distributed loads is determined. This results in the stiffness matrices which relate the forces developed at the element nodal points to the

corresponding element displacements.

3. Assembly of Elements. The nodal stiffness matrix for the complete structure is evaluated by superposition of the individual element stiffnesses contributing to each nodal point force. This involves only simple matrix addition when all element stiffnesses have been expressed in the same co-ordinate system.

4. Displacement Analysis. The nodal equilibrium equations, expressed by means of the structural stiffness matrix, are solved for the nodal displacements which resulted from the applied nodal forces.

5. Stress Analysis. The element stresses resulting from the computed nodal displacements are evaluated by means of element stress matrices.

6. Non-linear Creep Analysis. The above procedure is extended into the non-linear range by iterative and step-by-step procedures modified to include creep strains.

Mathematical Procedure

The finite element analysis, which was summarized in general terms will now be presented in more detailed mathematical form. Using the method presented by Zienkiewicz (48), the direct formulation of the finite element characteristics will be undertaken first. A general solution of

a linear axi-symmetric elastic problem will be presented, which will then be extended into the non-linear range and modified to include creep strains.

1. Displacement Function. Using a typical 'plane' finite element, e, defined as shown in Figure 4.3-B, with nodes i, j, and m numbered in an counter-clockwise order, the nodal displacement at node i is defined by its two components as

$$\{\delta_i\} = \begin{Bmatrix} u_i \\ v_i \end{Bmatrix} \tag{4.1}$$

and the six components of element displacements by the vector

$$\{\delta\}^e = \begin{Bmatrix} \delta_i \\ \delta_j \\ \delta_m \end{Bmatrix} . \tag{4.2}$$

The displacements within an element have to be uniquely defined by these six values (one value for each of the two degrees of freedom for each of the three nodal points). The simplest representation is given by two linear polynomials

$$\begin{aligned} u &= \alpha_1 + \alpha_2 r + \alpha_3 z \\ v &= \alpha_4 + \alpha_5 r + \alpha_6 z . \end{aligned} \tag{4.3}$$

The six constants α are evaluated by solving the two sets

of three simultaneous equations which arise when the nodal co-ordinates are inserted and the displacements equated to the appropriate nodal displacements. Writing, for example, for the radial displacements

$$\begin{aligned} u_i &= \alpha_1 + \alpha_2 r_i + \alpha_3 z_i \\ u_j &= \alpha_1 + \alpha_2 r_j + \alpha_3 z_j \\ u_m &= \alpha_1 + \alpha_2 r_m + \alpha_3 z_m \ , \end{aligned} \tag{4.4}$$

α_1, α_2, and α_3 are solved for in terms of displacements u_i, u_j, and u_m to obtain

$$u = \frac{1}{2\Delta}\left[\left(a_i + b_i r + c_i z\right) u_i + \left(a_j + b_j r + c_j z\right) u_j + \left(a_m + b_m r + c_m z\right) u_m\right] , \tag{4.5}$$

in which

$$\begin{aligned} a_i &= r_j z_m - r_m z_j \\ b_i &= z_j - z_m = z_{jm} \\ c_i &= r_m - r_j = r_{mj} \ . \end{aligned} \tag{4.5a}$$

The other coefficients are obtained by a cyclic permutation of subscripts in the order i, j, m, and

$$2\Delta = \det \begin{vmatrix} 1 & r_i & z_i \\ 1 & r_j & z_j \\ 1 & r_m & z_m \end{vmatrix} = 2(\text{area of triangle ijm}) \tag{4.6}$$

In a like manner, the equations for the vertical displacement yield

$$v = \frac{1}{2\Delta}\left[\left(a_i + b_i r + c_i z\right)v_i + \left(a_j + b_j r + c_j z\right)v_j + \left(a_m + b_m r + c_m z\right)v_m\right] . \quad (4.7)$$

In general, the standard matrix form for the displacement field is given by

$$\{f\}^e = [N]^e \{\delta\}^e , \quad (4.8)$$

and using Equation 4.5 and Equation 4.7,

$$\{f\}^e = \begin{Bmatrix} u(r,z) \\ v(r,z) \end{Bmatrix}^e = \left[I\ N_i,\ I\ N_j,\ I\ N_m\right] \{\delta\}^e , \quad (4.9)$$

where I is a 2 x 2 identity matrix, and

$$N_i = \left(a_i + b_i r + c_i z\right)/2\Delta, \text{ etc.} \quad (4.10)$$

Thus,

$$\begin{Bmatrix} u(r,z) \\ v(r,z) \end{Bmatrix}^e = \frac{1}{2\Delta}\begin{bmatrix} a_i+b_i r+c_i z, & 0, & a_j+b_j r+c_j z, \\ 0, & a_i+b_i r+c_i z, & 0, \\ 0, & a_m+b_m r+c_m z, & 0 \\ a_j+b_j r+c_j z, & 0, & a_m+b_m r+c_m z \end{bmatrix} \begin{Bmatrix} u_i \\ v_i \\ u_j \\ v_j \\ u_m \\ v_m \end{Bmatrix} \quad (4.11)$$

To verify that this choice of displacement function satisfies the basic requirements listed in an earlier section on convergence criteria, the displacements u and v are first investigated in their original form,

$$u = \alpha_1 + \alpha_2 r + \alpha_3 z$$
$$v = \alpha_4 + \alpha_5 r + \alpha_6 z \ , \tag{4.3}$$

where $\alpha_1, \ldots, \alpha_6$ are constant. These linear polynomials are obviously continuous as are their first partial derivatives. Thus, the first requirement is satisfied. The second requirement, for the special case of triangular two-dimensional elements, is that the displacement vary linearly in each direction. Again, this requirement is satisfied by these two linear polynomials. The third requirement is therefore also satisfied since, as required, the displacement function was chosen as linear functions of the displacements.

The fourth requirement is discussed in the next section on strains, where it is illustrated that constant strains are in fact obtained with a constant condition.

2. Strain. The total strain at any point within the element can be defined by the components which contribute to internal work. For the axi-symmetric system, these are the four non-zero components which are illustrated along

with the associated stresses in Figure 4.4. In terms of displacements, these strains are given by

$$\{\epsilon\}^e = \begin{Bmatrix} \epsilon_z \\ \epsilon_r \\ \epsilon_\theta \\ \gamma_{rz} \end{Bmatrix}^e = \begin{Bmatrix} \partial v/\partial z \\ \partial u/\partial r \\ u/r \\ \partial u/\partial z + \partial v/\partial r \end{Bmatrix}^e . \quad (4.12)$$

Using the displacement function defined by Equation 4.10, Equation 4.12 can be written in general as

$$\{\epsilon\}^e = [B]^e \{\delta\}^e , \quad (4.13)$$

and for the axi-symmetric problem as

$$\{\epsilon\}^e = [B_i, B_j, B_m] \{\delta\}^e , \quad (4.14)$$

in which

$$[B_i] = \frac{1}{2\Delta} \begin{bmatrix} 0 & , & c_i \\ b_i & , & 0 \\ a_i/r + b_i + c_i z/r & , & 0 \\ c_i & , & b_i \end{bmatrix} , \text{ etc.} \quad (4.15)$$

Thus,

$$\begin{Bmatrix} \epsilon_z \\ \epsilon_r \\ \epsilon_\theta \\ \gamma_{rz} \end{Bmatrix}^e = \frac{1}{2\Delta} \begin{bmatrix} 0 & , & c_i & , & 0 & , & c_j & , \\ b_i & , & 0 & , & b_j & , & 0 & , \\ a_i/r+b_i+c_i z/r & , & 0 & , & a_j/r+b_j+c_j z/r & , & 0 & , \\ c_i & , & b_i & , & c_j & , & b_j & , \end{bmatrix}$$

$$\begin{bmatrix} 0 & , & c_m \\ b_m & , & 0 \\ a_m/r+b_m+c_m z/r & , & 0 \\ c_m & , & b_m \end{bmatrix} \begin{Bmatrix} u_i \\ v_i \\ u_j \\ v_j \\ u_m \\ v_m \end{Bmatrix} . \quad (4.16)$$

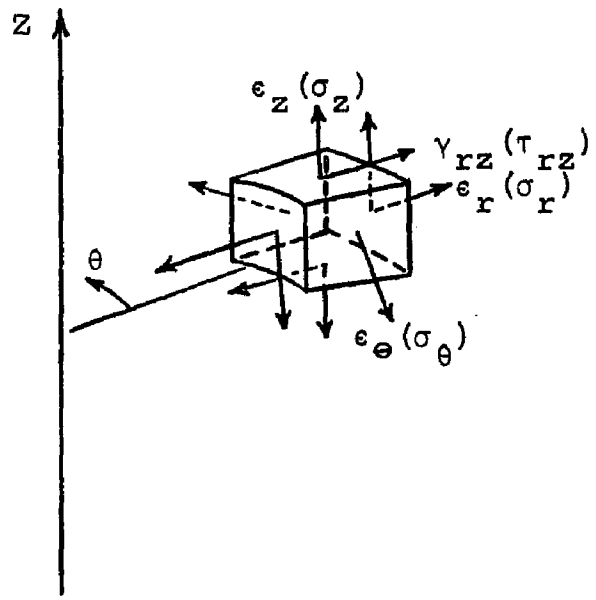

Figure 4.4. Strains and Stresses in Axi-Symmetric Solids

Since the matrix $[B]^e$ involves the co-ordinates r and z, the strains are not constant within the element as in the plane stress or plane strain case. This is due to the ϵ_θ term. Note, however, that if u is proportional to r, then the strains will be constant. As this is the only state of displacement coincident with a constant strain condition, it is clear that the displacement function satisfies the fourth convergence requirement.

3. Initial Strain (thermal strain). Initial strains are those that are independent of stress, and may be due to many causes. In general, for the axi-symmetric problem, four independent components of initial strain can result and are given by

$$\{\epsilon_o\}^e = \begin{Bmatrix} \epsilon_{zo} \\ \epsilon_{ro} \\ \epsilon_{\theta o} \\ \gamma_{rzo} \end{Bmatrix}^e . \qquad (4.17)$$

Although these initial strains may, in general, depend on the position within the element, they are usually defined by average, constant values, and this procedure will be used in this analysis.

The most frequently encountered case of initial strain is that due to a thermal expansion, which for the isotropic material considered here yields

$$\{\epsilon_o\}^e = \begin{Bmatrix} \alpha\theta^e \\ \alpha\theta^e \\ \alpha\theta^e \\ 0 \end{Bmatrix} , \qquad (4.18)$$

where θ^e is the average temperature rise in the element and α is the coefficient of thermal expansion.

In the generalization of the finite element method to account for creep in non-linear elastic problems, this initial strain in the 'incremental-initial strain' procedure is assumed to be composed of two parts. For each increment of time, the initial strain increment is assumed to be composed of both a thermal and a creep component, i.e.,

$$\Delta\{\epsilon_o\} = \Delta\{\epsilon_t\} + \Delta\{\epsilon_c\} . \qquad (4.19)$$

4. Elasticity Matrix. Assuming general elastic behaviour, the relationship between stresses and strains will be linear and of the general form

$$\{\sigma\}^e = [D]^e \left(\{\epsilon\}^e - \{\epsilon_o\}^e\right) , \qquad (4.20)$$

where $[D]^e$ is an elasticity matrix containing the appropriate material properties of the general element, e. For the axi-symmetric problem, this becomes

$$\begin{Bmatrix} \sigma_z \\ \sigma_r \\ \sigma_\theta \\ \tau_{rz} \end{Bmatrix}^e = [D]^e \left(\begin{Bmatrix} \epsilon_z \\ \epsilon_r \\ \epsilon_\theta \\ \gamma_{rz} \end{Bmatrix}^e - \begin{Bmatrix} \epsilon_{zo} \\ \epsilon_{ro} \\ \epsilon_{\theta o} \\ \gamma_{rzo} \end{Bmatrix}^e \right) . \qquad (4.21)$$

The elasticity matrix $[D]^e$ is derived by writing for the isotropic three-dimensional case considered here (ignoring the initial strains for convenience)

$$\begin{aligned}
\epsilon_z &= \frac{1}{E}\left(\sigma_z - \nu\left(\sigma_r + \sigma_\theta\right)\right) \\
\epsilon_r &= \frac{1}{E}\left(\sigma_r - \nu\left(\sigma_\theta + \sigma_z\right)\right) \\
\epsilon_\theta &= \frac{1}{E}\left(\sigma_\theta - \nu\left(\sigma_z + \sigma_r\right)\right) \\
\gamma_{rz} &= \frac{2(1+\nu)}{E}\left(\tau_{zr}\right),
\end{aligned} \tag{4.22}$$

and then solving for the stresses. This yields

$$\left[D\right]^e = \frac{E(1-\nu)}{(1+\nu)(1-2\nu)} \begin{bmatrix} 1 & \frac{\nu}{1-\nu} & \frac{\nu}{1-\nu} & 0 \\ & 1 & \frac{\nu}{1-\nu} & 0 \\ & & 1 & 0 \\ & \text{(symmetric)} & & \frac{1-2\nu}{2(1-\nu)} \end{bmatrix} \tag{4.23}$$

where, in general, each element may have different values for the material values E and ν.

5. The Stiffness Matrix. The stiffness matrix of the element ijm can now be computed according to the general relationship*

---

*Derivation of stiffness matrix in Appendix.

$$[k]^e = \int [B]^{e^T} [D]^e [B]^e d(vol) \ . \tag{4.24}$$

For the axi-symmetric problem, this becomes

$$[k]^e = 2\pi \int [B]^{e^T} [D]^e [B]^e r \, dr \, dz \ . \tag{4.25}$$

Since the matrix $[B]^e$ depends on the co-ordinates, the integration cannot be performed as easily as in the case of the plane stress problem. The simplest approximate procedure is to evaluate $[B]^e$ for a centroidal point

$$\begin{aligned} \bar{r} &= (r_i + r_j + r_m)/3 \\ \bar{z} &= (z_i + z_j + z_m)/3 \ , \end{aligned} \tag{4.26}$$

which gives as a first approximation

$$[k]^e \approx 2\pi \, [\bar{B}]^{e^T} [D]^e [\bar{B}]^e \, \bar{r} \, \Delta, \tag{4.27}$$

where Δ is the triangle area.

With the matrix $[B]^e$ of Equation 4.13 written as

$$\left[B\right]^e = \left[B_i, \ B_j, \ B_m\right] \tag{4.28}$$

and with $\left[B_i\right]$ given by Equation 4.15, the stiffness matrix, for computational convenience, can be written in a partitioned form as

$$[k]^e = \begin{bmatrix} k_{ii} & k_{ij} & k_{im} \\ k_{ji} & k_{jj} & k_{jm} \\ k_{mi} & k_{mj} & k_{mm} \end{bmatrix} \tag{4.29}$$

in which the 2 by 2 submatrices are built up as

$$\left[k_{rs}\right] = 2\pi \int \left[B_r\right]^T \left[D\right]^e \left[B_s\right] r \, dr \, dz \; . \tag{4.30}$$

At this stage, it is also useful to split up the submatrices $\left[B_i\right]$ into constant and variable parts

$$\left[B_i\right] = \left[\bar{B}_i\right] + \left[B_i'\right] \tag{4.31}$$

in which $\left[\bar{B}_i\right]$ is the value of $\left[B_i\right]$ at the centroid as in Equation 4.27 and $\left[B_i'\right]$ accounts for the variation from this value. Thus $\left[B_i'\right]$ is given by

$$\left[B_i'\right] = \begin{bmatrix} 0 & 0 \\ 0 & 0 \\ 1 & 0 \\ 0 & 0 \end{bmatrix} \left\{\left(a_i+c_i z\right)/r - \left(a_i+c_i \bar{z}\right)/\bar{r}\right\}/2\Delta . \tag{4.32}$$

Substituting the above expression into Equation 4.30 and noting that

$$\int \left[B_i'\right] r \, dr \, dz = [0] \; , \tag{4.33}$$

the following is obtained

$$\left[k_{rs}\right] = \left[\bar{k}_{rs}\right] + \left[k_{rs}'\right] \; , \tag{4.34}$$

in which the first term is given by

$$\left[\bar{k}_{rs}\right] = 2\pi \left[\bar{B}_r\right]^T \left[D\right]^e \left[\bar{B}_s\right] \bar{r}\, \Delta, \tag{4.35}$$

and the second term is a corrective term which is obtained from

$$\left[k_{rs}'\right] = \frac{2\pi}{(2\Delta)^2} \begin{bmatrix} 0 & 0 & 1 & 0 \\ 0 & 0 & 0 & 0 \end{bmatrix} \left[D\right]^e \begin{bmatrix} 0 & 0 \\ 0 & 0 \\ 1 & 0 \\ 0 & 0 \end{bmatrix} \cdot$$

$$\left[\int\left\{\left(a_r+c_r z\right)/r - \left(a_r+c_r \bar{z}\right)/\bar{r}\right\} \cdot \left\{\left(a_s+c_s z\right)/r \right.\right.$$

$$\left.\left. - \left(a_s+c_s \bar{z}\right)/\bar{r}\right\} r\, dr\, dz\right]. \tag{4.36}$$

If the various integrands are written in abbreviated notation

$$\begin{aligned} \int \frac{1}{r}\, dr\, dz &= \Delta I_1 \\ \int \frac{z}{r}\, dr\, dz &= \Delta I_2 \\ \int \frac{z^2}{r}\, dr\, dz &= \Delta I_3, \end{aligned} \tag{4.37}$$

then the corrective term becomes

$$\left[k_{rs}'\right] = \frac{\pi}{2\Delta} \begin{bmatrix} D_{33} & 0 \\ 0 & 0 \end{bmatrix} \left\{a_r a_s \left(I_1 - \frac{1}{\bar{r}}\right)\right. \tag{4.38}$$

$$\left. + \left(a_r c_s + a_s c_r\right)\left(I_2 - \frac{\bar{z}}{\bar{r}}\right) + c_r c_s \left(I_3 - \frac{\bar{z}^2}{\bar{r}}\right)\right\},$$

where the integrals I_1, I_2, and I_3 are evaluated explicitly in terms of the nodal co-ordinates..

6. External Nodal Forces. In the general axi-symmetric analysis, the nodal forces $\{R\}$ resulting from external loads represent a combined effect of the forces acting along the whole circumference of the circle forming the element 'node'. Thus, if $\bar{R}$ represents the radial component force per unit length of the circumference of a node (or a radius r), the external 'force' which will be introduced in the computation is

$$2\pi\ r\ \bar{R}\ . \tag{4.39a}$$

Similarly, in the axial direction, the combined effect of the axial forces is represented by

$$2\pi\ r\ \bar{Z}. \tag{4.39b}$$

Thus, in general for the axi-symmetric analysis,

$$\{R_i\} = \begin{Bmatrix} 2\pi\ r_i\ \bar{R}_i \\ 2\pi\ r_i\ \bar{Z}_i \end{Bmatrix} \tag{4.40}$$

7. Nodal Forces Due to Initial Strain. The general expression for the nodal forces due to initial strain* is

---

*See derivation of stiffness matrix in Appendix.

$$\left\{F\right\}^{e}_{\varepsilon_o} = - \int \left[B\right]^{e^T} \left[D\right]^{e} \left\{\varepsilon_o\right\}^{e} \, d(vol) \, . \qquad (4.41)$$

For the axi-symmetric analysis, this becomes

$$\left\{F\right\}^{e}_{\varepsilon_o} = - 2\pi \int \left[B\right]^{e^T} \left[D\right]^{e} \left\{\varepsilon_o\right\}^{e} \, r \, dr \, dz, \qquad (4.42)$$

and partitioning (noting that $\left[D\right]^{e} \left\{\varepsilon_o\right\}^{e}$ is constant over the element),

$$\left\{F_i\right\}_{\varepsilon_o} = - 2\pi \left(\int \left[B_i\right]^{T} r \, dr \, dz \right) \left[D\right]^{e} \left\{\varepsilon_o\right\}^{e} \, . \qquad (4.43)$$

As in the stiffness matrix determination, the approximate expression

$$\left\{\bar{F}_i\right\}_{\varepsilon_o} = - 2\pi \left[\bar{B}_i\right]^{T} \left[D\right]^{e} \left\{\varepsilon_o\right\}^{e} \bar{r} \, \Delta, \qquad (4.44)$$

together with a 'corrective' term can be used. This yields

$$\left\{F_i\right\}_{\varepsilon_o} = \left\{\bar{F}_i\right\}_{\varepsilon_o} + \left\{F_i'\right\}_{\varepsilon_o} \, . \qquad (4.45)$$

However, the corrective term is now zero since

$$\left\{F_i'\right\}_{\varepsilon_o} = 2\pi \left(\int \left[B_i'\right] r \, dr \, dz \right) \left[D\right]^{e} \left\{\varepsilon_o\right\} = 0. \qquad (4.46)$$

Therefore, this gives exactly

$$\left\{F_i\right\}_{\epsilon_o} = - 2\pi \left[\bar{B}_i\right]^T \left[D\right]^e \left\{\epsilon_o\right\}^e \bar{r}\, \Delta \,. \qquad (4.47)$$

8. Nodal Forces Due to Distributed Body Forces. The only distributed body forces (those acting on a unit volume of material within the element) in this specific axi-symmetric analysis will be that due to gravity, and in this analysis, it is insignificant and therefore, will be neglected. However, in a general problem, this contribution is written as

$$\left\{P\right\}^e = \left\{\begin{matrix} R \\ Z \end{matrix}\right\}^e , \qquad (4.48)$$

per unit volume of material in the r and z directions. The general expression for the nodal force due to distributed body forces* is

$$\left\{F\right\}_P^e = - \int \left[N\right]^{e^T} \left\{P\right\}^e d(\text{vol}). \qquad (4.49)$$

For the axi-symmetric analysis, this becomes

$$\left\{F\right\}_P^e = - 2\pi \int \left[N\right]^{e^T} \left\{\begin{matrix} R \\ Z \end{matrix}\right\}^e r\, dr\, dz, \qquad (4.50)$$

and partitioning,

$$\left\{F_i\right\}_P = - 2\pi \int \left\{\begin{matrix} R \\ Z \end{matrix}\right\} N_i\, r\, dr\, dz \,. \qquad (4.51)$$

---

*See derivation of stiffness matrix in Appendix.

Using a co-ordinate shift to the centroid of the triangular area and assuming the body forces are constant over this area,

$$\left\{\bar{F}_i\right\}_P = \left\{\bar{F}_j\right\}_P = \left\{\bar{F}_m\right\}_P = -\,2\pi \begin{Bmatrix} R \\ Z \end{Bmatrix} \frac{r\Delta}{3} \,. \tag{4.52}$$

9. Nodal Forces Due to Boundary Forces. Boundary elements, in general, are subjected to specified displacements and specified distributed external loading. The first presents no problem, but, a loading term has to be added to the nodes of the element which has a boundary face. By the virtual work consideration, this results in

$$\left\{F\right\}_b^e = -\int \left[N\right]^{e^T} \left\{g\right\} \, d(\text{area}), \tag{4.53}$$

where $\left\{g\right\}$ is the distributed external load per unit area and where the integration is taken over the boundary area of the element. For the axi-symmetric case and constant load $\left\{g\right\}$, this becomes

$$\left\{F\right\}_b^e = -\,2\pi \int \left[N\right]^{e^T} r \, dr \left\{g\right\} \,. \tag{4.54}$$

For the expression to be valid, $\left\{g\right\}$ must have the same number of components as $\left\{f\right\}$. Thus, for this particular analyses,

$$\left\{F\right\}_b^e = -\,2\pi \int \left[N\right]^{e^T} r \, dr \begin{Bmatrix} 0 \\ \sigma_z \end{Bmatrix} \,, \tag{4.55}$$

and partitioning,

$$\left\{F_i\right\}_b = - 2\pi \int N_i \, r \, dr \left\{\begin{matrix}0\\ \sigma_z\end{matrix}\right\} . \qquad (4.56)$$

In practice, an integration of this type is seldom explicitly carried out. This boundary loading is usually considered by the analyst to be represented simply by concentrated loads acting on the boundary nodes and are calculated by direct static procedures.

10. Assembly and Analysis. With the above formulae derived, the solution for nodal displacements and stresses now follows a standard structural routine. Assuming elastic behaviour of the element, the characteristic relation for the element is of the form

$$\left\{F\right\}^e = \left[k\right]^e \left\{\delta\right\}^e + \left\{F\right\}^e_{\varepsilon_o} + \left\{F\right\}^e_p + \left\{F\right\}^e_b , \qquad (4.57)$$

where $\left\{F\right\}^e$ is a matrix giving all the forces acting on the element, $[k]^e$ is defined by Equations 4.24 through 4.38, $\left\{\delta\right\}^e$ is defined by Equations 4.1 through 4.11, $\left\{F\right\}^e_{\varepsilon_o}$ represents the nodal forces required to balance any initial strain and is defined by Equations 4.41 through 4.47, $\left\{F\right\}^e_p$ represents the nodal forces required to balance any distributed loads acting on the element and is defined by Equations 4.48 through 4.52, and $\left\{F\right\}^e_b$ represents the nodal

forces required to balance distributed boundary loads and is defined by Equations 4.53 through 4.56. The first term, $[k]^e \{\delta\}^e$, represents the forces induced by displacements of the nodes.

A preliminary analysis is performed and this permits a unique definition of stresses or internal reactions at any specified point or points of the element in terms of the nodal displacements. Defining such stresses by a matrix $\{\sigma\}^e$, a relationship of the form

$$\{\sigma\}^e = [S]^e \{\delta\}^e + \{\sigma\}^e_{\epsilon_o} + \{\sigma\}^e_P + \{\sigma\}^e_b \qquad (4.58)$$

is obtained in which the last three terms are the stresses due to initial stresses, distributed element loads, and boundary loads respectively when no nodal displacement occurs.

To obtain a complete solution, the conditions of displacement compatibility and of equilibrium have to be satisfied throughout.

Any system of nodal displacements

$$\{\delta\} = \begin{Bmatrix} \delta_1 \\ \cdot \\ \cdot \\ \cdot \\ \delta_n \end{Bmatrix} , \qquad (4.59)$$

listed now for the whole structure in which all the elements participate, automatically satisfies the first condition.

As the conditions of overall equilibrium have already been satisfied within an element, all that is necessary is to establish equilibrium conditions at the nodes of the structure. The resulting equations contains the displacements as unknowns, and once these have been solved, the 'structural' problem is determined.

In a general analysis, the structure is loaded by external forces

$$\{R\} = \begin{Bmatrix} R_1 \\ \cdot \\ \cdot \\ \cdot \\ R_n \end{Bmatrix} , \qquad (4.60)$$

applied at the nodes in addition to the distributed loads applied to the individual elements. To establish the equilibrium conditions at a typical node, i, each component of R_i has, in turn, to be equated to the sum of the component forces contributed by the elements meeting at the nodes. Considering all the force components, this gives

$$\{R_i\} = \sum_e \{F_i\}^e , \qquad (4.61)$$

where the summation, $\sum_e$, is taken over all the elements of the structure. Substitution of Equation 4.57 for $\{F_i\}^e$

and using the submatrices of the stiffness matrix of Equation 4.29 to involve only the appropriate forces $\{F_i\}^e$, Equation 4.61 becomes

$$\{R_i\} = \sum_{m=1}^{n} \sum_{e} [k_{im}]^e \{\delta_m\} + \sum_{e} \{F_i\}^e_{\epsilon_o} + \sum_{e} \{F_i\}^e_P + \sum_{e} \{F_i\}^e_b \,. \tag{4.62}$$

If a particular element does not include the node in question, it will contain no submatrices with an i suffix and, therefore, its contribution will simply be zero. Once all nodes have been considered, the overall system of equations is established.

This system of equations can be written in matrix form as

$$[K]\{\delta\} = \{R\} - \{F\}_{\epsilon_o} - \{F\}_P - \{F\}_b \,, \tag{4.63}$$

in which the submatrices are

$$\begin{aligned} [K_{im}] &= \sum_e [k_{im}]^e \\ \{F_i\}_{\epsilon_o} &= \sum_e \{F_i\}^e_{\epsilon_o} \\ \{F_i\}_P &= \sum_e \{F_i\}^e_P \\ \{F_i\}_b &= \sum_e \{F_i\}^e_b \,, \end{aligned} \tag{4.64}$$

with the summations including all the elements.

The system of equations resulting from Equation 4.63 can be solved once the prescribed support displacements have been substituted. Without substitution of a minimum number of prescribed displacements to prevent rigid body movement of the structure, it is impossible to solve this system, because the displacements cannot be uniquely determined by the forces in such a situation. This physically obvious fact will result in the matrix [K] being singular, i.e., not possessing an inverse.

Once the solution of the unknown displacements has been obtained, the stresses at any part of the element can be found from its stress matrix. Substitution of Equation 4.13 into Equation 4.20 yields

$$\{\sigma\}^e = [D]^e [B]^e \{\delta\}^e - [D]^e \{\epsilon_o\}^e , \qquad (4.65)$$

where by comparing with Equation 4.58, $[D]^e [B]^e$ is recognized to be $[S]^e$ and $-[D]^e \{\epsilon_o\}^e$ is recognized to be $\{\sigma\}^e_{\epsilon_o}$. To account for the effect of the distributed body forces and the distributed boundary loads, these stress effects have to be added to Equation 4.65. This yields for the general analysis

$$\{\sigma\}^e = [D]^e [B]^e \{\delta\}^e - [D]^e \{\epsilon_o\}^e + \{\sigma\}^e_P + \{\sigma\}^e_b . \qquad (4.66)$$

This is just Equation 4.58 which established 'a prior' the characteristics for each element and is applied to each element in turn.

Due to the matrix [B] being a function of position in the element, the stresses, unlike the plane problem where the stresses are constant in the element, vary throughout the element. It is convenient now to evaluate the average stress at the centroid of the element. Thus, Equation 4.66 becomes

$$\{\bar{\sigma}\}^e = [D]^e[\bar{B}]^e\{\delta\}^e - [D]^e\{\epsilon_o\}^e + \{\sigma\}_p^e + \{\sigma\}_b^e . \tag{4.67}$$

Zienkiewicz (48) indicates that this procedure causes a certain amount of oscillation of stress values between elements to occur and that a better approximation can be achieved by averaging nodal stresses.

CHAPTER V

PROBLEM SOLUTION

INTRODUCTION

The creep laws and corresponding mechanical models for the salt pillar models which were presented in Chapter III neither satisfied this author nor did they meet the requirements of this analysis. Thus, in this section, an 'improved' creep law and its corresponding mechanical model is presented and justification for its adoption given.

The finite element analysis for axi-symmetric bodies which was developed in Chapter IV was modified to handle creep effects and was applied to the salt pillar model and programmed in Fortran IV for the IBM 7040 computer. The program followed the general format of an existing two-dimensional program (48), but with many modifications in order to apply it to this problem. Because of limited computer space, two sets of programs were run; one for the elastic analysis and one for the creep analysis.

A thorough series of checks of the main programs and of the subroutines were performed before any attempt was made to run the entire program. Included in the output of each of the two analyses were the displacements of the

nodal points, the new nodal point co-ordinates, and the stresses in each element. A program was then written to plot the nodal points in the salt pillar model at different stages of the analysis.

THE CREEP LAW ADOPTED FOR SALT

The creep laws proposed by Serata and Obert in their work with salt pillar models do not in either case truly represent the mechanical behaviour of salt.

Serata in his creep law and corresponding mechanical model fitted his constants to the creep data so that the flow of his viscoplastic unit (Bingham model) diminished within a relatively short period of time with the flow of his viscoelastic unit (Kelvin model) continuing for a very long or infinite length of time. This is rather confusing since this is just opposite to what one would expect from these two units. Also, his strain rate equation (Equation 3.2) involves a lateral stress (σ_{LA}) which he, in several places in his paper (18), implies is the lateral stress in the pillar, but, which actually is only the stress applied laterally at the roof and floor sections of his model. In the present analysis, this lateral stress at these two positions, in the interior, and in the pillar itself is one of the unknowns of the problem that is eventually solved for.

Obert's creep law and corresponding mechanical model (Burger's model) is a rather common one in rock mechanics and has been used by several other investigators (62,63, 64). Although it was used as the model for rock salt, it does not provide an exact representation of rock salt for two reasons. The first was indicated by Obert when he observed that no set of constants for his creep law (Equation 3.3) would provide a fit for a family of curves for rock salt primarily because $3\eta_m$ was not constant for different values of σ_{z_o}. The second becomes obvious after reviewing the literature on rock salt. Several investigators (15,18,20,21,23,24) have observed that rock salt's creep rate continues to decrease with time, a characteristic which can be classified as the 'age hardening' property. Obert's steady state creep rate, however, remains constant with time.

Since Bradshaw's data on creep with the salt pillar models appears to be the best documented and the most complete, involving also the temperature as one of the variables, a study was made of it in an attempt to use it to propose an approximate creep law for rock salt. In this process, the creep rate curve which he fitted to his data was separated into two components, a transient creep rate component and a steady creep rate component. The steady

creep rate component, unlike Obert's, was required to exhibit the 'age hardening' property of salt by having it fit the actual creep rate curve after the transient creep rate was no longer effective. Success was finally achieved with the following creep law for the salt pillar model which is proposed at this time:

$$\epsilon_{z_o} = \frac{\sigma_{z_o}}{E} + C_1 f_1(T) f_2(\sigma_{z_o}) \left[1-e^{-\alpha t}\right] + C_2 f_1(T) f_2(\sigma_{z_o}) \left[1-e^{-\beta t}\right], \tag{5.1}$$

where: $f_1(T) = T^{10.9}$

$f_2(\sigma_{z_o}) = \sigma_{z_o}^{3.2}$.

The first term on the right represents the elastic strain, the second represents the transient creep, and the third represents the steady state creep.

The mechanical model corresponding to this creep law is presented in Figure 5.1. It consists of a Hookean unit and two Kelvin units, with the steady creep Kelvin unit possessing a more viscous dashpot but a much weaker spring than the transient creep Kelvin unit. The following relations are implied:

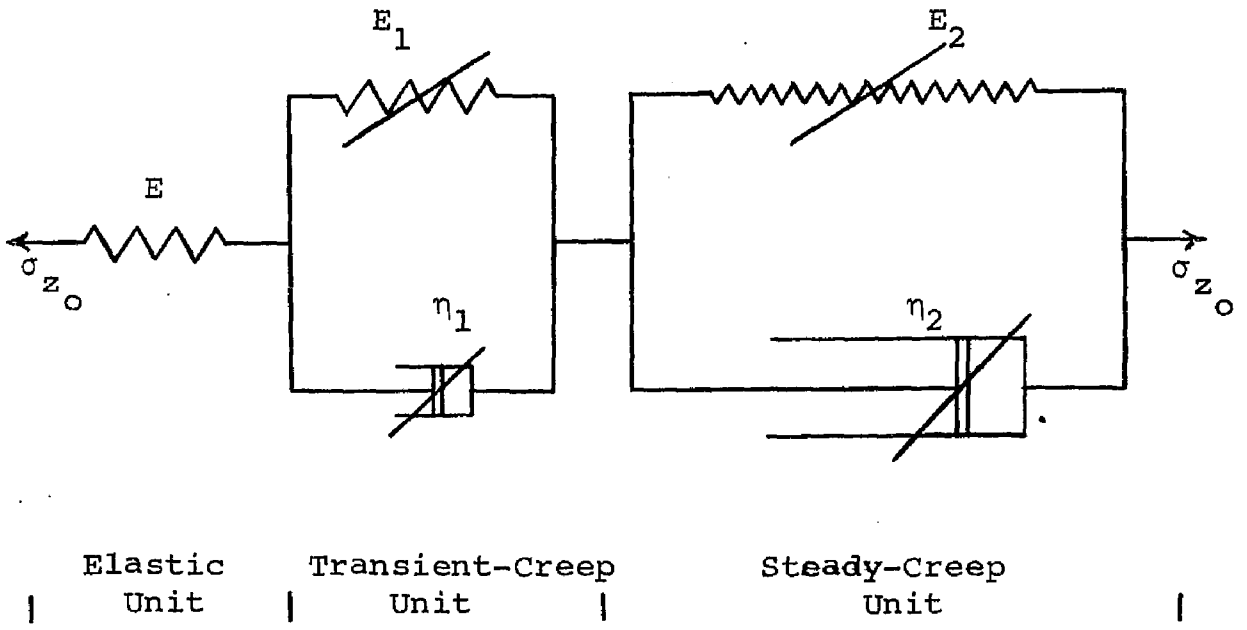

Figure 5.1. Mechanical Model Proposed for Rock Salt

$$C_1 T^{10.9} \sigma_{z_o}^{3.2} = \frac{\sigma_{z_o}}{E_1}$$

$$C_2 T^{10.9} \sigma_{z_o}^{3.2} = \frac{\sigma_{z_o}}{E_2} \qquad (5.2)$$

$$\alpha = \frac{E_1}{3\eta_1}$$

$$\beta = \frac{E_2}{3\eta_2} \quad .$$

The strain rate was obtained by taking a time derivative of Equation (5.2) to give

$$\dot{\epsilon}_{z_o} = (C_1\alpha) f_1(T) f_2(\sigma_{z_o}) e^{-\alpha t} + (C_2\beta) f_1(T) f_2(\sigma_{z_o}) e^{-\beta t}. \qquad (5.3)$$

The four constants, C_1, C_2, α and β were obtained by curve fitting to Equation (3.7) which represents Bradshaw's data. These constants are independent of time, stress and temperature.

The results of the curve fitting are presented in Figures 5.2 through 5.4. The first is a plot at constant temperature and various pillar stresses of the transient creep rate, the steady creep rate, the sum of these two components and also the creep rate as obtained by Bradshaw. The second is a plot at constant pillar stress and various temperatures of the same quantities. The third is a sample

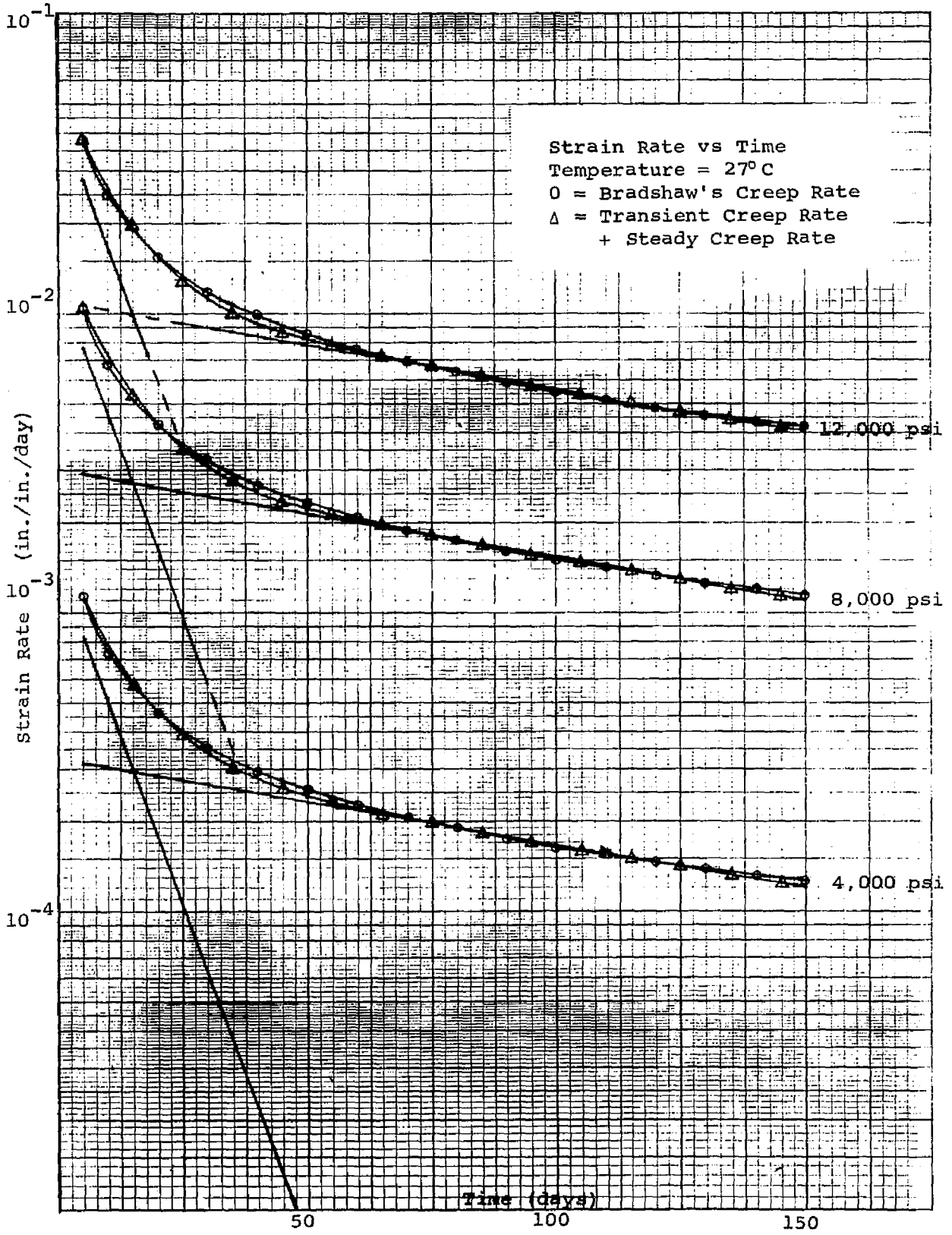

Figure 5.2. Strain Rate at Constant Temperature

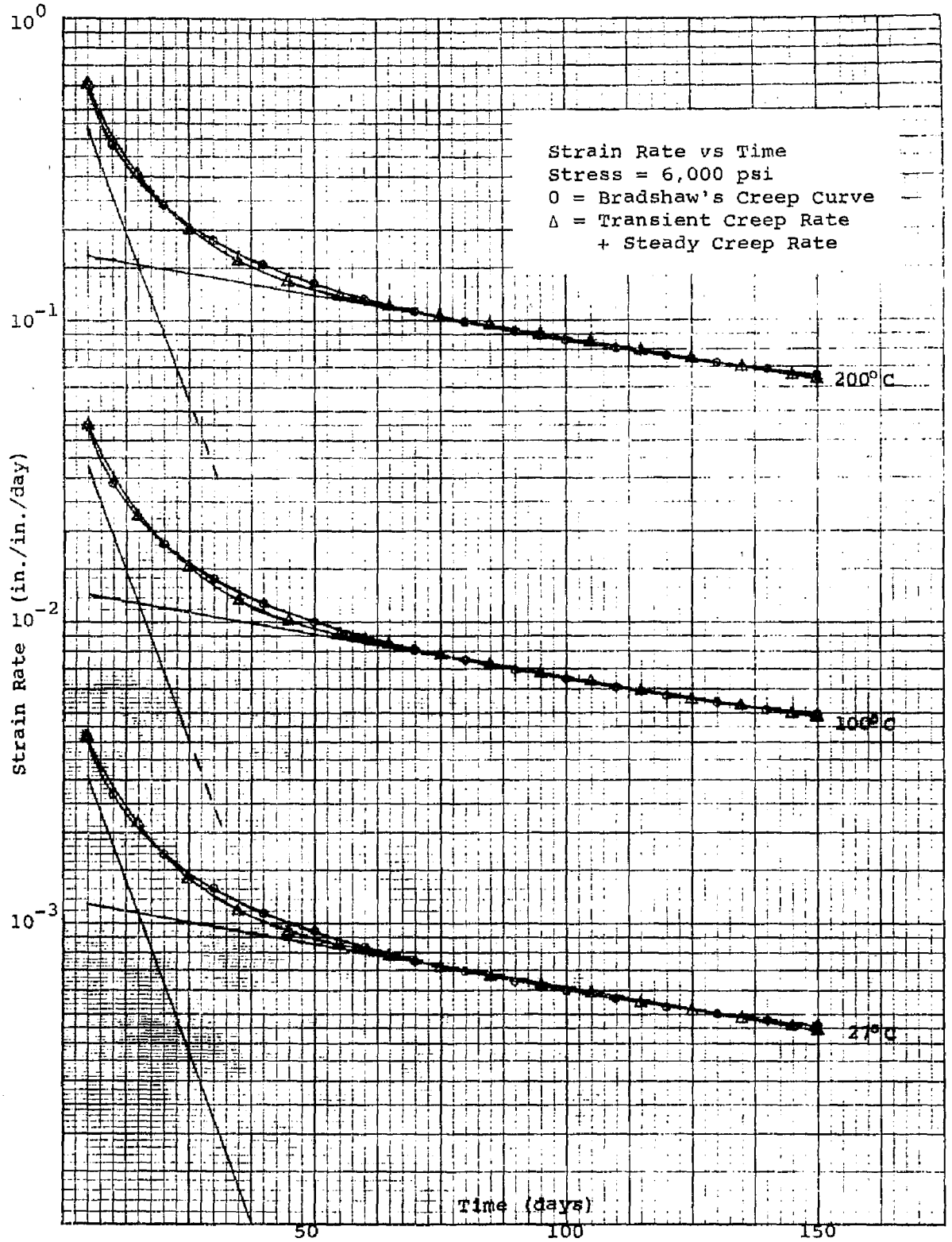

Figure 5.3. Strain Rate at Constant Stress

CREEP RATE CHECK BERGERON, W. MARCH 68 LSL

DELTA = 5. DAYS
STRESS = 6000. PSI
TEMP = 300. DEG. KEL.

C1A = 0.417CE-21
ALPHA = -0.104CE 00
C2B = 0.974CE-22
BETA = -0.670CE-02
CTR = 0.768CE-20

TIME	TCR	SCR	TR	TESTR
5.	3.0549798E-03	1.1606880E-03	4.2156678E-03	4.2130716E-03
10.	1.8162483E-03	1.1224491E-03	2.9386973E-03	2.6849076E-03
15.	1.0797569E-03	1.0854699E-03	2.1652668E-03	2.0628612E-03
20.	6.4196146E-04	1.0497090E-03	1.6916704E-03	1.7110388E-03
25.	3.8165927E-04	1.0151262E-03	1.3967855E-03	1.4800226E-03
30.	2.2690428E-04	9.8168279E-04	1.2085871E-03	1.3146208E-03
35.	1.3489926E-04	9.4934117E-04	1.0842404E-03	1.1892827E-03
40.	8.0200382E-05	9.1806503E-04	9.9826541E-04	1.0904113E-03
45.	4.7680773E-05	8.8781929E-04	9.3550007E-04	1.0100461E-03
50.	2.8347200E-05	8.5857001E-04	8.8691721E-04	9.4318925E-04
55.	1.6852993E-05	8.3028435E-04	8.4713734E-04	8.8653030E-04
60.	1.0019450E-05	8.0293056E-04	8.1295000E-04	8.3778198E-04
65.	5.9567693E-06	7.7647794E-04	7.8243470E-04	7.9530853E-04
70.	3.5414218E-06	7.5089681E-04	7.5443822E-04	7.5790648E-04
75.	2.1054479E-06	7.2615844E-04	7.2826388E-04	7.2466874E-04
80.	1.2517322E-06	7.0223509E-04	7.0348682E-04	6.9489766E-04
85.	7.4418049E-07	6.7909989E-04	6.7984406E-04	6.6804700E-04
90.	4.4243056E-07	6.5672689E-04	6.5716932E-04	6.4368250E-04
95.	2.6303406E-07	6.3509096E-04	6.3535400E-04	6.2145402E-04
100.	1.5637916E-07	6.1416782E-04	6.1432420E-04	6.0107594E-04
105.	9.2970623E-08	5.9393401E-04	5.9402698E-04	5.8231276E-04
110.	5.5272947E-08	5.7436681E-04	5.7442208E-04	5.6496831E-04
115.	3.2860903E-08	5.5544424E-04	5.5547711E-04	5.4887789E-04
120.	1.9536480E-08	5.3714509E-04	5.3716462E-04	5.3390197E-04
125.	1.1614839E-08	5.1944879E-04	5.1946040E-04	5.1992157E-04
130.	6.9052607E-09	5.0233550E-04	5.0234240E-04	5.0683450E-04
135.	4.1053195E-09	4.8578602E-04	4.8579012E-04	4.9455248E-04
140.	2.4406568E-09	4.6978176E-04	4.6978419E-04	4.8299888E-04
145.	1.4510444E-09	4.5430475E-04	4.5430620E-04	4.7210668E-04
150.	8.6267565E-10	4.3933764E-04	4.3933851E-04	4.6181713E-04

Figure 5.4. Sample of Results From Creep Rate Analysis

of the results obtained from the program which is included in the Appendix. As can be noted, a relatively good and consistent matching was obtained with the sum of the two creep rate components and Bradshaw's creep rate.

Assuming that the creep strain occurs without volume change, i.e., in a similar manner to the usual plastic strain assumption, the 'uniaxial' strain rate of Equation 5.3 is generalized to give

$$\frac{d}{dt}\begin{Bmatrix}\epsilon_z\\ \epsilon_r\\ \epsilon_\theta\\ \gamma_{rz}\end{Bmatrix} = \left(\left(C_1\alpha\right)e^{-\alpha t} + \left(C_2\beta\right)e^{-\beta t}\right)\left(T^{10.9}\right)$$

$$\left(K\bar{\sigma}^{-2.2}\right)\left[D_o\right]^{-1}\begin{Bmatrix}\sigma_z\\ \sigma_r\\ \sigma_\theta\\ \tau_{rz}\end{Bmatrix} , \qquad (5.4)$$

where the effective stress, $\bar{\sigma}$, is given by

$$\bar{\sigma} = \frac{1}{3}\sqrt{\left\{\left(\sigma_z-\sigma_r\right)^2 + \left(\sigma_r-\sigma_\theta\right)^2 + \left(\sigma_\theta-\sigma_z\right)^2\right\}} , \qquad (5.5)$$

and where $\left[D_o\right]^{-1}$ is that part of the elasticity matrix which depends on Poisson's ratio alone.

If Bradshaw's creep rate curve (Equation 3.7) had been obtained in axial tests of salt samples, then the five constants C_1, C_2, α, β, and K would in Equation 5.4 give the correct strain rate. His creep rate curve, however, was an expression for the creep rate of the pillar model in the

axial direction in terms of the average applied pillar stress. Since there are no data at this time from which to obtain the correct values of these constants, the values as obtained from Equation 3.7 will be used. Additional comments regarding the use of the above equations will appear in a later chapter.

CREEP EFFECTS MODIFICATIONS

In order to account for the time dependent strain (creep), the general format of the 'incremental-variable elasticity' procedure as suggested by Zienkiewicz (48) is followed, but with some additional modifications to fit the conditions of this analysis, i.e., instantaneous applied, constant pillar load, no separate component of plastic strain, and time dependent strain. The pillar load is instantaneously applied and maintained constant for a given increment of time with the nodal point displacements at the end of this increment found, by the use of a suitably modified elasticity matrix, as if the material was elastic.

For the elastic strain,

$$\{\epsilon_e\}^e = [D_e]^{e^{-1}} \{\sigma\}^e \quad . \tag{5.6}$$

For the creep strain,

$$\{\epsilon_c\}^e = c^e [D_o]^{e^{-1}} \{\sigma\}^e , \tag{5.7}$$

where

$$c^e = c^e(t, T, \bar{\sigma}) . \tag{5.8}$$

Thus,

$$\{\epsilon_e\}^e + \{\epsilon_c\}^e = \left([D_e]^{e^{-1}} + c^e [D_o]^{e^{-1}} \right) \{\sigma\}^e , \tag{5.9}$$

or,

$$\{\sigma\}^e = \left([D_e]^{e^{-1}} + c^e [D_o]^{e^{-1}} \right)^{-1} \left(\{\epsilon_e\}^e + \{\epsilon_c\}^e \right) . \tag{5.10}$$

This defines an 'elasto-creep' value of an elasticity matrix as

$$[D_{ec}]^e = \left([D_e]^{e^{-1}} + c^e [D_o]^{e^{-1}} \right)^{-1} . \tag{5.11}$$

In general, the complete problem is solved in an iterative way as described by the following steps:

1. The full load is applied to the structure and the elastic displacements, $\{\delta_e\}_i$, and stresses, $\{\sigma\}^e$, based on $E = E_e$ and $t = 0$ are determined respectively for each nodal point and each element.

2. For a fixed $\Delta t > 0$ (i.e., at a particular instant), a new value of $E = E_{ec}$ is determined for each element depending on the state of stress reached in that element in the preceeding step. The total displacement, $\{\delta_{ec}\}_i$, and the stress, $\{\sigma\}^e$, for Δt is then determined. This stress is now used in the first step of iteration in this particular time interval to find a better estimate of $\{\delta_{ec}\}^e$. The iteration procedure is used until reasonable convergence has occurred.

3. The new co-ordinates of each nodal point is found by $\begin{Bmatrix} r \\ z \end{Bmatrix}_{new_i} = \begin{Bmatrix} r \\ z \end{Bmatrix}_{old_i} + \{\delta_c\}$ and used to calculate a new stiffness matrix for the next time interval.

4. Step 1 is repeated with the new stiffness matrix.

5. Step 2 is repeated.

6. Step 3 is repeated, etc.

In reference to the iteration of the second step; Argyris (59) in a problem similar to this one, but involving plastic deformations with the 'incremental initial strain' method, suggested that it is sometimes not really necessary to perform this iteration procedure if the time interval is small enough, but that an improvement can be achieved

by specifying a limited number (two or three) iterations to be carried out in each time interval.

THE APPLICATION OF THE FINITE ELEMENT METHOD

The general finite element method presented in Chapter IV with the creep modifications developed in this chapter was adapted to the solution of displacements and stresses in the salt pillar model. The solution was carried out with a pillar stress of 6,000 psi and a temperature of 300°K using step 1 and step 2, with no iterations, completely through the first time interval of two days.

The assumptions which were discussed earlier in previous chapters and used in the application of this method to the axi-symmetric salt pillar model were:

1. Rock salt was homogeneous and isotropic.
2. The elastic properties measured by Serata (see Chapter III) were the ones which are most applicable to this problem and were used in the elastic analysis.
3. The creep curves of Bradshaw (see 'The Creep Law Adopted for Salt' in this chapter) are the most general and the best documented and were the ones used for the creep analysis.

4. The applied pillar load was instantaneously applied and maintained constant.
5. The only nodal forces were those due to the applied pillar loads.
6. The salt pillar model was maintained at constant temperature.
7. The initial strain was zero.
8. There was no separate component of plastic strain.
9. The stress in each element was evaluated at its centroidal point and was assumed constant over the element.

The axi-symmetric salt pillar model was divided into 'two-dimensional' elements as discussed in Chapter IV and illustrated in the top part of Figure 4.2-C. The division used produced 77 nodal points and 117 elements. (See plot of original nodal points by Calcomp 563 Plotter, Figure 5.12.) With two degrees of freedom associated with each nodal point, the solution of 154 simultaneous equations was required.

The linear elastic solution of these simultaneous equations for the displacements and then the stresses was accomplished by a program which followed the format of the one proposed by Zienkiewicz and Cheung (48) for plane stress

or plane strain triangular elements. The program was studied in detail and then altered to convert it to an axi-symmetric program, to account for the time dependent strain, and to implement it on the IBM 7040. Major changes were required in the main program and in all subroutines except 'Solve' and 'Matinv'. Because of limited space remaining in the computer, a separate program similar to the linear elasticity one, but with a few changes and additions, was written to include the effects of the time dependent strain. Flow charts of these two programs appear in Figure 5.5 and Figure 5.6, with the programs appearing in the Appendix. (See Appendix C and Appendix D.) Figures 5.7 through 5.10 contain the printed output of the creep analysis program for a 6,000 psi applied pillar load, 300°K constant temperature and for the first time increment of 2 days.

An important feature of these programs was the subdivision of the stiffness matrix into parts which were then written in a tridiagonalized manner. This allowed for the solution of the equations in steps by inverting only a small part of the overall stiffness matrix and not the entire matrix at one time. This was accomplished by dividing the idealized structure into segments called 'partitions'. In this analysis, five partitions were used

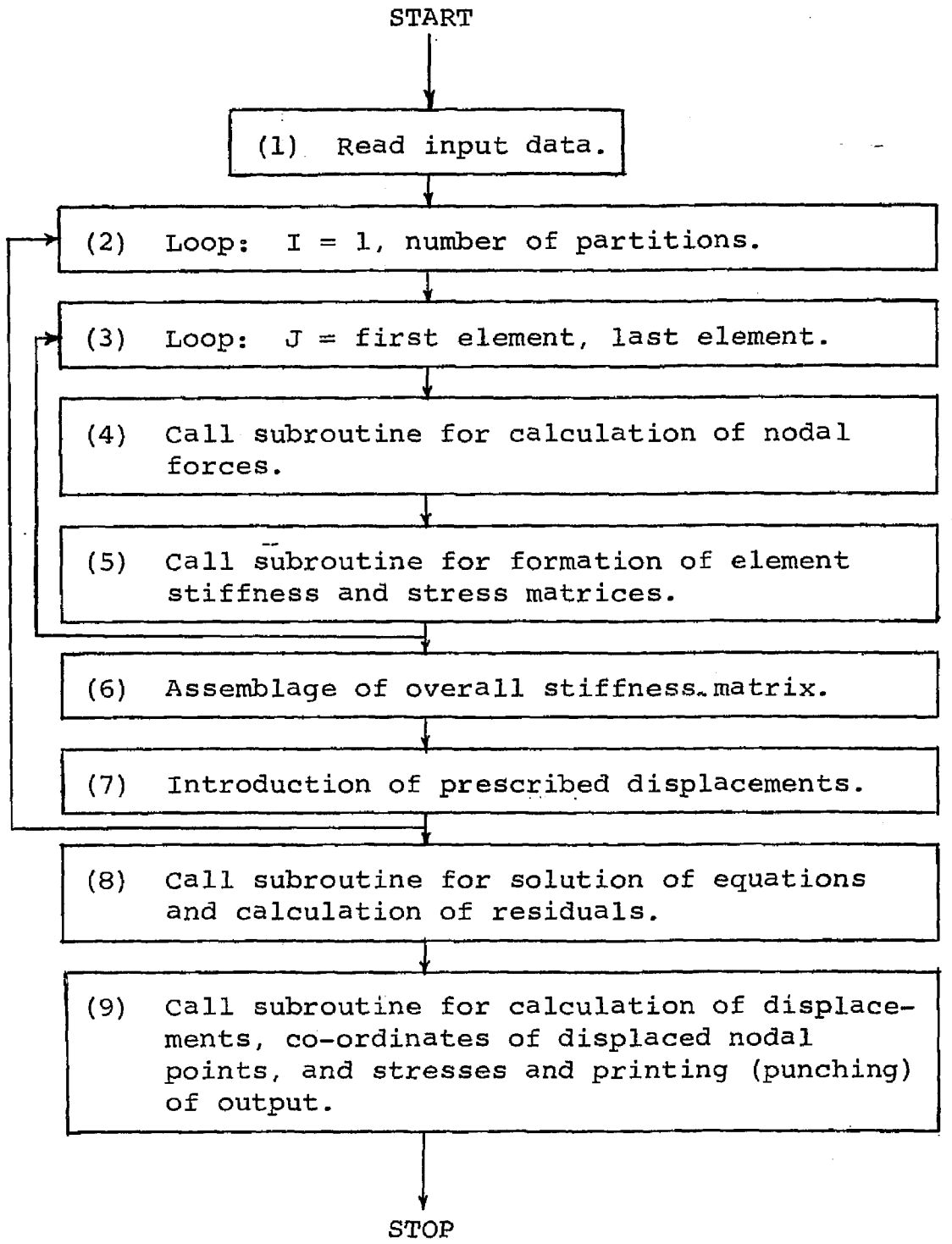

Figure 5.5. Flow Chart of Elastic Analysis Program.

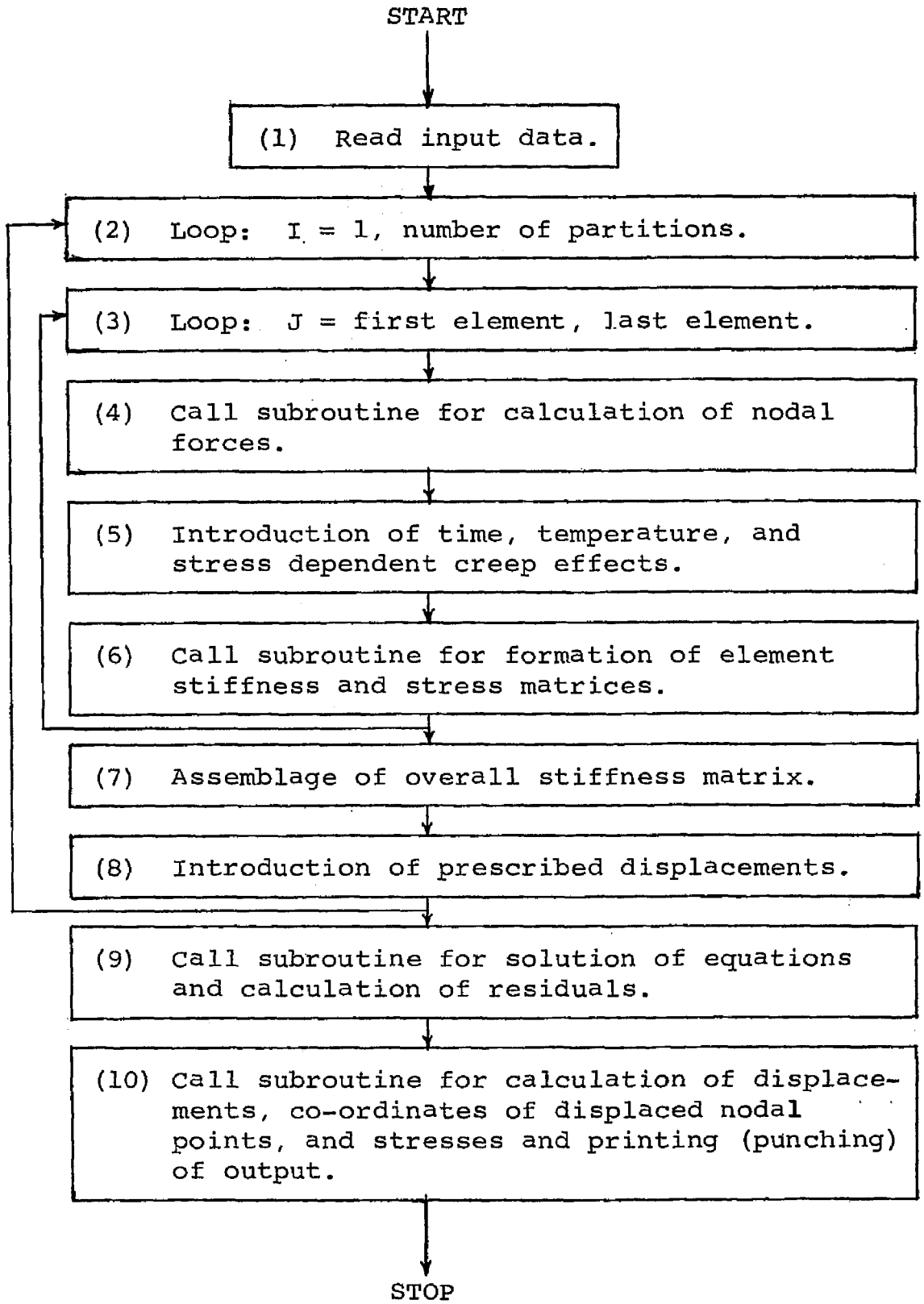

Figure 5.6. Flow Chart of Creep Modifications Program.

FINITE ELEMENT ANALYSIS OF SALT PILLAR MODELS
CREEP MODIFICATIONS

BERGERON, W. APRIL,1968 L.S.U.

AVERAGE PILLAR STRESS = 6000. PSI

NODE	R-DISPLACEMENTS	Z-DISPLACEMENTS	NEW R CO-ORD.	NEW Z CO-ORD.
1	1.2331854 E-14	-7.4107441 E-03	1.2331854 E-14	1.4925893 E 00
2	-9.6179373 E-16	-1.4361397 E-02	-9.6179373 E-16	1.1856386 E 00
3	-4.9637891 E-15	-1.9039243 E-02	-4.9637891 E-15	8.8096076 E-01
4	-8.9730265 E-16	-1.4678514 E-02	-8.9730265 E-16	5.8532149 E-01
5	-9.7668120 E-16	-9.0619384 E-03	-9.7668120 E-16	2.9093806 E-01
6	-1.6048551 E-22	-1.3878173 E-15	-1.6048551 E-22	-1.3878173 E-15
7	1.4776465 E-02	-2.2127226 E-02	3.1477647 E-01	1.4778728 E 00
8	-3.6119927 E-03	-3.3063364 E-03	2.9638801 E-01	1.1966937 E 00
9	-2.4588892 E-03	-9.5773141 E-03	2.9754111 E-01	8.9042268 E-01
10	2.0969080 E-03	-1.1321175 E-02	3.0209691 E-01	5.8867882 E-01
11	2.7537266 E-03	-6.5646273 E-03	3.0275373 E-01	2.9342538 E-01
12	4.5093043 E-03	-1.7881231 E-15	3.0450931 E-01	-1.7881231 E-15
13	1.8261214 E-02	-2.4883361 E-02	6.1826121 E-01	1.4751166 E 00
14	9.1584530 E-03	-1.3898030 E-02	6.0915845 E-01	1.1861020 E 00
15	-5.8466001 E-03	-1.7794838 E-03	5.9415340 E-01	8.9822051 E-01
16	5.0267100 E-04	-5.9659804 E-03	6.0050267 E-01	5.9402402 E-01
17	4.9812194 E-03	-5.4557344 E-03	6.0498121 E-01	2.9454427 E-01
18	7.3569512 E-03	-1.8310082 E-15	6.0735695 E-01	-1.8310082 E-15
19	2.1383336 E-02	-2.6114454 E-02	9.2138333 E-01	1.4738855 E 00
20	1.3389969 E-02	-1.7051671 E-02	9.1338997 E-01	1.1829483 E 00
21	4.5112753 E-03	-1.0118742 E-02	9.0451127 E-01	8.8988125 E-01
22	-2.3672160 E-03	-3.7514138 E-05	8.9763278 E-01	5.9996248 E-01
23	4.2330082 E-03	-1.9911887 E-03	9.0423300 E-01	2.9800881 E-01
24	9.6205685 E-03	-2.0891648 E-15	9.0962056 E-01	-2.0891648 E-15
25	3.3732335 E-02	-3.9303646 E-02	1.2337323 E 00	1.4606963 E 00
26	1.6510588 E-02	-2.0972666 E-02	1.2165106 E 00	1.1796273 E 00
27	8.0474951 E-03	-1.5007311 E-02	1.2080475 E 00	8.8495268 E-01
28	6.7658241 E-03	-9.8287782 E-03	1.2067658 E 00	5.9017122 E-01
29	2.0240059 E-03	3.9153470 E-04	1.2020240 E 00	3.0039154 E-01
30	9.2814814 E-03	-1.7415740 E-15	1.2092815 E 00	-1.7415740 E-15
31	3.7092321 E-02	-4.5715009 E-02	1.5370923 E 00	1.4542850 E 00
32	2.8158922 E-02	-3.5747690 E-02	1.5281589 E 00	1.1642523 E 00
33	1.0554038 E-02	-2.0566008 E-02	1.5105540 E 00	8.7943399 E-01
34	9.7248880 E-03	-1.6158675 E-02	1.5097249 E 00	5.8384132 E-01
35	1.0983280 E-02	-1.1105235 E-02	1.5109833 E 00	2.8889477 E-01
36	7.4646351 E-03	-2.9353384 E-15	1.5074646 E 00	-2.9353384 E-15
37	3.4308677 E-02	-6.3630320 E-02	1.8343087 E 00	1.4363697 E 00
38	3.1447937 E-02	-6.0756573 E-02	1.8314479 E 00	1.1392434 E 00
39	2.1387922 E-02	-5.3139996 E-02	1.8213879 E 00	8.4686000 E-01
40	1.2057446 E-02	-4.6571940 E-02	1.8120574 E 00	7.0342806 E-01
41	1.2583830 E-02	-4.3927275 E-02	1.8125838 E 00	5.5607273 E-01
42	1.2965022 E-02	-4.1569661 E-02	1.8129650 E 00	4.0843034 E-01
43	3.4237695 E-02	-2.8120473 E-02	1.8342317 E 00	2.7187953 E-01
44	1.8168686 E-02	-1.4517811 E-02	1.8181687 E 00	1.3548219 E-01
45	3.2846647 E-02	-1.1265635 E-15	1.8328466 E 00	-1.1265635 E-15
46	3.2595842 E-02	-8.5707020 E-02	2.1325958 E 00	1.4142930 E 00
47	2.8775902 E-02	-8.2930954 E-02	2.1287759 E 00	1.1170690 E 00
48	2.4316959 E-02	-8.1792202 E-02	2.1243170 E 00	8.1820779 E-01
49	1.5411525 E-02	-6.8338409 E-02	2.0154115 E 00	6.3166159 E-01

Figure 5.7. Results of Creep Analysis

50	1.4026394	E-02	-6.4020984	E-02	2.0140264	E 00	4.3597902 E-01
51	1.3579290	E-02	-5.5582043	E-02	1.9135793	E 00	5.9441795 E-01
52	4.8696245	E-02	-5.1629163	E-02	2.0486962	E 00	2.4837084 E-01
53	4.8561237	E-02	-4.4238413	E-18	2.0485612	E 00	-4.4238413 E-18
54	3.1168168	E-02	-9.6327188	E-02	2.4311682	E 00	1.4036728 E 00
55	2.7140380	E-02	-9.4018907	E-02	2.4271404	E 00	1.1059811 E 00
56	2.1554366	E-02	-9.2534364	E-02	2.4215544	E 00	8.0746563 E-01
57	1.8153191	E-02	-8.5424934	E-02	2.2181532	E 00	6.1457507 E-01
58	1.1675746	E-02	-8.6079879	E-02	2.2116758	E 00	4.1352012 E-01
59	1.6400937	E-02	-9.2336739	E-02	2.4164010	E 00	6.0766326 E-01
60	1.0763790	E-02	-9.2214531	E-02	2.4107638	E 00	4.0778547 E-01
61	2.9604919	E-02	-1.0345034	E-01	2.7296049	E 00	1.3965496 E 00
62	2.5827385	E-02	-1.0185015	E-01	2.7258274	E 00	1.0981499 E 00
63	2.0024796	E-02	-1.0049953	E-01	2.7200248	E 00	7.9950046 E-01
64	1.5355265	E-02	-9.7459652	E-02	2.6153553	E 00	6.0254034 E-01
65	1.0433754	E-02	-9.7218261	E-02	2.6104337	E 00	4.0278174 E-01
66	2.8055628	E-02	-1.0920576	E-01	3.0280556	E 00	1.3907942 E 00
67	2.4405762	E-02	-1.0804905	E-01	3.0244058	E 00	1.0915509 E 00
68	1.8587241	E-02	-1.0721928	E-01	3.0189873	E 00	7.9278071 E-01
69	1.4857694	E-02	-1.0225689	E-01	2.8148577	E 00	5.9774311 E-01
70	1.0156885	E-02	-1.0201391	E-01	2.8101569	E 00	3.9798609 E-01
71	1.4465698	E-02	-1.0678450	E-01	3.0144657	E 00	5.9321550 E-01
72	9.9640984	E-03	-1.0656721	E-01	3.0099641	E 00	3.9343279 E-01
73	2.7351911	E-02	-1.2118749	E-01	3.7773519	E 00	1.3788125 E 00
74	2.2776571	E-02	-1.2085263	E-01	3.7727766	E 00	1.0791474 E 00
75	1.7612233	E-02	-1.2088661	E-01	3.7676122	E 00	7.7911339 E-01
76	1.3816066	E-02	-1.2093641	E-01	3.7638161	E 00	5.7906359 E-01
77	9.9326946	E-03	-1.2090236	E-01	3.7599327	E 00	3.7909764 E-01

Figure 5.8. Results of Creep Analysis

ELEMENT NUMBER	Z-STRESS	R-STRESS	T-STRESS	RZ-STRESS
1	9.97567655E 04	1.0455850E 05	1.0324445E 05	2.623992CE 02
2	-1.74751566E 04	-1.85555543E 04	-1.85555547E 04	5.86295455E 02
3	-2.393124CE 04	-2.57321515E 04	-2.5627082E 04	9.0218473E 02
4	-1.5084476E 04	-1.6455C910E 04	-1.64550918E 04	9.0582327E 02
5	-5.91C8244E 04	-6.0356797E 04	-5.9698453E 04	7.5203954E 02
6	-1.2674594E 04	-1.0353891E 04	-1.0353902E 04	6.0326876E 02
7	-1.8068766E 04	-1.44883664E 04	-1.4311891E 04	7.0633011E 02
8	-1.0658855E 04	-5.5828281E 03	-5.5828437E 03	7.572238CE 02
9	-1.6638172E 04	-9.9351172E 03	-9.3036553E 03	2.6677875E 02
10	-9.3660351E 03	3.51C4688E 02	3.51046888E 02	-4.930676CE-10
11	6.0957531E 04	6.3030063E 04	6.3739718E 04	4.5451566E 02
12	-6.7441516E 04	-6.2669250E 04	-6.3830867E 04	5.8890137E 02
13	3.697625CE 04	4.1991398E 04	3.9406055E 04	4.4464771E 02
14	-5.05C3867E 03	-7.1290703E 03	-7.0411875E 03	7.15C1851E 02
15	-4.9343865E 04	-5.18C2322E 04	-5.1209263E 04	2.3508862E 02
16	1.2944465E 04	1.17C4793E 04	1.2309910E 04	1.4843738E 02
17	-3.9389703E 04	-3.9970086E 04	-3.8304738E 04	2.3468339E 02
18	-7.6377C7CE 03	-3.36C7930E 03	-3.2196445E 03	1.3842169E 02
19	-1.7899149E 04	-1.2323609E C4	-1.1749676E 04	-4.5965859E 02
20	-9.1118125E 03	-1.9497266E 03	-1.3353984E 03	-6.6793534E 02
21	4.4588172E 04	4.6321250E 04	4.6820C94E 04	4.8C90889E 02
22	-6.324475CE 04	-6.0887555E 04	-6.0639953E 04	4.6077980E 02
23	4.3922422E 04	4.6225344E 04	4.6050969E 04	5.8789714E 02
24	-4.5636715E 04	-4.C416207E 04	-4.2562414E 04	7.7411824E 02
25	-1.5723766E 04	-8.9664687E 03	-1.2543852E 04	-2.4146966E 02
26	1.5942164E 04	1.3185184E 04	1.3876072E 04	-8.220580CE 01
27	-4.0212239E 04	-4.2738155E 04	-4.1080271E 04	-1.7588679E 02
28	8.2964101E 03	8.1466407E 03	9.4912070E 03	-3.1909571E 02
29	-2.6940754E 04	-2.6092836E 04	-2.3976381E 04	-6.5590677E 02
30	-7.8736172E 03	-1.9156328E 03	-1.2415547E 03	-9.168254CE 02
31	3.2682965E 04	3.7020500E 04	3.6195188E 04	2.8506293E 02
32	-5.5632125E 04	-5.3718672E 04	-5.3403313E 04	3.1979338E 02
33	3.9071703E 04	4.0928328E 04	4.1005985E 04	4.6656723E 02
34	-5.5066937E 04	-5.2535781E 04	-5.2763375E 04	4.8235181E 02
35	5.9513360E 03	8.7576172E 03	8.1846C93E 03	-5.8073852E 02
36	-7.8472422E 03	-1.4423047E 02	-3.4484805E 03	-5.8386721E 02
37	-3.8155047E 04	-2.9271328E 04	-3.3213297E 04	-1.1641382E 03
38	1.0077459E 04	7.5322148E 03	9.1207383E 03	-1.2893804E 03
39	-2.6705533E 04	-2.8119273E 04	-2.615045CE 04	-1.3250409E 03
40	-2.5386563E 03	-1.3566016E 03	5.4128906E 02	-1.9273592E 03
41	2.9393813E 04	3.1325969E 04	3.1863875E 04	1.8282001E 02
42	-4.6351485E 04	-4.1520938E 04	-4.2433547E 04	1.9875098E 02
43	2.4260875E 04	2.9765844E 04	2.8190938E 04	2.8926026E 02
44	-5.1927929E 04	-4.9847344E 04	-4.9799602E 04	3.5664136E 02
45	6.9413438E 03	8.8485625E 03	8.7152500E 03	-6.523328CE 02
46	-2.4128461E 04	-2.0915688E 04	-2.1338735E 04	-9.9653662E 02
47	-1.0713984E 04	-7.6470938E 03	-8.0285782E 03	-1.4522561E 03
48	1.2100063E 04	2.1834524E 04	1.8059297E 04	-1.7142151E 03
49	-4.8547133E 04	-4.2733524E 04	-4.5055195E 04	-1.2353375E 03
50	1.4464219E 03	2.4207031E 02	2.0203125E 03	-1.9789513E 03
51	2.5649500E 04	2.5665063E 04	2.7194375E 04	-1.3030916E 03
52	-4.4027438E 04	-4.1669625E 04	-4.1203844E 04	-1.4174529E 03
53	2.7424438E 04	2.9809782E 04	3.0132469E 04	-1.6348512E 03
54	-4.3121438E 04	-3.6717156E 04	-3.8459422E 04	-1.8424812E 03
55	1.5816562E 04	2.1700813E 04	1.9676688E 04	-1.7077181E 03
56	-3.2536906E 04	-3.0580000E 04	-3.0548125E 04	-4.2354074E 03

Figure 5.9. Results of Creep Analysis

57	-2.88C1C63E 04	-2.6359C00E C4	-2.661CCCCE 04	-4.3189C14E 03
58	1.3259625E 04	1.5318687E 04	1.5109687E 04	-3.8C26671E 03
59	-2.48C8952E 04	-2.1271406E 04	-2.15C5102E 04	-6.7375411E 03
60	-1.8748563E 04	-1.1273312E 04	-1.4229188E C4	-4.4387521E 03
61	-1.866CC63E 04	-1.1493625E 04	-1.4266719E 04	1.C738771E 03
62	5.6042031E 03	1.0876C00E C4	9.1258594E 03	-7.16C3731E 02
63	-1.76C2578E 04	-1.1286375E C4	-1.3833156E 04	-1.7C36563E 03
64	1.8837938E C4	1.9147438E C4	2.1C3875CE 04	-2.6573278E 03
65	-3.8648563E 04	-3.86C1703E C4	-3.6826406E 04	-2.2416956E 03
66	2.721C668E 04	2.6563250E C4	2.947625CE 04	-3.7400247E 03
67	-4.3760964E 04	-4.C956078E C4	-4.C655C78E 04	-2.4725493E 03
68	1.0750937E 04	1.28C9875E C4	1.2851875E 04	-1.9642443E 03
69	-5.8335656E 04	-5.21C5344E 04	-5.4038265E 04	-2.358128CE 03
70	-1.14C825CE 04	-8.53C3750E 03	-9.2172500E C3	-3.8474979E 03
71	1.8918969E 04	2.1575157E 04	2.1144125E 04	-5.C354256E 03
72	-1.0359125E 04	-8.C671250E 03	-8.212125CE C3	-5.CCC7325E 03
73	-5.5558453E 04	-5.35C2141E 04	-5.3393203E 04	-5.3655C72E 03
74	-6.4256875E 03	-4.4252500E 03	-5.C690CCCE 03	-2.4426381E 03
75	-8.3729375E C3	-2.C465C00E 03	-4.2015625E C3	-5.C657047E 03
76	-1.C135437E 04	-4.C478750E C3	-6.C73750CE 03	-1.9454529E 02
77	-1.561CCCCE 03	5.3C53750E 03	2.5C3CCCCE C3	-5.9302406E 02
78	-1.15E2062E 04	-6.2043125E 03	-8.C68625CE 03	-1.5C04569E 03
79	9.67C625CE 03	1.2345750E 04	1.175025CE 04	-4.C312356E 03
80	1.2963187E 04	1.35C4812E C4	1.6813938E 04	-2.C273955E 03
81	-2.6975797E 04	-2.65C6688E C4	-2.4179141E 04	-1.4946997E 03
82	1.4521CCCE 04	1.4325750E C4	2.C797812E 04	-3.5582124E 03
83	-3.4464547E 04	-3.5433813E C4	-3.1759500E 04	-1.8752141E 03
84	1.21732E1E 04	7.7495938E C3	1.6516531E 04	-2.2410C49E 03
85	-3.8433813E 04	-2.9986500E C4	-3.C98450CE 04	-5.2722461E 03
86	-5.76C5CCCE 03	-2.9651406E 03	-3.4428281E C3	-3.1C88845E 03
87	-3.18C8CCCE 04	-3.4621125E 04	-3.113825CE 04	-7.2920398E 03
88	-3.5120375E 04	-4.35C6125E 04	-2.54C725CE 04	-4.7423770E 03
89	3.11C1782E 04	1.C476781E C4	3.7139985E 04	-1.86C8C08E 03
90	2.535875CE 03	-2.182C125E C4	4.1553125E 04	-7.7975743E 03
91	9.31CCCCCE 03	9.3512500E C3	1.48C7C62E 04	-1.8648393E 03
92	-1.884C797E 04	-1.8041719E 04	-1.4285234E 04	-1.5269214E 03
93	5.764625CE 03	5.8674375E 03	1.7127313E 04	-2.7718633E 03
94	-2.0054719E 04	-2.C172313E 04	-1.2759094E 04	-2.C501084E 03
95	1.9270625E 03	-6.5955625E 03	2.6955500E 04	-8.7783203E 02
96	1.6974485E 04	8.031CC00E 03	3.4253360E 04	1.6090625E 02
97	-5.2253438E 03	-3.1945157E 04	3.1567016E 04	7.4405938E 03
98	-4.3C575CCE 03	-1.4654250E 04	1.3611037E 05	-4.7973359E 03
99	6.3545CCCE 03	5.7826250E 03	1.2597812E 04	-1.638167CE 03
100	-1.3503812E 04	-1.3256172E C4	-7.3312812E 03	-1.6787135E 03
101	5.3364375E 03	2.8365C00E 03	1.8925438E 04	-1.6481387E 03
102	-9.6598594E 03	-8.52C2656E 03	3.6853281E 03	-1.6691973E 03
103	-1.8757187E 03	-6.4371563E 03	3.6291219E 04	3.7229531E 03
104	-1.5655CCCE 03	9.2712500E 02	3.1123813E 04	1.C518125E 03
105	4.4492656E 03	-1.3411031E 04	9.2123969E 04	4.3319375E 03
106	-1.684CCCCE 03	-5.1017500E 03	1.1C21537E 05	-4.7910235E 03
107	5.931625CE 03	7.6517500E 03	6.1767875E 04	-1.2237891E 02
108	1.6721875E 02	-1.2267031E 04	9.7051641E 04	7.225875CE 03
109	-2.9135CCCE 03	-1.6062500E 01	1.157246SE 05	-3.C566563E 03
110	1.13C0391E 02	2.4489746E 02	6.46C9141E 03	-2.8255664E 02
111	-2.5639144E 03	-1.3158696E 03	6.0156088E 03	-1.9130327E 03
112	8.0126172E 02	-8.9317188E 02	5.2922773E 03	5.5779785E 01
113	-1.7614170E 03	-1.07CC308E 03	4.9279437E 03	-6.2933105E 01
114	7.45E0469E 02	-7.9759707E 02	4.1209219E 03	2.9551709E 02
115	-1.2962930E 03	-3.2676953E 02	3.9056797E 03	1.4580161E 03
116	3.2764375E 02	-1.8808496E 02	3.1523086E 03	2.1358008E 02
117	-3.8748511E 02	3.8692871E 02	3.C3C8586E 03	1.3238437E 03

Figure 5.10. Results of Creep Analysis

with twelve to eighteen nodal points per partition. Thus, for this division, the largest to be inverted was a 36 x 36 matrix.

The main program and each subroutine was thoroughly checked out before any attempt was made to run the entire program. Many additional 'Write' statements were added (for checking analysis only) to check the formation of the matrices and the mathematical computation at different stages in the programs. Hand calculations were made to verify these checks. The final check was the introduction of a zero applied pillar stress which produced as expected: zero displacements, zero stress, and no change in nodal point co-ordinates.

Included in the programs was a calculation of residuals. These residuals were the difference between the original nodal forces and the nodal forces calculated from the newly solved displacements. As an example, in the second partition, the residuals were found from the matrix equation

$$-\{R_{II}\} = \{P_{II}\} - [C_I]^T\{\delta_I\} - [K_{II}]\{\delta_{II}\} - [C_{II}]\{\delta_{III}\}, \tag{5.12}$$

where: $\{R_{II}\}$ = residuals for second partition,

$\{P_{II}\}$ = nodal forces for second partition,

[C], [K] = parts of overall tridiagonalized stiffness matrix, and

$\{\delta\}$ = newly solved displacements.

For this analysis, the loads on the nodal rings due to the applied pillar load with the load distribution indicated in Figure 5.11 ranged from a low of 2,827.4 pounds to a high of 41,987 pounds. The residuals on the nodal rings for the elastic analysis ranged from a high of 0.07 pounds to a low of 10^{-38} pounds. The residuals for the creep analysis was somewhat larger, ranging in values from a high of 6.5 pounds to a low of 10^{-38} pounds. These residuals in relation to the magnitudes of the nodal forces were quite small and well within the range of accuracy expected in this analysis.

The final analysis of the results of this problem was performed by means of a plot program written for the Calcomp 563 Plotter. Plots of the original nodal points, the nodal points after elastic displacements, and the nodal points after elastic and creep displacements for total times of 10 days, 5 days, and 2 days were performed. This plot routine included the drawing of lines to represent

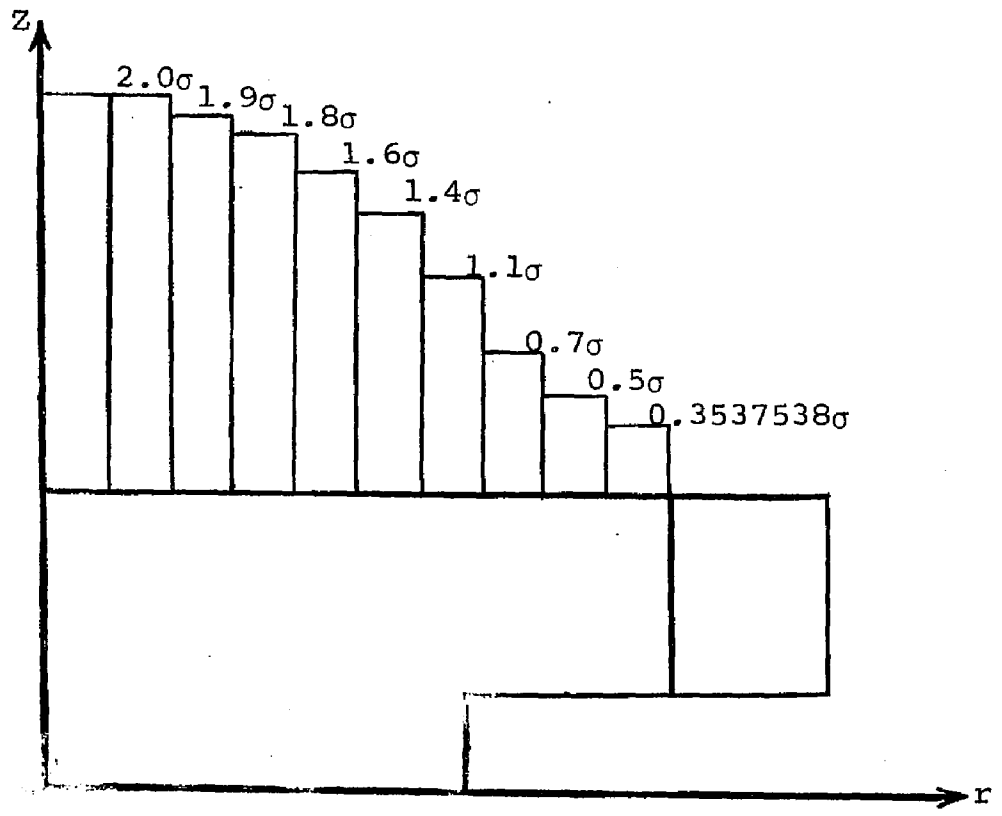

Figure 5.11. Pillar Load Distribution

the finite element, axi-symmetric body idealization, and was run in order to obtain a visual analysis of the deformations. Very little displacement occurred in the elastic analysis alone. In the creep analysis, however, the plots indicated, as expected, a rapid creep at first which decreased with time. Thus, only plots of the original nodal points and of the nodal points after elastic and creep displacements for the two days run were included. (See Figure 5.12 and Figure 5.13.) Included for comparison is Figure 5.14, which is a tracing of a photograph of a deformed salt pillar which appeared in Lomenick's Ph.D. Thesis (65) of March, 1968. Although the pillar load distributions were different, several significant similarities in the deformations of the physical pillar model and the finite element pillar model should be noted. These are:

1. The pillar section of each tended to flow up in a similar fashion into the roof portion of the model.
2. The pillar section of each bulged out in a similar fashion into the room area of the model.
3. The corner of the room area representing the pillar-roof joint in each deformed in a similar manner.

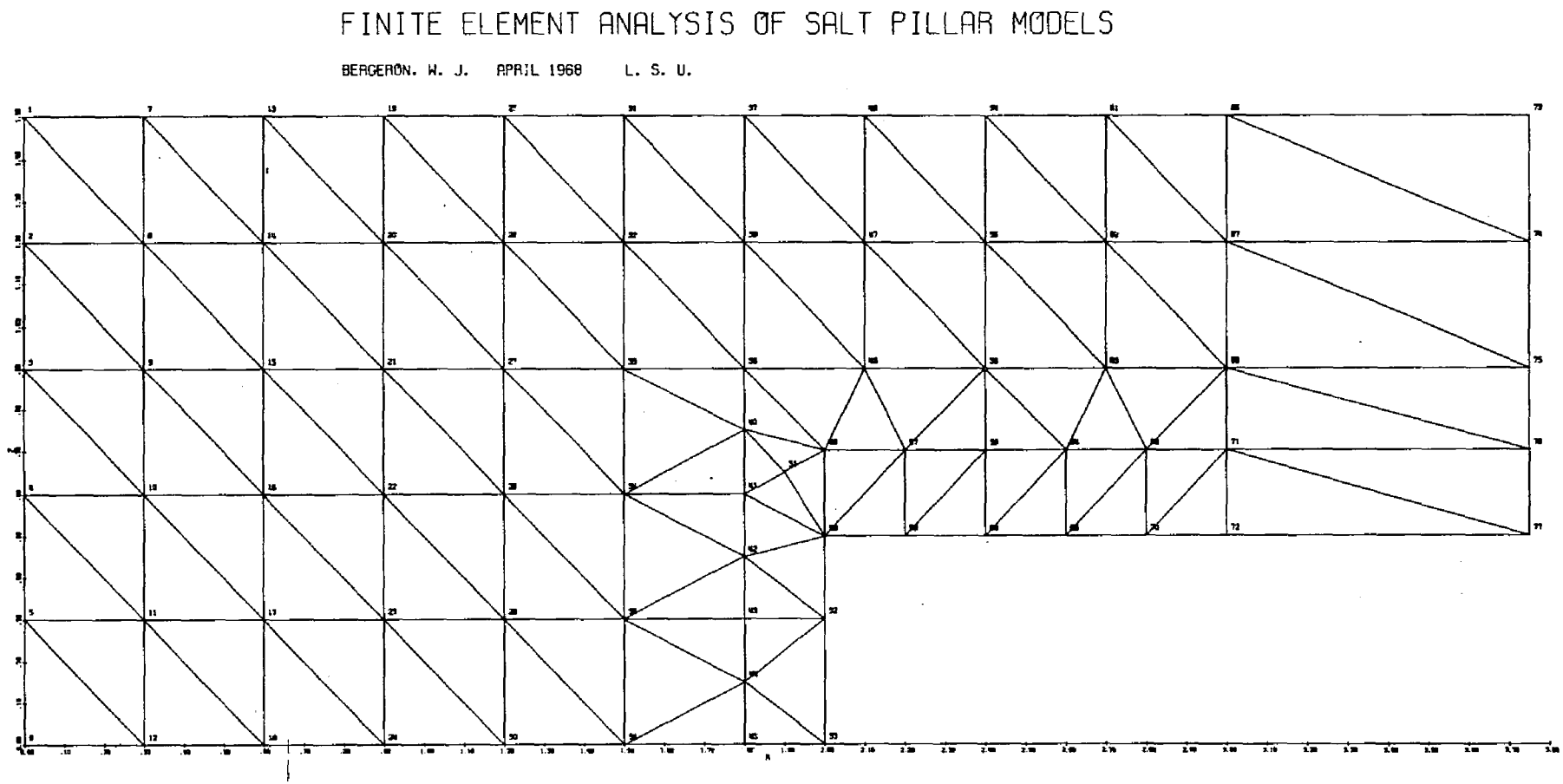

Figure 5.12. Plot of Original Nodal Points

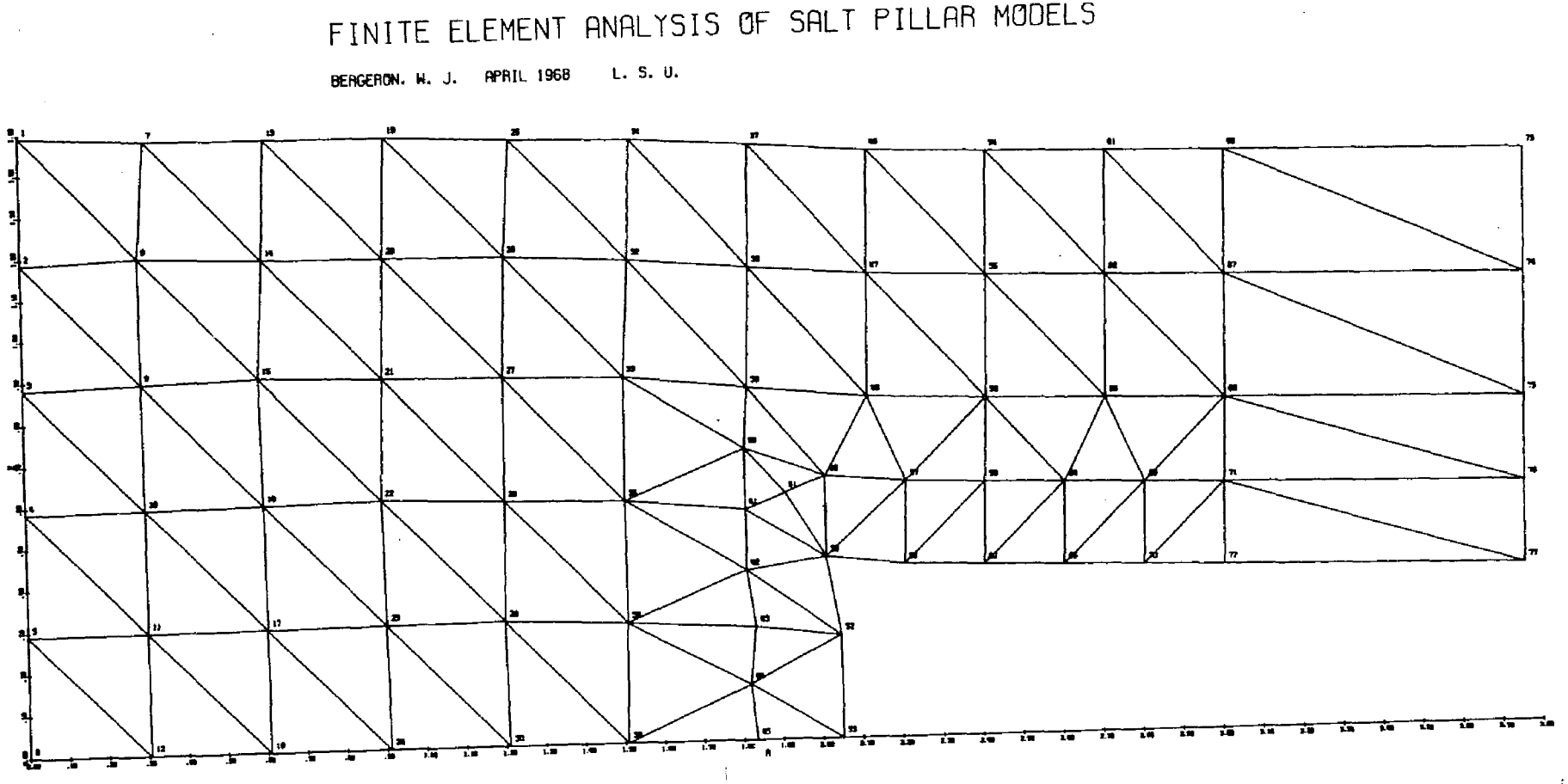

Figure 5.13. Plot of Nodal Points After Elastic and Creep Displacement (Two Days)

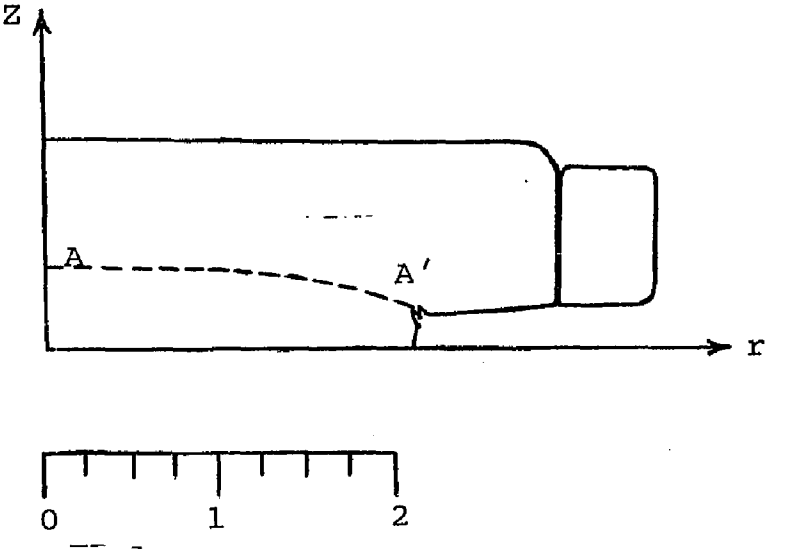

Figure 5.14. Tracing of a Photograph of a Deformed Salt Pillar Model (AA' Represents Original Top of Pillar Section of Model.)

Thus, the small residuals when combined with the excellent correlation between the actual deformed pillar model and the deformed finite element pillar model provided strong support to the validity of the proposed creep law, to the proposed creep modifications, to the basic assumptions made, and to the method of analysis used in this study.

CHAPTER VI

CONCLUSIONS

This was the initial study in this particular research program and no attempt was made to carry any one question to its final and absolute solution. Instead, much effort was spent in gathering background material for this program and in raising questions which this author felt could be at least partially answered by proposing new approaches and by using the existing data from other investigators. It is felt that the additional data required in future studies on any particular question can be obtained by the investigator at that time.

It should be noted that although the proposed creep modifications for the finite element technique and the proposed creep law with its corresponding mechanical model were developed independently of each other, they actually complement each other. This can be observed by considering the mechanical model by its two major components, the elastic component with it's elastic coefficient, D_e, connected in series with the creep component with its response coefficient, D_c. Two such components, by elementary analysis, combine to give the overall coefficient,

$\left(D_e^{-1} + D_c^{-1}\right)^{-1}$. But, this is just D_{ec}, the 'elasto-creep' coefficient as defined by the proposed creep modifications.

Lomenick (65) stated that a theoretical approach to the solution of the problem of creep in rock salt does not appear practical at the present time and also that the mechanisms of deformation within salt pillars are not fully understood. It is felt that this study not only clearly indicates that theoretical solutions are indeed practical, but also that it presents the method which will be used to analyze in detail the deformational mechanisms in the interior of these salt pillars.

Following are several projects which this author believes are within the realm of this research program and which he feels should be carried out by future investigators:

1. A study of the elastic behavior of salt with physical experiments to determine the elastic modulus and Poisson's ratio as functions of temperature. With these values, the original study could be extended into the temperature range expected in the mines.
2. A study of the heat conduction properties of salt and the temperature distribution in the

pillars. This should allow for the method of the original study to be used to account for variations of temperature with position and time in the model. Thus, it would be possible to account for thermal strains and strain rates which vary not only with time but also with temperature.

3. A study of the creep properties of salt which would include the obtaining of more accurate estimates of the uniaxial constants for Equation 5.3, the equation generalized to give the creep law used here.
4. An extension to the original analysis which would include introducing a flat steel plate on top and bottom of the pillar to give a constant displacement there and thus more closely simulate the actual model testing.
5. An extension to the original analysis which would carry it through a number of time steps with iterations in each time step and which would thus account for large displacements. (See outline of these steps in Chapter IV.)
6. An extension to the original analysis which would account for the fact that the hoop component of

stress is not constant through the element but, in fact, actually varies with position in the element.

7. A study with some or all of the above improvements which would include careful measurements of surface displacements of the physical salt pillar model and comparison to computed surface displacements of the finite element model under identical loads and at identical times.
8. A study using the methods indicated above, but with shale layers in the finite element model to determine the effect of shale partings in the mine pillars.

An extension to this work outside of this research program would be the study of other geologic materials which behave in a similar manner to rock salt. This was first proposed by Serata (18) when he observed that rock salt possessed all the important characteristics of rocks, and that the much more pronounced creep characteristics of rock salt should make possible an accurate study of the time dependent properties of the other rock.

BIBLIOGRAPHY

1. Parker, F. L., Hemphill, L., and Crowell, J., Status Report on Waste Disposal in Natural Salt Formations, ORNL - 2560, September, 1958.

2. Lane, J. A., "Determining Nuclear Fuel Requirements for Large-Scale Industrial Power," Nucleonics 12 10, 1954.

3. Regan, W. H. (ed.), Proceedings of the Symposium on the Solidification and Long-Term Storage of Highly Radioactive Wastes, Richland, Washington, CONF 660208, February, 1966.

4. Proceedings of the Princeton Conference on Disposal of Radioactive Wastes Products, Princeton University, Princeton, New Jersey, September 10-12, 1955.

5. Report of the Committee on Waste Disposal of the Division of Earth Sciences, "The Disposal of Radioactive Waste on Land," National Academy of Sciences - National Research Council Publication 519, Washington, D.C., September, 1957.

6. Mineral Resources of the United States, Public Affairs Press, 1958.

7. Birch, F., "Generation of Heat in Radioactive Wastes in Deep Reservoirs," Report for Committee on Waste Disposal of the Division of Earth Sciences, NAC - NRC, 1958.

8. Bradshaw, R. L., Empson, F. M., Boegly, W. J., Jr., Kubota, H., Parker, F. L., Struxhess, E. G., "Properties of Salt Important in Radioactive Waste Disposal," Proceedings of the International Conference on Saline Deposits, Houston, Texas, November 12-17, 1962, In press.

9. Bradshaw, R. L., et al., "Ultimate Storage of High-Level Waste Solids and Liquids in Salt Formations," Treatment and Storage of High-Level Radioactive Wastes, IAEA, Vienna, 1963.

10. Bradshaw, R. L., et al., "Ultimate Storage of High-level Waste Solids and Liquids in Salt Formations," Retention and Migration of Radioactive Ions in Soils, French University Press, Paris, 1963.

11. Boegly, W. J., Jr., Bradshaw, R. L., Empson, F. M., et al., "Project Salt Vault: Radioactive Waste Disposal in a Salt Mine," ORNL-P-1479, 1964.

12. Bradshaw, R. L., Blanche, J. O., Boegly, W. J., Jr., Empson, F. M., et al., "Deposits of High Activity Power Reactor Waste in Salt Mines: A Concept and Field Scale Demonstration," Nuclear Structure Engineering 2, October, 1965.

13. Empson, F. M., Boegly, W. J., Jr., McClain, W. C., et al., "Project Salt Vault: Design and Operation," Proceedings of International Symposium on the Solidification and Long-Term Storage of Highly Radioactive Wastes, Richland, Washington, February 14-18, 1966.

14. Boegly, W. J., Bradshaw, R. L., et al., "Project Salt Vault: A Demonstration Disposal of High-Level Radioactive Solids in Lyons, Kansas Salt Mines," Health Physics 12, March, 1966.

15. Bradshaw, R. L., Lomenick, T. F., McClain, W. C., Empson, F. M., et al., "Model and Underground Studies of the Influence of Stress, Temperature, and Radiation on Flow and Stability in Rock Salt Mines," Proceedings of the First Congress of the International Society of Rock Mechanics, Lisbon, Portugal, September 25 - October 2, 1966.

16. McClain, W. C., Bradshaw, R. L., Empson, F. M., "Disposal of High-Level Solidified Wastes in Salt Mines," ORNL-P-3053, 1967.

17. Morgan, K. Z., et al., Health Physics Division Annual Report, for period ending 31 July 1964, ORNL-3697, 1964.

18. Serata, S., "Theory and Model of Underground Opening and Support System," Proceedings of the Sixth Symposium on Rock Mechanics, Rolla, Missouri, pp. 260-292, October, 1964.

19. Obert, L., "Deformation Behavior of Model Pillars Made from Salt, Trona, and Potash Ore," Proceedings of the Sixth Symposium on Rock Mechanics, Rolla, Missouri, pp. 339-560, October, 1964.

20. Lomenick, T. F., Bradshaw, R. L., "Accelerated Deformation of Rock Salt at Elevated Temperature," Nature 207, pp. 158-159, July 10, 1965.

21. Bradshaw, R. L., Boegly, W. J., Jr., Empson, F. M., "Correlation of Convergence Measurements in Salt Mines with Laboratory Creep-test Data," Proceedings of the Sixth Symposium of Rock Mechanics, Rolla, Missouri, pp. 501-514, October, 1964.

22. Division of Engineering Laboratories, Bureau of Reclamation, Department of Interior, "Triaxial Compression Tests of Salt Rock Cores for the United States Atomic Energy Commission---Project Dribble," Laboratory Report No. C-1043, October, 1962.

23. Boresi, A. P., Deere, D. U., "Creep Closure of a Spherical Cavity in an Infinite Medium," report for Holmes and Narver, Inc., Las Vegas Division, May, 1963.

24. LeCompte, Paul, "Creep in Rock Salt," Journal of Geology 73, pp. 469-484, May, 1965.

25. Stocke, K., Borchert, H., "Fliessgrenzen von Salzgesteinen und Salztektonik," Kali, Vol. 20, 1936.

26. Griggs, David T., "Deformation of Rocks Under High Confining Pressures," Journal of Geology, Vol. 44, pp. 541-77, 1936.

27. Kendall, M. A., "An Investigation of the Creep Phenomena Exhibited by Solenhoten Limestone, Halite, and Cement Under Medium Confining Pressures," Master's Thesis, Agriculture and Mechanical College of Texas, p. 54, 1958.

28. Gunter, B. D., Parker, F. L., "Structural Properties of Rock Salt: Status Report on Waste Disposal in Natural Salt Formations; II," ORNL-2700, Radioactive Waste, p. 14-25, 1959.

29. Brown, K. E., Jessen, F. W., "Effect of Pressure and Temperature on Cavities in Salt," Journal of Petroleum Technology, pp. 341-345, 1959.

30. Serata, S., Gloyna, E. F., "Development of Design Principle for Disposal of Reactor Fuel Waste Into Underground Salt Cavities," Technical Report of University of Texas to Atomic Energy Commission, TID 6317, 1959.

31. Serata, S., Gloyna, E. F., "Principles of Structural Stability of Underground Salt Cavities," Journal of Geophysical Research, Volume 65, No. 9, pp. 2979-2987, September, 1960.

32. Corps of Engineers, "Project Dribble, Petrographic Examination and Physical Tests of Cores, Tatum Salt Dome, Mississippi," Technical Report No. 6-614, January, 1963.

33. Bradshaw, R. L., "Waste Treatment and Disposal, Quarterly Progress Report, May-October 1963," ORNL-TM-757, edit. by Blanco, R. E., and Parker, F. L., 132, 1964.

34. LeCompte, Paul, "Creep and Internal Friction in Rock Salt," Harvard University Doctoral Dissertation, 1960.

35. Turner, M. J., Clough, R. W., Martin, H. C., and Topp, L. J., "Stiffness and Deflection Analysis of Complex Structures," Journal of the Aeronautical Sciences, Vol. 23, No. 9, September, 1956.

36. Clough, R. W., "The Finite Element Method in Plane Stress Analysis," Proceedings, 2nd ASCE Conference on Electronic Computation, Pittsburgh, Pa., September, 1960.

37. Gallagher, R. H., Padlog, J., and Bijlaard, P. P., "Stress Analysis of Heated Complex Shapes," ARS J., 32, 700-707, 1962.

38. Wilson, F. L., "Finite Element Analysis of Two-Dimensional Structures," Structural Engineering Laboratory Report 63-2, University of California, Berkeley, California, June, 1963.

39. Clough, R. W., and Wilson, E. L., "Stress Analysis of a Gravity Dam by the Finite Element Method," RILEM Bulletin, No. 19, June, 1963.

40. Clough, R. W., and Raphael, J. M., "Stress Analysis in Non-Uniform Media by the Finite Element Method," Report No. SESM-63-2, Inst. of Engineering Research, University of California, Berkeley, California.

41. Clough, R. W., "The Finite Element in Structural Mechanics," in: Stress Analysis, Zienkiewicz, O. C. and Holister, G. S., eds., John Wiley, 1965.

42. Adini, A., and Clough, R. W., "Analysis of Plate Bending by the Finite Element Method," Report submitted to the National Science Foundation, Grant G7337, March, 1960.

43. Melosh, R. J., "A Stiffness Matrix for the Analysis of Thin Plates in Bending," Journal of the Aeronautical Sciences, Vol. 28, pp. 34-42, 1961.

44. Melosh, R. J., "Basis for Derivation of Matrices for the Direct Stiffness Method," Journal of the American Institute for Aeronautics and Astronautics, Vol. 1, pp. 1631-1636, July, 1963.

45. Grafton, P. E. and Strome, D. R., "Analysis of Axi-symmetrical Shells by the Direct Stiffness Method," Journal of the American Institute for Aeronautics and Astronautics, Vol. 1, pp. 2342-2347, October, 1963.

46. Popov, E. P., Penzien, J., and Lu, Z. A., "Finite Element Solution of Axi-symmetric Shells," Proceedings of American Society of Civil Engineers, Engineering Mechanics Division, pp. 119-145, 1964.

47. Fraeijs de Veubeke, B., "Displacement and Equilibrium Models in the Finite Element Method," in: Stress Analysis, Zienkiewicz, O. C. and Holister, G. S., eds., John Wiley, 1965.

48. Zienkiewicz, O. C., The Finite Element Method in Structural and Continuum Mechanics, McGraw-Hill, 1967.

49. Zienkiewicz, O. C. and Cheung, Y. K., "Finite Elements in the Solution of Field Problems," The Engineer, pp. 507-510, September 24, 1965.

50. Visser, W., "A Finite Element Method for the Determination of Non-Stationary Temperature Distribution and Thermal Deformations," Prof. Conference on Matrix Methods in Structural Mechanics, Air Force Inst. of Techn., Ohio, October, 1965.

51. Zienkiewicz, O. C., Mayer, P., and Cheung, Y. K., "Solution of Anisotropic Seepage Problems by Finite Elements," Proceedings of the American Society of Civil Engineering, 92, EMI, pp. 111-120, 1966.

52. Wilson, E. L. and Nickell, R. E., "Application of the Finite Element Method to Heat Conduction Analysis," Nuclear Engineering and Design 4, pp. 276-286, 1966.

53. Melosh, R. J., "Structural Analysis of Solids," Journal of the Structural Division, ASCE, Vol. 89, No. ST4, Proc. Paper 3593, August, 1963.

54. Argyris, J. H., "Matrix Analysis of Three-Dimensional Elastic Media - Small and Large Displacement," Journal of American Institute of Aeronautics and Astronautics 3, pp. 45-51, January, 1965.

55. Argyris, J. H., "Three-Dimensional Anisotropic and Inhomogeneous Media - Matrix Analysis for Small and Large Displacements," Ingenious Archives,34, pp. 33055, 1965.

56. Clough, R. W. and Rashid, Y., "Finite Element Analysis of Axi-symmetric Solids," Journal of the Engineering Mechanics Division 91, pp. 71-85, February, 1965.

57. Rashid, Y., "Analysis of Axi-symmetric Composite Structures by the Finite Element Method," Nuclear Engineering and Design 3, pp. 163-182, 1966.

58. Wilson, E. L., "Structural Analysis of Axi-symmetric Solids," Journal of American Institute of Aeronautics and Astronautics 3, pp. 2269-2274, December, 1965.

59. Argyris, J. H., "Elasto-lastic Matrix Displacement Analysis of Three-Dimensional Continua," Journal of the Royal Aeronautical Society 69, pp. 633-635, September, 1965.

60. Marcal, P. V. and King, I. P., "Elastic-plastic Analysis of Two-Dimensional Stress Systems by the Finite Element Method," International Journal of Mechanical Sciences 9, 3, pp. 143-155, March 1967.

61. Fraeijs de Veubeke, B., "Duality Between Displacement and Equilibrium Method with a View to Obtaining Upper and Lower Bounds to Static Influence Coefficients," Proceedings, 14th Meeting of AGARD Structures and Materials Panel, Paris, July, 1962.

62. Shoua, Ezra D., "Effects of Confining Pressure on Polycrystalline Rock Behavior Analysed by Rheological Theory," Proceedings of the First Congress of the International Society of Rock Mechanics, Lisbon, Portugal, September 25-October 1, 1966.

63. Hardy, H. R., Jr., "Analysis of the Inelastic Deformation of Geologic Materials in Terms of Mechanical Models," Proceedings of the Society for Experimental Stress Analysis 1967 Spring Meeting, Ottawa, Ontario, Canada, May 16-19, 1967.

64. Duvall, W. I. and Obert, L., Rock Mechanics and the Design of Structures in Rocks, John Wiley and Sons, Inc., 1967.

65. Lomenick, T. F., "Accelerated Deformation of Rock Salt at Elevated Temperature and Pressure and its Implications for High Level Radioactive Waste Disposal," Ph.D. Thesis, University of Tennessee, March, 1968.

APPENDIX A

DERIVATION OF THE STIFFNESS MATRIX

APPENDIX A

DERIVATION OF THE STIFFNESS MATRIX

In order to make the nodal forces,

$$\{F\}^e = \begin{Bmatrix} F_i \\ F_j \\ F_m \end{Bmatrix} , \tag{A.1}$$

statically equivalent to the actual boundary stresses and distributed loads, an arbitrary (virtual) nodal displacement, $\{\delta^*\}^e$, is imposed and the external and internal work done by the various forces during that displacement are equated.

Equation 4.8 and Equation 4.13 for the displacements and strains within the element yield respectively

$$\{f^*\}^e = [N]^e \{\delta^*\}^e , \text{ and}$$

$$\{\epsilon^*\}^e = [B]^e \{\delta^*\}^e . \tag{A.2}$$

The external work done by the nodal forces is given by

$$\{\delta^*\}^{eT} \{F\}^e . \tag{A.3}$$

The internal work per unit volume done by the stresses and distributed forces is given by

$$\{\epsilon^*\}^{eT} \{\sigma\}^e - \{f^*\}^{eT} \{p\} , \tag{A.4}$$

and using Equations A.2, this becomes

$$\{\delta^*\}^{e^T} \left([B]^{e^T} \{\sigma\}^e - [N]^{e^T} \{p\} \right) . \qquad (A.5)$$

Similarly, the internal work per unit area done by the boundary forces is given by

$$- \{\delta^*\}^{e^T} [N]^{e^T} \{g\} . \qquad (A.6)$$

Equating the external work and the total internal work yields

$$\{\delta^*\}^{e^T} \{F\}^e = \{\delta^*\}^{e^T} \left(\int [B]^{e^T} \{\sigma\}^e \, d(vol) \right. \qquad (A.7)$$

$$- \int [N]^{e^T} \{p\} \, d(vol) - \int [N]^{e^T}$$

$$\left. \{g\} \, d(area) \right) .$$

For arbitrary virtual displacements and with Equation 4.13 and Equation 4.20 substituted into Equation A.7,

$$\{F\}^e = \left(\int [B]^{e^T} [D]^e [B]^e \, d(vol) \right) \{\delta\}^e - \int [B]^{e^T} [D]^e$$

$$\{\epsilon_o\}^e \, d(vol) - \int [N]^{e^T} \{p\} \, d(vol) - \int [N]^{e^T}$$

$$\{g\} \, d(area) . \qquad (A.8)$$

Comparison of Equation A.8 with the general characteristic relation of a structural element (Equation 4.57)

allows the following terms to be defined:

$$\left[K\right]^{e} = \int \left[B\right]^{e^T} \left[D\right]^{e} \left[B\right]^{e} \, d(vol), \tag{A.9}$$

$$\left\{F\right\}^{e}_{\varepsilon_o} = - \int \left[B\right]^{e^T} \left[D\right]^{e} \left\{\varepsilon_o\right\}^{e} \, d(vol), \tag{A.10}$$

$$\left\{F\right\}^{e}_{p} = - \int \left[N\right]^{e^T} \left\{p\right\} \, d(vol), \text{ and} \tag{A.11}$$

$$\left\{F\right\}^{e}_{b} = - \int \left[N\right]^{e^T} \left\{g\right\} \, d(area). \tag{A.12}$$

APPENDIX B

PROGRAM LISTING FOR CREEP RATE ANALYSIS

```
$JOB            BERGERON, W.
$EXECUTE        WATFOR
$ID             00 04 1306 53029                BERGERON, W.
          C     BERGERON W 1306-53029
          C     TRANSIENT CREEP RATE AND STEADY CREEP RATE CHECK2
          C
     1     50   READ(5,20)DELTA,STRESS,TEMP,C1A,ALPHA,C2B,BETA,CTR
     2     20   FORMAT(3F7.0,5E10.4)
     3          IF(STRESS)90,90,51
     4     51   WRITE(6,60)
     5     60   FORMAT(1H1,48HCREEP RATE CHECK   BERGERON, W.   MARCH 68   LSU//)
     6          WRITE(6,61)DELTA,STRESS,TEMP,C1A,ALPHA,C2B,BETA,CTR
     7     61   FORMAT(1X,9HDELTA  = ,F7.0,6H  DAYS/1X,9HSTRESS = ,F7.0,5H  PSI/
               1  1X,9HTEMP    = ,F7.0,11H  DEG. KEL.//1X,
               2  9HC1A     = ,E15.4,/1X,9HALPHA  = ,E15.4,/1X,9HC2B     = ,E15.4,/
               3  1X,9HBETA   = ,E15.4,/1X,9HCTR    = ,E15.4,///1X,4HTIME,8X,
               4  4HTCR ,13X,3HSCR,13X,3HTR ,12X,5HTESTR//)
     10         TIME=DELTA
     11    32   TCR = C1A*TEMP**10.9*STRESS**3.2*EXP(ALPHA*TIME)*10.0**(-20)
     12         SCR=C2B*TEMP**10.9*STRESS**3.2*EXP(BETA*TIME)*10.0**(-20)
     13         TR=TCR+SCR
     14         TESTR=CTR*TEMP**10.9*STRESS**3.2*(TIME*24.)**(-0.65)*10.0**(-20)
     15         WRITE(6,62)TIME,TCR,SCR,TR,TESTR
     16    62   FORMAT(1X,F5.0,1P5E16.7)
     17         TIME=TIME+DELTA
     20         IF(TIME-150.)32,32,50
     21    90   STOP
     22         END
          $ENTRY
```

APPENDIX C

PROGRAM LISTING FOR SALT PILLAR MODEL ANALYSIS

(Linear Elasticity)

```
      BERGERON, h.                          PREPROCESSOR - JOB CCCCCC

$FILE   BERGFN   'FTC02.',U16,U16,BLOCK=2635,SINGLE,LRL=2635,RCT=1,
$ETC             REEL,ERR=RERRX.,EOF=RECFX.,ECR=REORX.
$FILE   BERGFN   'FTC03.',U13,U13,BLOCK=38,DOUBLE,LRL=36,RCT=1,
$ETC             REEL,ERR=RERRX.,EOF=RECFX.,ECR=REORX.
```

FORTRAN SOURCE LIST

```
ISN      SOURCE STATEMENT

  0 $IBFTC
    C      BERGERON W 1306-53025
    C      FINITE ELEMENT ANALYSIS OF SALT PILLAR MODELS
    C      ELASTIC ANALYSIS
    C
    C      MAIN PROGRAM
    C
  1        DIMENSION X(100,2),XE(3,2),NF(15),NB(15,2),BV(15,2),NEP(150),
           1NOD(150,3),E(2),P(2),GE(2),NLBE(10),FPL(10),NSTART(10),
           2NEND(10),NFIRST(10),NLAST(10)
    C
  2        COMMON C(6,6),CBA(4,6),DB(4,6),A(6,6),B(4,6),ST(50,100),U(200,4),
           1XNEW(100,8)
    C
  3        CALL FPTRAP(-3)
  4        REWIND1
  5        REWIND4
    C
    C      READING AND PRINTING OF DATA
    C
    C      READ CONSTANTS
  6        READ(5,10)NPART,NPOIN,NELEM,NBOUN,NODLN,NYM,NFREE,NBEL
 17   10   FORMAT(10I4)
    C      READ NODAL POINT CO-ORDINATES
 20        DO30I=1,NPOIN
 21   30   READ(5,35)X(I,1),X(I,2)
    C      X(I,1)=R CO-ORDINATE OF NODAL POINT I
    C      X(I,2)=Z CO-ORDINATE OF NODAL POINT I
 23   35   FORMAT(5F14.6)
    C      READ ELEMENT NODAL NUMBER AND ELEMENT PROPERTY NUMBER
 24        DO40I=1,NELEM
 25   40   READ(5,10)(NOD(I,J),J=1,3),NEP(I)
    C      NOD(I,J)=NODAL NUMBER OF J NODE OF ELEMENT I
    C      NEP(I)=1 IF ELEMENT IS SALT OR =2 IF STEEL
    C      READ PRESCRIBED DISPLACEMENTS
 33        DO50I=1,NBOUN
 34   50   READ(5,45)NF(I),NB(I,1),NB(I,2),BV(I,1),BV(I,2)
    C      NF(I)=NODAL POINT NUMBER OF FIRST NODAL POINT WITH PRESC. DISP.
 36   45   FORMAT(3I4,2F16.8)
    C      READ FIRST AND LAST ELEMENTS AND NODAL POINTS IN EACH PARTITION
 37        DO60I=1,NPART
 40   60   READ(5,10)NSTART(I),NEND(I),NFIRST(I),NLAST(I)
    C      READ ELASTICITY VALUES
 42        DO61I=1,NYM
 43   61   READ(5,35)E(I),P(I),GE(I)
    C      READ LOADED BOUNDARY ELEMENT NUMBERS AND FPL ON EACH
 45        READ(5,10)(NLBE(I),I=1,NBEL)
    C      NLBE(1)=ELEMENT NUMBER OF FIRST LOADED BOUNDARY ELEMENT
 52        READ(5,11)(FPL(I),I=1,NBEL)
 57   11   FORMAT(9F6.4,F12.8)
    C
    C      ABOVE DATA REMAINS CONSTANT FOR ALL PILLAR LOADS
 60        WRITE(6,2)
 61   2    FORMAT(1H1,45HFINITE ELEMENT ANALYSIS OF SALT PILLAR MODELS//,1X,
           1  35HBERGERON, W.   APRIL, 1968   L.S.U.//)
```

```
                                                FORTRAN SOURCE LIST
ISN       SOURCE STATEMENT

      C
      C       R/W PILLAR LOAD
   62  1      READ(5,62)PILLD
   63  62     FORMAT(F10.0)
   64         WRITE(6,63)PILLD
   65  63     FORMAT(1H ,20HAV. PILLAR STRESS = ,F10.0,5H  PSI/)
      C
      C       CALCULATION OF NODAL LOADS DUE TO PILLAR LOAD
   66  800    NCOLN=NCOLN+1
   67         CALL LOPIL(),XE,NOD,NCOLN,NPOIN,NBEL,NLBE,FPL,PILLD)
      C       FORMATION OF MATRICES
   70         INTER=0
   71         DO70II=1,NPART
   72         DO75I=1,50
   73         DO75J=1,100
   74  75     ST(I,J)=0.
   77         NST=NSTART(II)
  100         NEN=NEND(II)
  101         K=NFIRST(II)
  102         L=NLAST(II)
  103         MINUS=K-1
  104         DO 8000 LK=NST,NEN
  105         MM=LK-INTER
  106         DO85I=1,3
  107         JJ=NOD(LK,I)
  110         XE(I,1)=X(JJ,I)
  111  85     XE(I,2)=X(JJ,2)
  113         J=MEP(LK)
  114         YM=E(J)
  115         PR=P(J)
  116         G=GE(J)
      C
      C       CALCULATION OF ELEMENT STIFFNESS AND STRESS MATRICES
  117         CALL FEM(XE,YM,PR,G,MM)
  120         DO 801  LL=1,3
  121         DO80KK=1,3
  122         IF(NOD(LK,KK)-K)80,131,131
  123  131    IF(NOD(LK,KK)-L)132,132,80
  124  132    M=NFREE*(NOD(LK,KK)-K)
  125         N=NFREE*(NOD(LK,LL)-K)
  126         I=NFREE*(KK-1)
  127         J=NFREE*(LL-1)
  130         IF(N)80,900,900
  131  900    DO5NJ=1,NFREE
  132         DO5MI=1,NFREE
  133         MMI=M+MI
  134         NNJ=N+NJ
  135         IMI=I+MI
  136         JNJ=J+NJ
  137  5      ST(MMI,NNJ)=ST(MMI,NNJ)+C(IMI,JNJ)
  142  80     CONTINUE
  144  801    CONTINUE
  146  8000   CONTINUE
      C
      C       INTRODUCTION OF PRESCRIBED DISPLACEMENTS
```

FORTRAN SOURCE LIST

```
ISN        SOURCE STATEMENT

150        DO290I=1,NBCON
151        M=NF(I)-K
152        MM=NF(I)-1
153        IF(M)290,242,242
154   242  IF(NF(I)-L)243,243,290
155   243  DO230J=1,NFREE
156        IF(NB(I,J))230,345,230
157   345  NMI=NFREE*M+J
160        ST(NMI,NMI)=ST(NMI,NMI)*.1E+12
161        DO233JJ=1,NCOLN
162        JNJ=NFREE*MM+J
163   233  U(JNJ,JJ)=ST(NMI,NMI)*BV(I,J)
165   230  CONTINUE
167   290  CONTINUE
171        INTER=NEN
172        MI=NFREE*MINUS+1
173        NJ=NFREE*L
174        M=NJ-MI+1
175        IF(II-NPART)115,116,115
176   115  NA=NFREE*(NLAST(II+1)-MINUS)
177        GO TO 117
200   116  NA=M+1
201   117  N=NA-M
202        MM=M+1
203   70   WRITE(4)M,N,((ST(I,J),I=1,M),J=1,M),((ST(I,J),I=1,M),J=MM,NA),
          1((U(I,J),I=MI,NJ),J=1,NCOLN)
235        REWIND1
236        REWIND2
237        REWIND3
240        REWIND4
     C
     C     SOLUTION OF TRIDIAGONAL MATRICES AND CALCULATION OF RESIDUALS
241        CALL SOLVE (NPART,NCOLN)
242   8005 REWIND 3
243        CALL STRESS(NPART,NFIRST,NLAST,NCOLN,NELEM,NCC,NFREE,NPOIN,
          1PILLO,X)
244        NCOLN=NCOLN-1
245   20   STOP
246        END
```

FORTRAN SOURCE LIST

```
ISN        SOURCE STATEMENT

  0 $IBFTC LOPIL
  1        SUBROUTINE LOPIL(X,XE,NOD,NCOLN,NPOIN,NBEL,NLBE,FPL,PILLO)
    C      BERGERON W 1306-53029
    C      SUBROUTINE FOR CALCULATION OF LOADS DUE TO PILLAR LOAD
  2        DIMENSION X(100,2),XE(3,2),NOD(150,3),NLBE(10),FPL(10)
  3        COMMON C(6,6),DBA(4,6),DB(4,6),A(6,6),B(4,6),ST(50,100),L(200,4),
          1XNEW(100,8)
    C
  4        NPOIN2=NPOIN*2
  5        DO10I=1,NPOIN2
  6   10   U(I,NCOLN)=0.
 10        DO20II=1,NBEL
 11        CON=FPL(II)*PILLO
 12        IJ=NLBE(II)
 13        DO85I=1,3
 14        JJ=NOD(IJ,I)
    C      IJ IS THE ELEMENT NO. AND JJ IS THE NODAL NO. OF I NODE OF IJ
 15   85   XE(I,1)=X(JJ,1)
 17        ELH=-1.57079632*(XE(3,1)**2-XE(1,1)**2)*CON
 20        DO86I=1,3,2
 21        JJ=NOD(IJ,I)
 22   86   U(2*JJ,NCOLN)=L(2*JJ,NCOLN)+ELH
 24   20   CONTINUE
 26        RETURN
 27        END
```

FORTRAN SOURCE LIST

```
ISN       SOURCE STATEMENT

  0 $IBFTC FEM
  1       SUBROUTINE FEM(XE,YM,PR,G,MM)
    C     BERGERON W 1306-53025
    C     SUBROUTINE FOR FORMATION OF ELEMENT STIFFNESS AND STRESS MATRICES
    C     FOR AXI-SYMETRIC PROBLEM
  2       DIMENSION D(4,4),XE(3,2),ZW(3),ZX(3),ZY(3)
  3       COMMON C(6,6),CBA(4,6),DB(4,6),A(6,6),B(4,6),ST(50,100),U(200,4),
         1XNEW(100,8)
    C
  4       DO20J=1,6
  5       DO21I=1,4
  6       B(I,J)=0.
  7       DB(I,J)=0.
 10    21 CBA(I,J)=0.
 12       DO20I=1,6
 13       A(I,J)=0.
 14    20 C(I,J)=0.
 17       DO22J=1,4
 20       DO22I=1,4
 21    22 D(I,J)=0.
 24       THIRD=1./3.
 25       CRX=(XE(1,1)+XE(2,1)+XE(3,1))*THIRD
 26       CRY=(XE(1,2)+XE(2,2)+XE(3,2))*THIRD
 27       ZW(1)=XE(2,1)*XE(3,2)-XE(3,1)*XE(2,2)
 30       ZW(2)=XE(3,1)*XE(1,2)-XE(1,1)*XE(3,2)
 31       ZW(3)=XE(1,1)*XE(2,2)-XE(2,1)*XE(1,2)
 32       DO5I=1,3
 33       XE(I,1)=XE(I,1)-CRX
 34    5  XE(I,2)=XE(I,2)-CRY
 36       ZX(1)=XE(2,2)-XE(3,2)
 37       ZX(2)=XE(3,2)-XE(1,2)
 40       ZX(3)=XE(1,2)-XE(2,2)
 41       ZY(1)=XE(3,1)-XE(2,1)
 42       ZY(2)=XE(1,1)-XE(3,1)
 43       ZY(3)=XE(2,1)-XE(1,1)
 44       ZK=XE(2,1)*XE(3,2)-XE(3,1)*XE(2,2)
 45       Z=2.*ZK
    C
    C     ELASTICITY MATRIX FOR AXI-SYMMETRIC CASE
 46       DCON=(YM*(1.-PR))/((1.+PR)*(1.-2.*PR))
 47       DCON2=PR/(1.-PR)
 50       D(1,1)=DCON
 51       D(1,2)=DCON*DCON2
 52       D(1,3)=D(1,2)
 53       D(1,4)=0.
 54       D(2,1)=D(1,2)
 55       D(2,2)=DCON
 56       D(2,3)=D(1,2)
 57       D(2,4)=0.
 60       D(3,1)=D(1,3)
 61       D(3,2)=D(2,3)
 62       D(3,3)=DCON
 63       D(3,4)=0.
 64       D(4,1)=D(1,4)
 65       D(4,2)=D(2,4)
```

FORTRAN SOURCE LIST FEM

```
ISN         SOURCE STATEMENT

 66         C(4,3)=D(3,4)
 67         C(4,4)=G
     C
     C      B MATRIX FOR AXI-SYMMETRIC CASE
 70         B(1,2)=ZY(1)
 71         B(1,4)=ZY(2)
 72         B(1,6)=ZY(3)
 73         B(2,1)=ZX(1)
 74         B(2,3)=ZX(2)
 75         B(2,5)=ZX(3)
 76         QUC=ORY/ORX
 77         B(3,1)=ZW(1)/CRX+ZX(1)+ZY(1)*QUC
100         B(3,3)=ZW(2)/CRX+ZX(2)+ZY(2)*QUC
101         B(3,5)=ZW(3)/CRX+ZX(3)+ZY(3)*QUC
102         B(4,1)=ZY(1)
103         B(4,2)=ZX(1)
104         B(4,3)=ZY(2)
105         B(4,4)=ZX(2)
106         B(4,5)=ZY(3)
107         B(4,6)=ZX(3)
110         DO40I=1,4
111         DO40J=1,6
112         DO40K=1,4
113   40    DB(I,J)=DB(I,J)+C(I,K)*B(K,J)/Z
117         VOL=3.14159265*Z*ORX
120         DO60I=1,6
121         DO60J=1,6
122         DO60K=1,4
123   60    C(I,J)=C(I,J)+B(K,I)*DB(K,J)*VOL/Z
127         IF(MM)128,128,127
130   127   WRITE(1)((DB(I,J),I=1,4),J=1,6),CRX,CRY
141   128   RETURN
142         END
```

FORTRAN SOURCE LIST

```
ISN       SOURCE STATEMENT

  0 $IBFTC SOLVE
  1       SUBROUTINE SOLVE(NPART,NCOLN)
    C     BERGERON W 1306-5302S
    C     SUBROUTINE FOR SOLUTION OF EQUATIONS
  2       DIMENSION AM(50,50),BM(50,50),YM(50,50),TF(50,4),RS(50,4),F(50,4),
         1DIS(50,4)
  3       COMMON C(6,6),CBA(4,6),DB(4,6),A(6,6),B(4,6),ST(50,100),L(200,4),
         1XNEW(100,8)
    C
  4       DO140I=1,50
  5       DO141J=1,NCOLN
  6       TF(I,J)=0.
  7   141 RS(I,J)=0.
 11       DO140J=1,50
 12   140 YM(I,J)=0.
 15       DO144LL=1,NPART
 16       READ(4)M,N,((AM(I,J),I=1,M),J=1,M),((BM(I,J),I=1,M),J=1,N),
         1((F(I,J),I=1,M),J=1,NCOLN)
 51   150 DO424I=1,M
 52       DO425J=1,NCOLN
 53       F(I,J)=F(I,J)-TF(I,J)
 54   425 DIS(I,J)=F(I,J)
 56       DO424J=1,M
 57   424 AM(I,J)=AM(I,J)-YM(I,J)
 62       CALL MATINV(AM,M,DIS,NCOLN)
 63       WRITE(2)M,N,((AM(I,J),I=1,M),J=1,M),((BM(I,J),I=1,M),J=1,N),
         1((F(I,J),I=1,M),J=1,NCOLN)
114       IF(NPART-LL)437,437,432
115    432 CALL MATM(AM,F,DIS,M,M,NCOLN)
116       CALL MATTM(BM,DIS,TF,N,M,NCOLN)
117       DO110J=1,N
120       DO110I=1,M
121       YM(I,J)=0.
122       DO110K=1,M
123   110 YM(I,J)=YM(I,J)+AM(I,K)*BM(K,J)
127       DO111J=1,N
130       DO111I=1,N
131       AM(I,J)=0.
132       DO111K=1,M
133   111 AM(I,J)=AM(I,J)+BM(K,I)*YM(K,J)
137       DO112I=1,N
140       DO112J=1,N
141   112 YM(I,J)=AM(I,J)
144   144 CONTINUE
146   437 REWIND4
147       WRITE(3)((DIS(I,J),I=1,M),J=1,NCOLN)
160       IF(NPART-1)600,600,601
161   601 NA=NPART-1
162       DO441LL=1,NA
163       BACKSPACE2
164       BACKSPACE2
165       READ(2)M,N,((AM(I,J),I=1,M),J=1,M),((BM(I,J),I=1,M),J=1,N),
         1((F(I,J),I=1,M),J=1,NCOLN)
220       CALL MATM(BM,DIS,TF,M,N,NCOLN)
221       DO444J=1,NCOLN
```

FORTRAN SOURCE LIST SOLVE

```
ISN        SOURCE STATEMENT

222        DO444I=1,M
223   444  F(I,J)=F(I,J)-TF(I,J)
226        CALL MATM(AM,F,DIS,M,M,NCOLN)
227   441  WRITE(3)((DIS(I,J),I=1,M),J=1,NCOLN)
241        WRITE(6,515)
242   515  FORMAT(10H RESIDUALS/)
243        DO5COLL=1,NPART
244        READ(4)M,N,((AM(I,J),I=1,M),J=1,M),((BM(I,J),I=1,M),J=1,N),
          1((F(I,J),I=1,M),J=1,NCOLN)
277        BACKSPACE3
300        READ(3)((DIS(I,J),I=1,M),J=1,NCOLN)
311        IF(LL-NPART)508,505,505
312   505  DO506J=1,NCOLN
313        DO506I=1,N
314   506  TF(I,J)=0.
317        GO TO 509
320   508  BACKSPACE3
321        BACKSPACE3
322        READ(3)((TF(I,J),I=1,N),J=1,NCOLN)
333   509  DO510J=1,NCOLN
334        DO510I=1,M
335        F(I,J)=F(I,J)-RS(I,J)
336        DO512K=1,M
337   512  F(I,J)=F(I,J)-AM(I,K)*DIS(K,J)
341        DO510L=1,N
342   510  F(I,J)=F(I,J)-BM(I,L)*TF(L,J)
346        CALL MATTM(BM,DIS,RS,N,M,NCOLN)
347        WRITE(6,516)LL
350   516  FORMAT(1X,12HPART. NO.  =,I4,)
351   500  WRITE(6,31)((F(I,J),I=1,M),J=1,NCOLN)
363   31   FORMAT(1X,12E9.2)
364   600  CONTINUE
365         RETURN
366        END
```

FORTRAN SOURCE LIST

```
ISN       SOURCE STATEMENT

  0 $IBFTC MATM
  1       SUBROUTINE MATM(XMAT,YMAT,PMAT,M,N,NCOLN)
    C     BERGERON W 1306-53029
    C     MATRIX MULTIPLICATION
  2       DIMENSION XMAT(50,50),YMAT(50,4),PMAT(50,4)
  3       COMMON C(6,6),CBA(4,6),DB(4,6),A(6,6),B(4,6),ST(50,100),L(200,4),
         1XNEW(100,8)
    C     XMAT IS M BY N LEFT MATRIX TO BE MULTIPLIED
    C     YMAT IS N BY NCOLN RIGHT MATRIX TO BE MULTIPLIED
    C     PMAT IS M BY NCOLN PRODUCT MATRIX
    C
  4       DO10I=1,M
  5       DO10J=1,NCOLN
  6       PMAT(I,J)=0.
  7       DO10K=1,N
 10   10    PMAT(I,J)=PMAT(I,J)+XMAT(I,K)*YMAT(K,J)
 14       RETURN
 15       END
```

FORTRAN SOURCE LIST

```
ISN       SOURCE STATEMENT

  0 $IBFTC MATTM
  1       SUBROUTINE MATTM(XMAT,YMAT,PMAT,N,M,NCOLN)
    C     BERGERON W 1306-53029
    C     MATRIX MULTIPLICATION WITH XMAT TRANSPOSED
  2       DIMENSION XMAT(50,50),YMAT(50,4),PMAT(50,4)
  3       COMMON C(6,6),DBA(4,6),DB(4,6),A(6,6),B(4,6),ST(50,100),L(200,4),
         1XNEW(100,8)
    C     XMAT IS M BY N LEFT MATRIX
    C     YMAT IS M BY NCOLN RIGHT MATRIX
    C     PMAT IS N BY NCOLN PRODUCT OF XMAT TRANSPOSED AND YMAT
    C
  4       DO 10 I=1,N
  5       DO 10 J=1,NCOLN
  6       PMAT(I,J)=0.
  7       DO 10 K=1,M
 10    10 PMAT(I,J)=PMAT(I,J)+XMAT(K,I)*YMAT(K,J)
 14       RETURN
 15       END
```

FORTRAN SOURCE LIST

```
ISN       SOURCE STATEMENT

  0 $IBFTC STRESS
  1       SUBROUTINE STRESS(NPART,NFIRST,NLAST,NCOLN,NELEM,NOD,NFREE,NPOIN,
         1PILLD,X)
    C     BERGERON W 1306-53029
    C     SUBROUTINE FOR CALCULATION OF STRESSES
  2       DIMENSION NOD(150,3),NFIRST(15),NLAST(15),X(100,2)
  3       COMMON C(6,6),DBA(4,6),DB(4,6),A(6,6),B(4,6),ST(50,100),U(200,4),
         1XNEW(100,8)
    C
  4       DO6O I=1,NPART
  5       JJ=NPART+1-II
  6       M=NFREE*(NFIRST(JJ)-1)+1
  7       N=NFREE*NLAST(JJ)
 10  600  READ(3)((U(I,J),I=M,N),J=1,NCOLN)
 22       DO5O I=1,NPOIN
 23       DO5O J=1,NCOLN
 24       XNEW(I,2*J-1)=X(I,1)+U(2*I-1,J)
 25  50   XNEW(I,2*J)=X(I,2)+U(2*I,J)
 30       WRITE(6,613)
 31  613  FORMAT(1H1,45HFINITE ELEMENT ANALYSIS OF SALT PILLAR MODELS/,1X,
         1  16HELASTIC ANALYSIS//,1X,26HBERGERON, W.   APRIL, 1968,3X,
         2  6HL.S.U.//)
 32       WRITE(6,614)PILLD
 33  614  FORMAT(1X,24HAVERAGE PILLAR STRESS = ,F10.0,5H  PSI/)
 34       WRITE(6,615)
 35  615  FORMAT(1H ,40HNODE   R-DISPLACEMENTS   Z-DISPLACEMENTS,5X,
         1  31HNEW R CO-ORD.      NEW Z CO-ORD./)
 36       WRITE(6,32)((I,U(2*I-1,J),U(2*I,J),XNEW(I,2*J-1),XNEW(I,2*J),
         1II=1,NPOIN),J=1,NCOLN)
 47  32   FORMAT(1X,I4,1P4E18.8)
 50       WRITE(7,33)((U(2*I-1,J),U(2*I,J),I=1,NPOIN),J=1,NCOLN)
 61  33   FORMAT(2E16.8)
 62       WRITE(6,635)
 63  635  FORMAT(1H1,15HELEMENT NUMBER ,16H    Z-STRESS    ,
         1  16H    R-STRESS    ,16H    T-STRESS    ,16H    RZ-STRESS   /)
    C
 64       DO2OLL=1,NELEM
 65       READ(1)((CB(I,J),I=1,4),J=1,6),CRX,CRY
 76       DO62OJ=1,NCOLN
 77       DO62OI=1,3
100       JJ=NOD(LL,I)
101       C(2*I-1,J)=U(2*JJ-1,J)
102  620  C(2*I,J)=U(2*JJ,J)
105       DO63OJ=1,NCOLN
106       DO63OI=1,4
107       DBA(I,J)=0.
110       DO63OK=1,6
111  630  DBA(I,J)=DBA(I,J)+DB(I,K)*C(K,J)
115       WRITE(6,31)LL,((DBA(I,J),I=1,4),J=1,NCOLN)
126  31   FORMAT(6X,I4,5X,1P4E16.7)
127       WRITE(7,46)((DBA(I,J),I=1,4),J=1,NCOLN)
140  46   FORMAT(4E16.8)
141  20   CONTINUE
143       WRITE(7,45)((XNEW(I,2*J-1),XNEW(I,2*J),I=1,NPOIN),J=1,NCOLN)
154  45   FORMAT(2F14.6)
```

FORTRAN SOURCE LIST STRESS

```
ISN       SOURCE STATEMENT

155        RETURN
156       END
```

FORTRAN SOURCE LIST

```
ISN        SOURCE STATEMENT

  0 $IBFTC MATINV
  1        SUBROUTINE MATINV(A,N,B,M)
           C      MATRIX INVERSION WITH ACCOMPANYING SOLUTION OF LINEAR EQUATIONS
           C
           C      INITIALIZATION
  2        DIMENSION IPIVOT(50),A(50,50),B(50,4),INDEX(50,2),PIVOT(50)
  3     10 DETERM=1.0
  4     15 DO 20 J=1,N
  5     20 IPIVOT(J)=0
  7     30 DO 550 I=1,N
           C
           C      SEARCH FOR PIVOT ELEMENT
 10     40 AMAX=0.0
 11     45 DO 105 J=1,N
 12     50 IF(IPIVOT(J)-1)60,105,60
 13     60 DO 100 K=1,N
 14     70 IF(IPIVOT(K)-1)80,100,740
 15     80 IF(ABS(AMAX)-ABS(A(J,K)))85,100,100
 16     85 IROW=J
 17     90 ICOLUM=K
 20     95 AMAX=A(J,K)
 21    100 CONTINUE
 23    105 CONTINUE
 25    110 IPIVOT(ICOLUM)=IPIVOT(ICOLUM)+1
           C
           C      INTERCHANGE ROWS TO PUT PIVOT ELEMENT ON DIAGONAL
 26    130 IF(IROW-ICOLUM)140,260,140
 27    140 DETERM=-DETERM
 30    150 DO 200 L=1,N
 31    160 SWAP=A(IROW,L)
 32    170 A(IROW,L)=A(ICOLUM,L)
 33    200 A(ICOLUM,L)=SWAP
 35    205 IF(M)260,260,210
 36    210 DO 250 L=1,M
 37    220 SWAP=B(IROW,L)
 40    230 B(IROW,L)=B(ICOLUM,L)
 41    250 B(ICOLUM,L)=SWAP
 43    260 INDEX(I,1)=IROW
 44    270 INDEX(I,2)=ICOLUM
 45    310 PIVOT(I)=A(ICOLUM,ICOLUM)
 46    320 DETERM=DETERM*PIVOT(I)
           C
           C      DIVIDE PIVOT ROW BY PIVOT ELEMENT
 47    330 A(ICOLUM,ICOLUM)=1.0
 50    340 DO 350 L=1,N
 51    350 A(ICOLUM,L)=A(ICOLUM,L)/PIVOT(I)
 53    355 IF(M)380,380,360
 54    360 DO 370 L=1,M
 55    370 B(ICOLUM,L)=B(ICOLUM,L)/PIVOT(I)
           C      REDUCE NON-PIVOT ROWS
 57     380 DO 545 L1=1,N
 60     391 IF(L1-ICOLUM)400,545,400
 61    400 T=A(L1,ICOLUM)
 62    420 A(L1,ICOLUM)=0.0
 63    430 DO 450 L=1,N
```

FORTRAN SOURCE LIST MATINV

```
ISN        SOURCE STATEMENT

 64   450   A(L1,L)=A(L1,L)-A(ICOLUM,L)*T
 66    456  IF(M)545,545,460
 67   460   DO500L=1,M
 70   500   B(L1,L)=B(L1,L)-B(ICOLUM,L)*T
 72    545  CONTINUE
 74   550   CONTINUE
    C
    C      INTERCHANGE COLUMNS
 76   600   DO710I=1,N
 77   610   L=N+1-I
100   620   IF(INDEX(L,1)-INDEX(L,2))630,710,630
101   630   JROW=INDEX(L,1)
102   640   JCOLUM=INDEX(L,2)
103   650   DO705K=1,N
104   660   SWAP=A(K,JROW)
105   670   A(K,JROW)=A(K,JCOLUM)
106   700   A(K,JCOLUM)=SWAP
107   705   CONTINUE
111   710   CONTINUE
113   740   RETURN
114   750   END
```

APPENDIX D

PROGRAM LISTING FOR SALT PILLAR ANALYSIS

(Creep Effects Modification)

```
      BERGERON, W.                          PREPROCESSOR - JOB 000000

$FILE   BERGRN   'FT002.',U16,U16,BLOCK=2635,SINGLE,LRL=2635,RCT=1,
$ETC             REEL,ERR=RERRX.,EOF=RECFX.,ECR=REORX.
$FILE   BERGRN   'FT003.',U13,U13,BLOCK=38,DOUBLE,LRL=36,RCT=1,
$ETC             REEL,ERR=RERRX.,EOF=RECFX.,ECR=RECRX.
```

FORTRAN SOURCE LIST

```
ISN       SOURCE STATEMENT

  0 $IBFTC
    C      BERGERON W 1306-53025
    C      FINITE ELEMENT ANALYSIS OF SALT PILLAR MODELS
    C      CREEP MODIFICATIONS
    C
    C      MAIN PROGRAM
    C
  1        DIMENSION X(100,2),XE(3,2),NF(15),NB(15,2),BV(15,2),NEP(150),
           1NOD(150,3),E(2),P(2),GE(2),NLBE(10),FPL(10),NSTART(10),
           2NEND(10),NFIRST(10),NLAST(10),STRESS(150,3)
    C
  2        COMMON C(6,6),CBA(4,6),DB(4,6),A(6,6),B(4,6),ST(50,100),U(200,4),
           1XNEW(100,8)
    C
  3        CALL FPTRAP(-3)
  4        REWIND1
  5        REWIND4
    C
    C      READING AND PRINTING OF DATA
    C
    C      READ CONSTANTS
  6        READ(5,10)NPART,NPOIN,NELEM,NBOUN,NODUN,NYM,NFREE,NBEL
 17   10   FORMAT(10I4)
    C      READ NODAL POINT CO-ORDINATES
 20        DO30I=1,NPOIN
 21   30   READ(5,35)X(I,1),X(I,2)
    C      X(I,1)=R CO-ORDINATE OF NODAL POINT I
    C      X(I,2)=Z CO-ORDINATE OF NODAL POINT I
 23   35   FORMAT(5F14.6)
    C      READ ELEMENT NODAL NUMBER AND ELEMENT PROPERTY NUMBER
 24        DO40I=1,NELEM
 25   40   READ(5,10)(NOD(I,J),J=1,3),NEP(I)
    C      NOD(I,J)=NODAL NUMBER OF J NODE OF ELEMENT I
    C      NEP(I)=1 IF ELEMENT IS SALT OR =2 IF STEEL
    C      READ PRESCRIBED DISPLACEMENTS
 33        DO50I=1,NBOUN
 34   50   READ(5,45)NF(I),NB(I,1),NB(I,2),BV(I,1),BV(I,2)
    C      NF(1)=NODAL POINT NUMBER OF FIRST NODAL POINT WITH PRESC. DISP.
 36   45   FORMAT(3I4,2F16.8)
    C      READ FIRST AND LAST ELEMENTS AND NODAL POINTS IN EACH PARTITION
 37        DO60I=1,NPART
 40   60   READ(5,10)NSTART(I),NEND(I),NFIRST(I),NLAST(I)
    C      READ ELASTICITY VALUES
 42        DO61I=1,NYM
 43   61   READ(5,35)E(I),P(I),GE(I)
    C      READ LOADED BOUNDARY ELEMENT NUMBERS AND FPL ON EACH
 45        READ(5,10)(NLBE(I),I=1,NBEL)
    C      NLBE(1)=ELEMENT NUMBER OF FIRST LOADED BOUNDARY ELEMENT
 52        READ(5,11)(FPL(I),I=1,NBEL)
 57   11   FORMAT(9F6.4,F12.8)
    C
    C      ABOVE DATA REMAINS CONSTANT FOR ALL PILLAR LOADS
 60        WRITE(6,2)
 61   2    FORMAT(1H1,45HFINITE ELEMENT ANALYSIS OF SALT PILLAR MODELS//,1X,
           1  35HBERGERON, W.   APRIL, 1968   L.S.U.//)
```

FORTRAN SOURCE LIST

```
ISN        SOURCE STATEMENT

     C
     C     R/W PILLAR LOAD
  62  1    READ(5,62)PILLO
  63  62   FORMAT(F10.0)
  64       WRITE(6,63)PILLO
  65  63   FORMAT(1H ,20HAV. PILLAR STRESS = ,F10.0,5H  PSI/)
     C
     C     READ STRESS FROM PROGRAM NO. 1, STRESS(I,J)
     C     I=ELEMENT NO., J=1,2,3 FOR Z,R,T STRESS
  66       DO 64 I=1,NELEM
  67  64   READ(5,65)(STRESS(I,J),J=1,3)
  75  65   FORMAT(3E16.8)
  76       READ(5,66)TIME,DTIME,TEMP
  77  66   FORMAT(3F8.0)
     C
     C     CALCULATION OF NODAL LOADS DUE TO PILLAR LOAD
 100  800  NCOLN=NCOLN+1
 101       CALL LDPIL(X,XE,NOD,NCOLN,NPOIN,NBEL,NLBE,FPL,PILLO)
     C     FORMATION OF MATRICES
 102       INTER=0
 103       DO 70 II=1,NPART
 104       DO 75 I=1,50
 105       DO 75 J=1,100
 106  75   ST(I,J)=0.
 111       NST=NSTART(II)
 112       NEN=NEND(II)
 113       K=NFIRST(II)
 114       L=NLAST(II)
 115       MINUS=K-1
 116       DO 8000 LK=NST,NEN
 117       MM=LK-INTER
 120       DO 85 I=1,3
 121       JJ=NOD(LK,I)
 122       XE(I,1)=X(JJ,1)
 123  85   XE(I,2)=X(JJ,2)
 125       J=NEP(LK)
 126       YM=E(J)
 127       PR=P(J)
 130       G=GE(J)
 131       SZ=STRESS(LK,1)
 132       SR=STRESS(LK,2)
 133       STAN=STRESS(LK,3)
     C
     C     CALCULATION OF ELEMENT STIFFNESS AND STRESS MATRICES
 134       CALL FEM(XE,YM,PR,G,MM,TIME,DTIME,TEMP,J,SZ,SR,STAN)
 135       DO 801  LL=1,3
 136       DO 80 KK=1,3
 137       IF(NOD(LK,KK)-K)80,131,131
 140  131  IF(NOD(LK,KK)-L)132,132,80
 141  132  M=NFREE*(NOD(LK,KK)-K)
 142       N=NFREE*(NOD(LK,LL)-K)
 143       I=NFREE*(KK-1)
 144       J=NFREE*(LL-1)
 145       IF(N)80,900,900
 146  900  DO 5 NJ=1,NFREE
```

FORTRAN SOURCE LIST

```
ISN        SOURCE STATEMENT

147        DO5MI=1,NFREE
150        MMI=M+MI
151        NNJ=N+NJ
152        IMI=I+MI
153        JNJ=J+NJ
154   5    ST(MMI,NNJ)=ST(MMI,NNJ)+C(IMI,JNJ)
157   80   CONTINUE
161   801  CONTINUE
163   80CC CONTINUE
      C
      C    INTRODUCTION OF PRESCRIBED DISPLACEMENTS
165        DO290I=1,NBCUN
166        M=NF(I)-K
167        MM=NF(I)-1
170        IF(M)290,242,242
171   242  IF(NF(I)-L)243,243,290
172   243  DO230J=1,NFREE
173        IF(NB(I,J))230,345,230
174   345  MMI=NFREE*M+J
175        ST(MMI,MMI)=ST(MMI,MMI)*.1E+12
176        DO233JJ=1,NCOLN
177        JNJ=NFREE*MM+J
200   233  U(JNJ,JJ)=ST(MMI,MMI)*BV(I,J)
202   230  CONTINUE
204   290  CONTINUE
206        INTER=NEN
207        MI=NFREE*MINUS+1
210        NJ=NFREE*L
211        M=NJ-MI+1
212        IF(II-NPART)115,116,115
213   115  NA=NFREE*(NLAST(II+1)-MINUS)
214        GO TO 117
215   116  NA=M+1
216   117  N=NA-M
217        MM=M+1
220   70   WRITE(4)M,N,((ST(I,J),I=1,M),J=1,M),((ST(I,J),I=1,M),J=MM,NA),
          1((L(I,J),I=MI,NJ),J=1,NCOLN)
252        REWIND1
253        REWIND2
254        REWIND3
255        REWIND4
      C
      C    SOLUTION OF TRIDIAGONAL MATRICES AND CALCULATION OF RESIDUALS
256        CALL SOLVE (NPART,NCOLN)
257   800S REWIND 3
260        CALL TOTDIS(NPART,NFIRST,NLAST,NCOLN,NELEM,NCC,NFREE,NPOIN,
          1PILLD,X)
261        NCOLN=NCOLN-1
262   20   STOP
263        END
```

FORTRAN SOURCE LIST

```
ISN        SOURCE STATEMENT

  0 $IBFTC LCPIL
  1        SUBROUTINE LCPIL(X,XE,NOD,NCOLN,NPOIN,NBEL,NLBE,FPL,PILLC)
    C      BERGERON W 1306-5302S
    C      SUBROUTINE FOR CALCULATION OF LOADS DUE TO PILLAR LOAD
  2        DIMENSION X(100,2),XE(3,2),NOD(150,3),NLBE(10),FPL(10)
  3        COMMON C(6,6),CBA(4,6),DB(4,6),A(6,6),B(4,6),ST(50,100),U(200,4),
          1XNEW(100,8)
    C
  4        NPOIN2=NPOIN*2
  5        DO10I=1,NPOIN2
  6   10   U(I,NCOLN)=0.
 10        DO20II=1,NBEL
 11        CON=FPL(II)*PILLC
 12        IJ=NLBE(II)
 13        DO85I=1,3
 14        JJ=NOD(IJ,I)
    C      IJ IS THE ELEMENT NO. AND JJ IS THE NODAL NO. OF I NODE OF IJ
 15   85   XE(I,1)=X(JJ,1)
 17        ELH=-1.57079632*(XE(3,1)**2-XE(1,1)**2)*CON
 20        DO86I=1,3,2
 21        JJ=NOD(IJ,I)
 22   86   U(2*JJ,NCOLN)=U(2*JJ,NCOLN)+ELH
 24   20   CONTINUE
 26        RETURN
 27        END
```

FORTRAN SOURCE LIST

```
ISN       SOURCE STATEMENT

  0 $IBFTC FEM
  1       SUBROUTINE FEM(XE,YM,PR,G,MM,TIME,CTIME,TEMP,JJ,SZ,SR,STAN)
    C     BERGERON W 1306-53029
    C     SUBROUTINE FOR FORMATION OF ELEMENT STIFFNESS AND STRESS MATRICES
    C     FOR AXI-SYMETRIC PROBLEM
  2       DIMENSION D(50,50),XE(3,2),ZW(3),ZX(3),ZY(3),DEI(4,4),DDI(4,4),
         1DUM(50,1)
  3       COMMON C(6,6),CBA(4,6),DB(4,6),A(6,6),B(4,6),ST(50,100),U(200,4),
         1XNEW(100,8)
    C
  4       DO20J=1,6
  5       DO21I=1,4
  6       B(I,J)=0.
  7       DB(I,J)=0.
 10  21   DBA(I,J)=0.
 12       DO20I=1,6
 13       A(I,J)=0.
 14  20   C(I,J)=0.
 17       THIRD=1./3.
 20       CRX=(XE(1,1)+XE(2,1)+XE(3,1))*THIRD
 21       CRY=(XE(1,2)+XE(2,2)+XE(3,2))*THIRD
 22       ZW(1)=XE(2,1)*XE(3,2)-XE(3,1)*XE(2,2)
 23       ZW(2)=XE(3,1)*XE(1,2)-XE(1,1)*XE(3,2)
 24       ZW(3)=XE(1,1)*XE(2,2)-XE(2,1)*XE(1,2)
 25       DO5I=1,3
 26       XE(I,1)=XE(I,1)-CRX
 27  5    XE(I,2)=XE(I,2)-CRY
 31       ZX(1)=XE(2,2)-XE(3,2)
 32       ZX(2)=XE(3,2)-XE(1,2)
 33       ZX(3)=XE(1,2)-XE(2,2)
 34       ZY(1)=XE(3,1)-XE(2,1)
 35       ZY(2)=XE(1,1)-XE(3,1)
 36       ZY(3)=XE(2,1)-XE(1,1)
 37       ZK=XE(2,1)*XE(3,2)-XE(3,1)*XE(2,2)
 40       Z=3.*ZK
 41       IF(JJ-2)1,2,2
    C
    C     INVERTED ELASTICITY MATRIX FOR AXI-SYM. CASE
 42  1    PE=-PR/YM
 43       DEI(1,1)=1./YM
 44       DEI(1,2)=PE
 45       DEI(1,3)=PE
 46       DEI(1,4)=0.0
 47       DEI(2,1)=PE
 50       DEI(2,2)=DEI(1,1)
 51       DEI(2,3)=PE
 52       DEI(2,4)=0.0
 53       DEI(3,1)=PE
 54       DEI(3,2)=PE
 55       DEI(3,3)=DEI(1,1)
 56       DEI(3,4)=0.0
 57       DEI(4,1)=0.0
 60       DEI(4,2)=0.0
 61       DEI(4,3)=0.0
 62       DEI(4,4)=1./G
```

FORTRAN SOURCE LIST FEP

```
ISN       SOURCE STATEMENT

    C
    C     INVERTED CREEP MATRIX FOR AXI-SYM. CASE
 63         FES=(1./2.**1.1)*(((SZ-SR)**2+(SR-STAN)**2+(STAN-SZ)**2)**1.1)
 64         TMT=10.**(-20)
 65         CC=.768*TMT*TEMP**10.9*(TIME*24.)**(-0.65)*FES*DTIME*TMT
 66         CP=-CC/2.
 67         DCI(1,1)=CC
 70         DCI(1,2)=CP
 71         DCI(1,3)=CP
 72         DCI(1,4)=0.0
 73         DCI(2,1)=CP
 74         DCI(2,2)=CC
 75         DCI(2,3)=CP
 76         DCI(2,4)=0.0
 77         DCI(3,1)=CP
100         DCI(3,2)=CP
101         DCI(3,3)=CC
102         DCI(3,4)=0.0
103         DCI(4,1)=0.0
104         DCI(4,2)=0.0
105         DCI(4,3)=0.0
106         DCI(4,4)=3.*CC
107         DO 3 J=1,4
110         DO 3 I=1,4
111    3    D(I,J)=DEI(I,J)+DCI(I,J)
114         CALL MATINV(D,4,DUM,0)
115         GO TO 4
    C
    C     ELASTICITY MATRIX FOR AXI-SYMMETRIC CASE
116    2    DCON=(YM*(1.-PR))/((1.+PR)*(1.-2.*PR))
117         DCON2=PR/(1.-PR)
120         D(1,1)=DCON
121         D(1,2)=DCON*DCON2
122         D(1,3)=D(1,2)
123         D(1,4)=0.
124         D(2,1)=D(1,2)
125         D(2,2)=DCON
126         D(2,3)=D(1,2)
127         D(2,4)=0.
130         D(3,1)=D(1,3)
131         D(3,2)=D(2,3)
132         D(3,3)=DCON
133         D(3,4)=0.
134         D(4,1)=D(1,4)
135         D(4,2)=D(2,4)
136         D(4,3)=D(3,4)
137         D(4,4)=G
    C
    C     B MATRIX FOR AXI-SYMMETRIC CASE
140    4    B(1,2)=ZY(1)
141         B(1,4)=ZY(2)
142         B(1,6)=ZY(3)
143         B(2,1)=ZX(1)
144         B(2,3)=ZX(2)
145         B(2,5)=ZX(3)
```

FORTRAN SOURCE LIST FEM

```
ISN        SOURCE STATEMENT

146        GLC=ORY/ORX
147        B(3,1)=ZW(1)/ORX+ZX(1)+ZY(1)*GLC
150        B(3,3)=ZW(2)/ORX+ZX(2)+ZY(2)*GLC
151        B(3,5)=ZW(3)/ORX+ZX(3)+ZY(3)*GLC
152        B(4,1)=ZY(1)
153        B(4,2)=ZX(1)
154        B(4,3)=ZY(2)
155        B(4,4)=ZX(2)
156        B(4,5)=ZY(3)
157        B(4,6)=ZX(3)
160        DO40I=1,4
161        DO40J=1,6
162        DO40K=1,4
163   40   DB(I,J)=DB(I,J)+C(I,K)*B(K,J)/Z
167        VOL=3.14159265*Z*ORX
170        DO60I=1,6
171        DO60J=1,6
172        DO60K=1,4
173   60   C(I,J)=C(I,J)+B(K,I)*DB(K,J)*VOL/Z
177        IF(MM)128,128,127
200   127  WRITE(1)((DE(I,J),I=1,4),J=1,6),ORX,ORY
211   128  RETURN
212        END
```

FORTRAN SOURCE LIST

```
ISN       SOURCE STATEMENT

  0 $IBFTC SOLVE
  1        SUBROUTINE SOLVE(NPART,NCOLN)
    C      BERGERON W 1306-5302S
    C      SUBROUTINE FOR SOLUTION OF EQUATIONS
  2        DIMENSION AM(50,50),BM(50,50),YM(50,50),TF(50,4),RS(50,4),F(50,4),
          1DIS(50,4)
  3        COMMON C(6,6),CBA(4,6),DB(4,6),A(6,6),B(4,6),ST(50,100),L(200,4),
          1XNEW(100,8)
  4        EQUIVALENCE(YM(1,1),ST(1,1))
    C
  5        DO140I=1,50
  6        DO141J=1,NCOLN
  7        TF(I,J)=0.
 10  141   RS(I,J)=0.
 12        DO140J=1,50
 13  140   YM(I,J)=0.
 16        DO144LL=1,NPART
 17        READ(4)M,N,((AM(I,J),I=1,M),J=1,M),((BM(I,J),I=1,M),J=1,N),
          1((F(I,J),I=1,M),J=1,NCOLN)
 52  150   DO424I=1,M
 53        DO425J=1,NCOLN
 54        F(I,J)=F(I,J)-TF(I,J)
 55  425   DIS(I,J)=F(I,J)
 57        DO424J=1,M
 60  424   AM(I,J)=AM(I,J)-YM(I,J)
 63        CALL MATINV(AM,M,DIS,NCOLN)
 64        WRITE(2)M,N,((AM(I,J),I=1,M),J=1,M),((BM(I,J),I=1,M),J=1,N),
          1((F(I,J),I=1,M),J=1,NCOLN)
115        IF(NPART-LL)437,437,432
116   432  CALL MATM(AM,F,DIS,M,M,NCOLN)
117        CALL MATTM(BM,DIS,TF,N,M,NCOLN)
120        DO110J=1,N
121        DO110I=1,M
122        YM(I,J)=0.
123        DO110K=1,M
124  110   YM(I,J)=YM(I,J)+AM(I,K)*BM(K,J)
130        DO111J=1,N
131        DO111I=1,N
132        AM(I,J)=0.
133        DO111K=1,M
134  111   AM(I,J)=AM(I,J)+BM(K,I)*YM(K,J)
140        DO112I=1,N
141        DO112J=1,N
142  112   YM(I,J)=AM(I,J)
145  144   CONTINUE
147  437   REWIND4
150        WRITE(3)((DIS(I,J),I=1,M),J=1,NCOLN)
161        IF(NPART-1)600,600,601
162  601   NA=NPART-1
163        DO441LL=1,NA
164        BACKSPACE2
165        BACKSPACE2
166        READ(2)M,N,((AM(I,J),I=1,M),J=1,M),((BM(I,J),I=1,M),J=1,N),
          1((F(I,J),I=1,M),J=1,NCOLN)
221        CALL MATM(BM,DIS,TF,M,N,NCOLN)
```

FORTRAN SOURCE LIST SOLVE

```
ISN        SOURCE STATEMENT

222        DO444J=1,NCOLN
223        DO444I=1,M
224   444  F(I,J)=F(I,J)-TF(I,J)
227        CALL MATM(AM,F,DIS,M,M,NCOLN)
230   441  WRITE(3)((DIS(I,J),I=1,M),J=1,NCOLN)
242        WRITE(6,515)
243   515  FORMAT(10H RESIDUALS/)
244        DO500LL=1,NPART
245        READ(4)M,N,((AM(I,J),I=1,M),J=1,M),((BM(I,J),I=1,M),J=1,N),
          1((F(I,J),I=1,M),J=1,NCOLN)
300        BACKSPACE3
301        READ(3)((DIS(I,J),I=1,M),J=1,NCOLN)
312        IF(LL-NPART)508,505,505
313   505  DO506J=1,NCOLN
314        DO506I=1,N
315   506  TF(I,J)=0.
320        GO TO 509
321   508  BACKSPACE3
322        BACKSPACE3
323        READ(3)((TF(I,J),I=1,N),J=1,NCOLN)
334   509  DO510J=1,NCOLN
335        DO510I=1,M
336        F(I,J)=F(I,J)-RS(I,J)
337        DO512K=1,M
340   512  F(I,J)=F(I,J)-AM(I,K)*DIS(K,J)
342        DO510L=1,N
343   510  F(I,J)=F(I,J)-BM(I,L)*TF(L,J)
347        CALL MATTM(BM,DIS,RS,N,M,NCOLN)
350        WRITE(6,516)LL
351   516  FORMAT(1X,12HPART. NO.  =,I4,)
352   500  WRITE(6,31)((F(I,J),I=1,M),J=1,NCOLN)
364   31   FORMAT(1X,12E9.2)
365   600  CONTINUE
366         RETURN
367        END
```

FORTRAN SOURCE LIST

```
ISN       SOURCE STATEMENT

  0 $IBFTC MATM
  1       SUBROUTINE MATM(XMAT,YMAT,PMAT,M,N,NCOLN)
    C     BERGERON W 1306-53029
    C     MATRIX MULTIPLICATION
  2       DIMENSION XMAT(50,50),YMAT(50,4),PMAT(50,4)
  3       COMMON C(6,6),CBA(4,6),CB(4,6),A(6,6),B(4,6),ST(50,100),L(200,4),
         1XNEW(100,8)
    C     XMAT IS M BY N LEFT MATRIX TO BE MULTIPLIED
    C     YMAT IS N BY NCOLN RIGHT MATRIX TO BE MULTIPLIED
    C     PMAT IS M BY NCOLN PRODUCT MATRIX
    C
  4       DO10I=1,M
  5       DO10J=1,NCOLN
  6       PMAT(I,J)=0.
  7       DO10K=1,N
 10   10    PMAT(I,J)=PMAT(I,J)+XMAT(I,K)*YMAT(K,J)
 14       RETURN
 15       END
```

FORTRAN SOURCE LIST

```
ISN        SOURCE STATEMENT

  0 $IBFTC MATTM
  1        SUBROUTINE MATTM(XMAT,YMAT,PMAT,N,M,NCOLN)
    C      BERGERON W 1306-5302
    C      MATRIX MULTIPLICATION WITH XMAT TRANSPOSED
  2        DIMENSION XMAT(50,50),YMAT(50,4),PMAT(50,4)
  3        COMMON C(6,6),CBA(4,6),DB(4,6),A(6,6),B(4,6),ST(50,100),L(200,4),
          1XNEW(100,8)
    C      XMAT IS M BY N LEFT MATRIX
    C      YMAT IS M BY NCOLN RIGHT MATRIX
    C      PMAT IS N BY NCOLN PRODUCT OF XMAT TRANSPOSED AND YMAT
    C
  4        DO 10 I=1,N
  5        DO 10 J=1,NCOLN
  6        PMAT(I,J)=0.
  7        DO 10 K=1,M
 10   10   PMAT(I,J)=PMAT(I,J)+XMAT(K,I)*YMAT(K,J)
 14        RETURN
 15        END
```

FORTRAN SOURCE LIST

```
ISN       SOURCE STATEMENT

  0 $IBFTC TOTDIS
  1       SUBROUTINE TOTDIS(NPART,NFIRST,NLAST,NCOLN,NELEM,NOD,NFREE,NPOIN,
         1PILLD,X)
    C     BERGERON W 1306-53029
    C     SUBROUTINE FOR CALCULATION OF TOTAL DISPLACEMENTS
  2       DIMENSION NOD(150,3),NFIRST(15),NLAST(15),X(100,2)
  3       COMMON C(6,6),DBA(4,6),DB(4,6),A(6,6),B(4,6),ST(50,100),U(200,4),
         1XNEW(100,8)
    C
  4       DO60II=1,NPART
  5       JJ=NPART+1-II
  6       M=NFREE*(NFIRST(JJ)-1)+1
  7       N=NFREE*NLAST(JJ)
 10   600  READ(3)((U(I,J),I=M,N),J=1,NCOLN)
 22       DO50I=1,NPOIN
 23       DO50J=1,NCOLN
 24       XNEW(I,2*J-1)=X(I,1)+U(2*I-1,J)
 25   50  XNEW(I,2*J)=X(I,2)+U(2*I,J)
 30       WRITE(6,613)
 31   613  FORMAT(1H1,45HFINITE ELEMENT ANALYSIS OF SALT PILLAR MODELS/,1X,
         119HCREEP MODIFICATIONS//,1X,32HBERGERON, W.  APRIL,1968  U.S.U.//)
 32       WRITE(6,614)PILLD
 33   614  FORMAT(1X,24HAVERAGE PILLAR STRESS = ,F10.0,5H  PSI/)
 34       WRITE(6,615)
 35   615  FORMAT(1H ,40HNODE   R-DISPLACEMENTS   Z-DISPLACEMENTS,5X,
         1  31HNEW R CO-ORD.     NEW Z CO-ORD./)
 36       WRITE(6,32)((I,U(2*I-1,J),U(2*I,J),XNEW(I,2*J-1),XNEW(I,2*J),
         1I=1,NPOIN),J=1,NCOLN)
 47   32   FORMAT(1X,I4,1P4E18.8)
 50       WRITE(7,33)((U(2*I-1,J),U(2*I,J),I=1,NPOIN),J=1,NCOLN)
 61   33   FORMAT(2E16.8)
 62       WRITE(6,635)
 63   635  FORMAT(1H1,15HELEMENT NUMBER ,16H    Z-STRESS    ,
         1  16H    R-STRESS    ,16H    T-STRESS    ,16H    RZ-STRESS   /)
    C
 64       DO20LL=1,NELEM
 65       READ(1)((DB(I,J),I=1,4),J=1,6),CRX,CRY
 76       DO620J=1,NCOLN
 77       DO620I=1,3
100       JJ=NOD(LL,I)
101       C(2*I-1,J)=U(2*JJ-1,J)
102   620  C(2*I,J)=U(2*JJ,J)
105       DO630J=1,NCOLN
106       DO630I=1,4
107       DBA(I,J)=0.
110       DO630K=1,6
111   630  DBA(I,J)=DBA(I,J)+DB(I,K)*C(K,J)
115       WRITE(6,31)LL,((DBA(I,J),I=1,4),J=1,NCOLN)
126   31   FORMAT(6X,I4,5X,1P4E16.7)
127       WRITE(7,46)((DBA(I,J),I=1,4),J=1,NCOLN)
140   46   FORMAT(4E16.8)
141   20   CONTINUE
143       WRITE(7,45)((XNEW(I,2*J-1),XNEW(I,2*J),I=1,NPOIN),J=1,NCOLN)
154   45   FORMAT(2F14.6)
155        RETURN
```

FORTRAN SOURCE LIST TCTDIS

ISN	SOURCE STATEMENT
156	END

FORTRAN SOURCE LIST

```
ISN        SOURCE STATEMENT

  0 $IBFTC MATINV
  1        SUBROUTINE MATINV(A,N,B,M)
    C      MATRIX INVERSION WITH ACCOMPANYING SOLUTION OF LINEAR EQUATIONS
    C
    C      INITIALIZATION
  2        DIMENSION IPIVOT(50),A(50,50),B(50,4),INDEX(50,2),PIVOT(50)
  3   10   DETERM=1.0
  4   15   DO20J=1,N
  5   20   IPIVOT(J)=0
  7   30   DO550I=1,N
    C
    C      SEARCH FOR PIVOT ELEMENT
 10   40   AMAX=0.0
 11   45   DO105J=1,N
 12   50   IF(IPIVOT(J)-1)60,105,60
 13   60   DO100K=1,N
 14   70   IF(IPIVOT(K)-1)80,100,740
 15   80   IF(ABS(AMAX)-ABS(A(J,K)))85,100,100
 16   85   IROW=J
 17   90   ICOLUM=K
 20   95   AMAX=A(J,K)
 21  100   CONTINUE
 23  105   CONTINUE
 25  110   IPIVOT(ICOLUM)=IPIVOT(ICOLUM)+1
    C
    C      INTERCHANGE ROWS TO PUT PIVOT ELEMENT ON DIAGONAL
 26  130   IF(IROW-ICOLUM)140,260,140
 27  140   DETERM=-DETERM
 30  150   DO200L=1,N
 31  160   SWAP=A(IROW,L)
 32  170   A(IROW,L)=A(ICOLUM,L)
 33  200   A(ICOLUM,L)=SWAP
 35  205   IF(M)260,260,210
 36  210   DO250L=1,M
 37  220   SWAP=B(IROW,L)
 40  230   B(IROW,L)=B(ICOLUM,L)
 41  250   B(ICOLUM,L)=SWAP
 43  260   INDEX(I,1)=IROW
 44  270   INDEX(I,2)=ICOLUM
 45  310   PIVOT(I)=A(ICOLUM,ICOLUM)
 46  320   DETERM=DETERM*PIVOT(I)
    C
    C      DIVIDE PIVOT ROW BY PIVOT ELEMENT
 47  330   A(ICOLUM,ICOLUM)=1.0
 50  340   DO350L=1,N
 51  350   A(ICOLUM,L)=A(ICOLUM,L)/PIVOT(I)
 53  355   IF(M)380,380,360
 54  360   DO370L=1,M
 55  370   B(ICOLUM,L)=B(ICOLUM,L)/PIVOT(I)
    C      REDUCE NON-PIVOT ROWS
 57   380  DO545 L1=1,N
 60   391  IF(L1-ICOLUM)400,545,400
 61  400   T=A(L1,ICOLUM)
 62  420   A(L1,ICOLUM)=0.0
 63  430   DO450L=1,N
```

FORTRAN SOURCE LIST MATINV

```
ISN        SOURCE STATEMENT

 64   450   A(L1,L)=A(L1,L)-A(ICOLUM,L)*T
 66    456  IF(M)545,545,460
 67   460   DO500L=1,M
 70   500   B(L1,L)=B(L1,L)-B(ICOLUM,L)*T
 72    545  CONTINUE
 74   550   CONTINUE
     C
     C      INTERCHANGE COLUMNS
 76   600   DO710I=1,N
 77   610   L=N+1-I
100   620   IF(INDEX(L,1)-INDEX(L,2))630,710,630
101   630   JROW=INDEX(L,1)
102   640   JCOLUM=INDEX(L,2)
103   650   DO705K=1,N
104   660   SWAP=A(K,JROW)
105   670   A(K,JROW)=A(K,JCOLUM)
106   700   A(K,JCOLUM)=SWAP
107   705   CONTINUE
111   710   CONTINUE
113   740   RETURN
114   750   END
```

APPENDIX E

PROGRAM LISTING FOR PLOT OF NODAL POINTS

FORTRAN SOURCE LIST

```
ISN       SOURCE STATEMENT

  0 $IBFTC PLOTNP
    C      PLOT OF NODAL POINTS
  1        DIMENSION BUFFER(6000),XAR(102),YAR(102),NOD(150,3),A(5),B(5)
  2        DIMENSION HEAD1(8),HEAD2(8)
  3        DIMENSION XBP(14),YBP(14),NOBP(12)
  4        NOBP(1)=1
  5        NOBP(2)=7
  6        NOBP(3)=13
  7        NOBP(4)=19
 10        NOBP(5)=25
 11        NOBP(6)=31
 12        NOBP(7)=37
 13        NOBP(8)=46
 14        NOBP(9)=54
 15        NOBP(10)=61
 16        NOBP(11)=66
 17        NOBP(12)=73
 20        READ(5,10)NPART,NPOIN,NELEM
 24   10   FORMAT(10I4)
 25        DATA HEAD2/45HBERGERON, W. J.   APRIL 1968      L. S. U.    /
 26        DO40I=1,NELEM
 27   40   READ(5,10)(NOD(I,J),J=1,3)
 35        READ(5,45) (XAR(I),YAR(I),I=1,NPOIN)
 42   45   FORMAT (2F14.6)
 43        CALL PLOTS(BUFFER,6000)
 44        XAR(NPOIN+1)=0.
 45        XAR(NPOIN+2)=10.
 46        DATA TITLEX/6H  R   /
 47        DATA TITLEY/6H  Z   /
 50        DATA HEAD1/45HFINITE ELEMENT ANALYSIS OF SALT PILLAR MODELS/
 51        CALL AXIS(0.,0.,TITLEX,-6, 38.0 ,0.,0.,.1,10.)
 52        CALL AXIS(0.,0.,TITLEY,6,15.,90.,0.,.1,10.)
 53        B(4)=0.
 54        CALL SYMBOL(8.,17.,.5,HEAD1,0.,45)
 55        CALL SYMBOL(8.,16.,.25,HEAD2,0.,45)
 56        A(4)=0.
 57        A(5)=.1
 60        B(5)=.1
 61        DO60I=1,NELEM
 62        DO50J=1,3
 63        K=NOD(I,J)
 64        A(J)=XAR(K)
 65   50   B(J)=YAR(K)
    C      JOIN 3 NODAL PTS FOR AN ELEMENT
 67   60   CALL LINE(A,B,3,1,0,0)
    C      NEXT NUMBER EACH POINT
 71        DO70I=1,NPOIN
 72        X=XAR(I)*10.+.125
 73        Y=YAR(I)*10.+.125
 74        FPN=I
 75        CALL NUMBER (X,Y,.125,FPN,0.,-1)
 76   70   CONTINUE
100        DO 500 I=1,12
101        J=NOBP(I)
102        XBP(I)=XAR(J)
```

FORTRAN SOURCE LIST PLOTNP

```
ISN        SOURCE STATEMENT

103        YBP(I)=YAR(J)
104   500  CONTINUE
106        XBP(13)=0.
107        XBP(14)=.1
110        YBP(13)=0.
111        YBP(14)=.1
112        CALL LINE(XBP,YBP,12,1,0,0)
113        CALL PLOT(30.,5.,-3)
114        CALL PLOT(0.,0.,999)
115        STOP
116        END
```

VITA

William Joseph Bergeron was born in Eunice, Louisiana on June 9, 1934. He attended public school in Eunice and graduated from Eunice High School in May, 1952. He entered Southwestern Louisiana Institute in Lafayette, Louisiana, completed his freshman year there, and then joined the U.S. Air Force. In June, 1954, he married a girl from Eunice and at present is the father of three girls and a boy. Upon completion of his service obligation, he returned to Southwestern Louisiana Institute and in June, 1959, he received the degree of Bachelor of Science in Petroleum Engineering. He then worked as an engineer with Halliburton until January, 1960, at which time he enrolled in the Graduate School of Louisiana State University. He completed the requirements for the degree of Master of Science in Engineering Mechanics in August, 1961. He then joined the staff in the Physics Department at the University of Southwestern Louisiana and remained there until August, 1965 when he re-entered the Graduate School at Louisiana State University. He is now a candidate for the degree of Doctor of Philosophy in the Department of Engineering Mechanics.

EXAMINATION AND THESIS REPORT

Candidate: William Joseph Bergeron

Major Field: Engineering Mechanics

Title of Thesis: "Finite Element Analysis of Salt Pillar Models"

Approved:

Robert J. Thoma
Major Professor and Chairman

R D Anderson
Dean of the Graduate School

EXAMINING COMMITTEE:

Robert J. Thoma

Oscar W. Albritton

Edwin P. Chilcott

Daniel R. Yannitell

Dan K. Sokol

Date of Examination:

June 6, 1968